# Temporal and spatial scales of temperature, salinity and current velocity on the Newfoundland Grand Banks and in the Gulf of St. Lawrence

M. Ouellet, B. Petrie, J. Chassé and D. Gilbert

Ocean Sciences Division
Fisheries and Oceans Canada
Bedford Institute of Oceanography
P.O. Box 1006
Dartmouth, Nova Scotia, B2Y 4A2

2011

Canadian Technical Report of
Hydrography and Ocean Sciences 272

Fisheries and Oceans Canada | Pêches et Océans Canada

Canada

Canadian Technical Report of Hydrography and Ocean Sciences
No. 272

2011

# Temporal and spatial scales of temperature, salinity and current velocity on the Newfoundland Grand Banks and in the Gulf of St. Lawrence

by

M. Ouellet[1], B. Petrie[2], J. Chassé[3] & D. Gilbert[4]

[1]Ocean Sciences - Canadian Hydrographic Service
Fisheries and Oceans Canada
Integrated Science Data Management
200 Kent Street
Ottawa, Ontario, K1A 0E6

[2]Ocean Sciences Division
Fisheries and Oceans Canada
Bedford Institute of Oceanography
P.O. Box 1006
Dartmouth, Nova Scotia, B2Y 4A2

[3]Aquatic Resources Division
Fisheries and Oceans Canada
Gulf Fisheries Centre
343 Université Avenue, PO Box 5030
Moncton, New Brunswick, E1C 9B6

[4]Direction des sciences océaniques et de l'environnement
Pêches et Océans Canada
Institut Maurice-Lamontagne
850, Route de la Mer, C.P. 1000
Mont-Joli, Québec, G5H 3Z4

© Her Majesty the Queen in Right of Canada, 2011.
PDF version: Cat. No. Fs 97-18/272E-PDF ISSN 1488-5417
PRINT version: Cat. No. Fs 97-18/272E ISSN 0711-6764

Published by:

Fisheries and Oceans Canada
200 Kent Street
Ottawa, Ontario
K1A 0E6

Correct citation for this publication:

Ouellet, M., Petrie, B., Chassé, J. and Gilbert, D. 2011. Temporal and spatial scales of temperature, salinity and current velocity on the Newfoundland Grand Banks and in the Gulf of St. Lawrence. Can. Tech. Rep. Hydrogr. Ocean Sci. No. 272: vi + 78 p.

# TABLE OF CONTENTS

TABLE OF CONTENTS ..... iii
LIST OF FIGURES ..... iv
LIST OF TABLES ..... v
ABSTRACT ..... vi
RÉSUMÉ ..... vi

1.0 INTRODUCTION ..... 1
2.0 METHOD ..... 2
2.1. CALCULATION OF COEFFICIENTS ..... 3
2.2 EQUATION FITTING ..... 4
3.0 DATA ..... 4
3.1 RESAMPLING ..... 5
3.2 SUBSEQUENT FILTERING ..... 6
3.3 CURRENT ROTATION ..... 7
4.0 ANALYSIS ..... 8
4.1 NEWFOUNDLAND SHELF AND GRAND BANKS ..... 8
4.1.1 AVALON CHANNEL ARRAY ..... 10
4.1.2 FLEMISH PASS ARRAY ..... 13
4.1.3 CASP2 ARRAY ..... 17
4.1.4 SOUTHEAST SHOAL ARRAY ..... 21
4.2 GULF OF ST. LAWRENCE AND ST. LAWRENCE ESTUARY ..... 24
4.2.1 CABOT STRAIT ..... 24
4.2.2 ST. LAWRENCE ESTUARY ..... 30
4.2.3 CENTRAL GULF ..... 35
4.2.4 GASPÉ CURRENT ..... 39
4.2.5 JACQUES-CARTIER PASSAGE ..... 44
4.2.6 STRAIT OF BELLE ISLE ..... 53
5.0 CONCLUSION ..... 57
5.1 NEWFOUNDLAND SHELF AND GRAND BANKS ..... 57
5.2 GULF OF ST. LAWRENCE AND ST. LAWRENCE ESTUARY ..... 60
5.3 REPRESENTATIVITY OF SAMPLING ALONG AZMP SECTIONS ..... 63
6.0 ACKNOWLEDGEMENTS ..... 63
7.0 REFERENCES ..... 63

APPENDIX I ..... 67

# LIST OF FIGURES

Figure 1. Map of AZMP sections and fixed stations ..... 1
Figure 2. Newfoundland Shelf and Position of Arrays ..... 5
Figure 3.Gulf of St. Lawrence and Position of Arrays ..... 5
Figure 4.Newfoundland Shelf and Velocity Decomposition Axis ..... 8
Figure 5.Gulf of St. Lawrence and Velocity Decomposition Axis ..... 9
Figure 6.1 Avalon Channel Array ..... 10
Figure 6.2 Horizontal correlation across Avalon Channel ..... 12
Figure 6.3 Vertical correlation in Avalon Channel ..... 12
Figure 6.4 Temporal auto-correlation in Avalon Channel ..... 13
Figure 7.1 Flemish Pass Array ..... 17
Figure 7.2 Horizontal correlation along Flemish Pass ..... 15
Figure 7.3 Horizontal correlation across Flemish Pass ..... 15
Figure 7.4 Vertical correlation at Flemish Pass ..... 16
Figure 7.5 Temporal auto-correlation in Flemish Pass ..... 16
Figure 8.1 CASP2 Array ..... 16
Figure 8.2 Horizontal correlation Across-Shelf during CASP2 ..... 18
Figure 8.3 Horizontal correlation Along-Shelf during CASP2 ..... 19
Figure 8.4 Vertical correlation during CASP2 ..... 20
Figure 8.5 Temporal auto-correlation during CASP2 ..... 20
Figure 9.1 Southeast Shoal Array ..... 22
Figure 9.2 Horizontal correlation Across-Shelf at Southeast Shoal ..... 23
Figure 9.3 Vertical correlation at Southeast Shoal ..... 23
Figure 9.4 Temporal auto-correlation at Southeast Shoal ..... 24
Figure 10.1 Cabot Strait Array ..... 27
Figure 10.2 Horizontal correlation along Cabot Strait ..... 27
Figure 10.3 Vertical correlation in Cabot Strait ..... 27
Figure 10.4 Temporal auto-correlation in Cabot Strait ..... 29
Figure 11.1 St. Lawrence Estuary Array ..... 31
Figure 11.2 Horizontal correlation along St. Lawrence Estuary ..... 32
Figure 11.3 Horizontal correlation across St. Lawrence Estuary ..... 32
Figure 11.4 Vertical correlation in St. Lawrence Estuary ..... 33
Figure 11.5 Temporal auto-correlation in St. Lawrence Estuary ..... 34
Figure 12.1 Central Gulf Array ..... 36
Figure 12.2 Horizontal correlation along Honguedo Strait ..... 37
Figure 12.3 Horizontal correlation across Honguedo Strait ..... 37
Figure 12.4 Vertical correlation in Central Gulf ..... 38
Figure 12.5 Temporal auto-correlation in Central Gulf ..... 38
Figure 13.1 Gaspé Current Array ..... 40
Figure 13.2 Horizontal correlation along 100 m isobath ..... 41
Figure 13.3 Horizontal correlation across Gaspé Current ..... 41
Figure 13.4 Vertical correlation in Gaspé Current ..... 42
Figure 13.5 Temporal auto-correlation in Gaspé Current ..... 43
Figure 14.1 Jacques-Cartier Passage Array ..... 45
Figure 14.2 Summer horizontal correlation along Jacques-Cartier Passage ..... 46

Figure 14.3 Winter horizontal correlation along Jacques-Cartier Passage ..... 46
Figure 14.4 Horizontal correlation along Anticosti shore ..... 48
Figure 14.5 Summer horizontal correlation across Jacques-Cartier Passage ..... 48
Figure 14.6 Winter horizontal correlation across Jacques-Cartier Passage ..... 49
Figure 14.7 Summer vertical correlation in Jacques-Cartier Passage ..... 49
Figure 14.8 Winter vertical correlation in Jacques-Cartier Passage ..... 50
Figure 14.9 Summer temporal auto-correlation in Jacques-Cartier Passage ..... 51
Figure 14.10 Winter temporal auto-correlation in Jacques-Cartier Passage ..... 52
Figure 15.1 Strait of Belle Isle Array ..... 54
Figure 15.2 Horizontal correlation across Strait of Belle Isle ..... 55
Figure 15.3 Vertical correlation in Strait of Belle Isle ..... 56
Figure 15.4 Temporal auto-correlation in Strait of Belle Isle ..... 57
Figure 16.1 Horizontal correlation scales of temperature on Newfoundland Shelf ..... 59
Figure 16.2 Horizontal correlation scales of salinity on Newfoundland Shelf ..... 59
Figure 17.1 Horizontal correlation scales of temperature in the G. of St. Lawrence ..... 62
Figure 17.2 Horizontal correlation scales of salinity in the Gulf of St. Lawrence ..... 62

## LIST OF TABLES

Table 1 Datasets used ..... 4
Table 2 Variance accounted for by the filtered series ..... 8
Table 3 Velocity coordinates ..... 9
Table 4 Summary of Newfoundland Shelf correlation scales ..... 58
Table 5 Summary of Gulf of St. Lawrence correlation scales ..... 61
Table 6 AZMP Sections, average station distance and corresponding arrays ..... 63

## ABSTRACT

Ouellet, M., B. Petrie, J. Chassé and D. Gilbert. 2011. Spatial and temporal scales of temperature, salinity and current velocity on the Newfoundland Grand Banks and in the Gulf of St. Lawrence. Can. Tech. Rep. Hydrogr. Ocean Sci. No. 272: vi+ 78 p.

In order to assess the representativity of the Atlantic Zonal Monitoring Program (AZMP) stations, an analysis of the spatial and temporal variability of temperature, salinity and current velocity in Canadian Atlantic waters is presented here using historic mooring series. Spatial correlation functions are estimated in the horizontal and vertical directions between simultaneous sensors. Temporal auto-correlation is used to investigate the temporal scales. The analysis focuses on two regions: Newfoundland Grand Banks and Gulf of St. Lawrence. In the Grand Banks, Avalon Peninsula, Flemish pass, SouthEast Shoal and the CASP2 zone. In the Gulf, Strait of Belle Isle, Jacques Cartier Passage, St. Lawrence Estuary, Gaspé Current, Central Gulf and Cabot Strait.



## RÉSUMÉ

Ouellet, M., B. Petrie, J. Chassé et D. Gilbert. 2011. Spatial and temporal scales of temperature, salinity and current velocity on the Newfoundland Grand Banks and in the Gulf of St. Lawrence. Can. Tech. Rep. Hydrogr. Ocean Sci. No. 272: vi + 78 p.

Afin d'évaluer la représentativité du Programme de Monitorage de la Zone Atlantique (PMZA), nous présentons une analyse de la variabilité spatiale et temporelle de la température, de la salinité et du courant dans les eaux atlantiques canadiennes, à partir de données historiques de mouillages. Des fonctions de corrélation spatiale sont estimées dans les directions verticale et horizontale entre des données simultanées de capteurs séparés. Les échelles temporelles sont évaluées au moyen de la fonction d'auto corrélation temporelle. L'analyse se concentre sur deux régions: les Grand Bancs de Terre-Neuve et le golfe du Saint-Laurent. Sur les Grand Bancs, la péninsule d'Avalon, le col Flamand, le plateau du Sud-Est et les lieux de CASP2. Dans le golfe, le détroit de Belle Isle, le détroit de Jacques-Cartier, l'estuaire Saint-Laurent, le courant de Gaspé, le centre du golfe et le détroit de Cabot.

## 1.0 Introduction

The Atlantic Zonal Monitoring Program (AZMP) is an operational marine research program conducted by DFO in the eastern Canadian waters (Therriault et al., 1998). Its observation component requires, among other tasks, bi-weekly hydrographic sampling (temperature, salinity, nutrients, plankton) at seven (7) fixed stations and seasonal hydrographic sampling along thirteen (13) sections (Therriault et al., 1998). The coverage of physical, chemical and biological variables is limited by technical, financial and physical constraints. The locations of the regularly sampled stations and sections were based on analyses of mainly physical variables with emphasis on the Scotian Shelf (Therriault et al., 1998; Petrie and Dean-Moore, 1996). Determination of the temporal and spatial scales of variability is very important in order to assess the sampling strategy employed by the AZMP over the whole Canadian Atlantic region and to resolve the fundamental biological, chemical and physical processes.

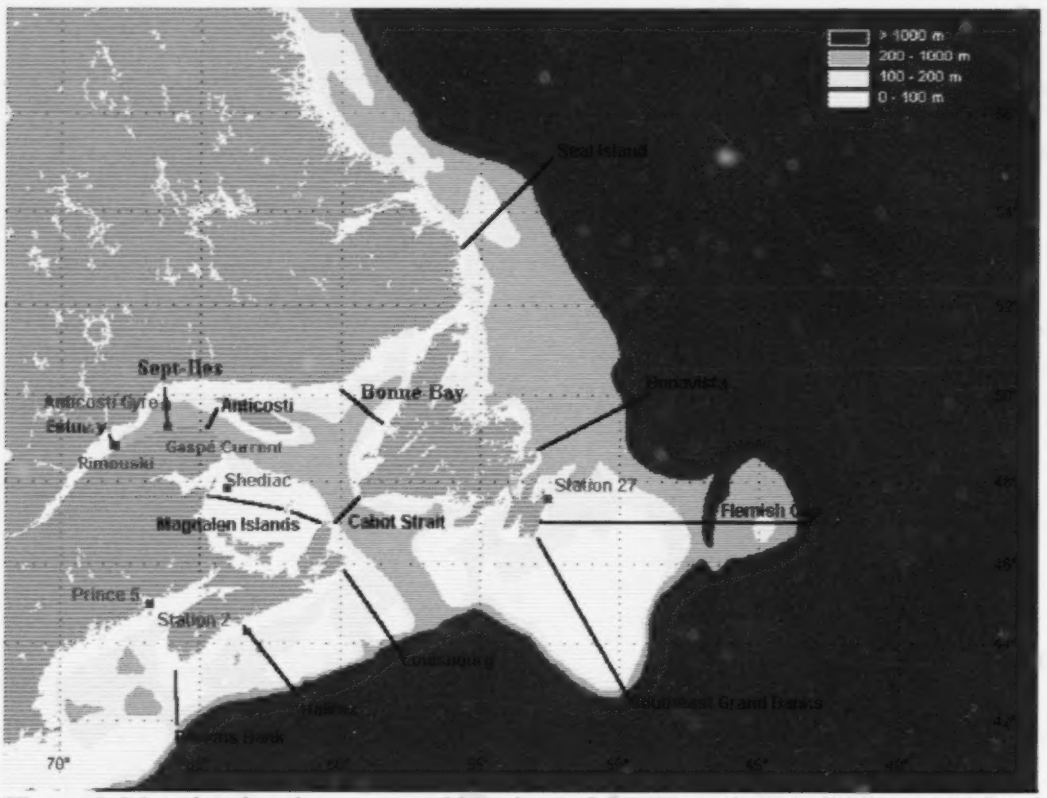


**Figure 1.** Map showing the names and locations of AZMP sections (solid lines) and fixed stations (squares).

Petrie and Dean-Moore (1996) used the data from five instrumented arrays on the Scotian Shelf to derive spatial and temporal scales of variability for temperature and salinity. Ouellet et al. (2003) conducted an analysis of sea surface temperature and determined spatial and temporal scales of variability for the region from the Labrador Shelf to the Gulf of Maine. In this report, we extend the two earlier studies and present the results of an investigation of the spatial and temporal scales of variability in eastern Canadian

waters using data from fixed arrays of current meters, thermistor chains and moored pressure gauges. The temporal scales of variability that can be addressed with these datasets are limited by the length of the data records; the spatial scales of variability are limited by the design of the array.

## 2.0 Method

The method involves the estimation of correlation coefficients (r) and their variation as a function of vertical and horizontal distance, and time lag. This is similar to the first steps of the statistical optimal interpolation method introduced by Gandin (1967), which is frequently used in meteorology. An estimation of correlation functions was used by the Climate Research Branch of the Meteorological Service of Canada (Milewska and Hogg, 2001) in an analysis of the Canadian climate network.

The correlation function is dependent on the four dimensions of space (x and y, horizontal separations, and z, vertical separation) and time (t). With data from an array of fixed instruments, correlations and their distributions can be calculated for a single dimension holding the other three fixed. We usually refer to the correlation function in the time dimension as the temporal auto-correlation. There are two steps in the estimation of the space and time scales of variability: the actual calculation of the individual correlation coefficients and the fitting of a smoothly varying function to these values.

### 2.1. Calculation of coefficients

For an array with instruments at the same depths on different moorings, the correlation coefficients as a function of the *horizontal* distance can be determined. Moreover, often there are sufficient data to calculate the coefficients along and across bathymetric contours or relative to coastlines. For a single mooring with several instruments, the correlation coefficients as a function of *vertical* separation can be computed. For any instrument, the *temporal* auto-correlation can be calculated.

Spatial correlation coefficients are computed typically in 3 dimensions: two axes in the horizontal (*x, y; along and across isobaths; along and perpendicular to coastlines*) and one in the vertical (*z*). For the two horizontal dimensions, the instruments for each correlation coefficient pair should be ideally at the same depths; for the work presented in this report, depth offsets of 5 m and less have been tolerated and are considered to be at the same depth. Frequently the instrument depths are not known to any accuracy of less than 5 m. It is usually convenient to set $x$ and $y$ either along/across an isobath, a shoreline, a known current trajectory or a front, when sampling configuration permits it. The vertical correlation coefficients can be computed from any two instruments moored on the same line.

For series $x$ and $y$ of $N$ observations sampled simultaneously by two instruments separated by a horizontal or vertical distance $d$, the correlation coefficient is given by:

$$C_d = \frac{\sum_{i=1}^{N}(x_i - \bar{x})(y_i - \bar{y})}{\sqrt{\sum_{i=1}^{N}(x_i - \bar{x})^2 \sum_{i=1}^{N}(y_i - \bar{y})^2}}$$

where the overbar denotes a time average. In this report, spatial coefficients were computed only for overlapping series of 30 days duration or longer. For $n$ instruments located along one dimension and sampled during a common time interval, the number of possible correlation coefficients is equal to $n*(n-1)/2$.

Temporal auto-correlation coefficients for a series of lags indexed by a number $k$ are given by:

$$C_k = \frac{\sum_{n=1}^{N-k}(x_n - \bar{x})(x_{n+k} - \bar{x})}{\sqrt{\sum_{n=1}^{N-k}(x_n - \bar{x})^2 \sum_{n=1}^{N-k}(x_{n+k} - \bar{x})^2}}$$

Temporal coefficients were computed for time series of observations of 40 days or longer, with selected lags of 6, 12, 24, 48, 72, 96, 120, 240, 360, 480 and 960 hours (a quarter of a day to 40 days) whenever possible.

2.2 Equation fitting

Once the correlation coefficients between all pairs of instruments are known, the second step consists of fitting a function that will represent the spatial or temporal scale of variability. We selected an exponential form, and fitted it to the raw correlation coefficients using Gauss-Newton's non-linear least square regression method (Dennis, 1977). The e-folding scale (distance or time at which the fitted correlation function equals $e^{-1}$, *~0.37*) is taken as the estimate of the correlation scale.

Prior to the exponential fitting, we considered whether or not results could be combined into a single group or had to be separated on a case by case basis. For example, horizontal scales of variability could differ depending on whether the data were from the shallow mixed layer, the pycnocline or deeper.

In some instances, the correlation scale could not be resolved. This can be because of the scarcity of correlation coefficients, because the e-folding scale is greater than the largest separation value between simultaneous instrument pairs, or because the e-folding scale is smaller than the smallest separation value between pairs. In those cases, the e-folding value represents only the upper or lower limit of the correlation scale.

In cases when all correlation coefficients were negative, an exponential function is not a good representation of the scale; the upper limit of correlation scale was set as the smallest separation between simultaneous instruments.

**Table 1**. Datasets used

| Region | Array name | Start Time | End Time | ODI cruise # | Project | Reference (if available) or project leader |
|---|---|---|---|---|---|---|
| Grand Banks | Avalon | 21-Jun-80 | 23-Oct-80 | 80019 | | Petrie (1991) |
| | | 23-Oct-80 | 23-Apr-81 | 80034 | | Petrie (1991) |
| | Flemish | 14-Oct-85 | 01-Feb-86 | 85929<br>85930 | Labrador Current Variability Study | Lively and Petrie (1990) |
| | CASP2 | 29-Nov-91 | 21-May-92 | 91059 | Canadian Atlantic Storm Program II | Lively (1994) |
| | SEShoal | 18-Apr-86 | 17-Oct-86 | 86005 | | Ross, Loder and Graca (1988) |
| | | 3-May-87 | 19-Oct-87 | 87012<br>87999 | | Ross, Loder and Graca (1988) |
| Gulf of St. Lawrence | Cabot | 10-Aug-66 | 10-Sep-66 | 66021 | | Lawrence (1968) |
| | | 13-Jun-67 | 07-Sep-67 | 67018 | | Farquharson (1970) |
| | | 01-Oct-83 | 24-Dec-83 | 83938 | Petro-Canada Bow Drill 1 | Gregory, Nadeau and Lefaivre (1989) |
| | | 04-Jun-93 | 21-Oct-93 | 93600 | Cape North 1993 | Castonguay and Gilbert (1994), Desruisseaux (1996) |
| | | 23-Oct-95 | 23-Jun-96 | 95600 | Golfe Hiver 1996 | Gilbert and Smith |
| | | 10-May-96 | 01-May-97 | 96600 | | Gilbert and Smith |
| | | 01-May-97 | 05-Dec-97 | 97003 | | Smith |
| | SLE | 19-May-79 | 07-Dec-79 | 79010 | | El-Sabh, Lie and Koutitonsky (1982) |
| | | 11-Apr-82 | 11-Sep-82 | 82007 | | Tee and Lim (1987) |
| | Central Gulf | 14-Jun-67 | 25-Jul-67 | 67018 | | Lomas and Lawrence (1973) |
| | | 29-Jan-70 | 27-Apr-70 | 70001 | | Gregory, Nadeau and Lefaivre (1989) |
| | | 15-May-79 | 06-Dec-79 | 79010 | | Gregory, Nadeau and Lefaivre (1989) |
| | | 06-Dec-79 | 19-Apr-80 | 79031 | | Gregory, Nadeau and Lefaivre (1989) |
| | | 19-Apr-80 | 12-Nov-80 | 80007 | | Gregory, Nadeau and Lefaivre (1989) |
| | | 02-Dec-80 | 29-Apr-81 | 80040 | | Gregory, Nadeau and Lefaivre (1989) |
| | Gaspé | 16-Jun-78 | 30-Sep-78 | 78017<br>78018 | Gaspé Current Project | Tang and Bennett (1981) |
| | JCP | 26-May-86 | 20-May-88 | 86600 | COHJAC | Bourque and Kelley (1995), Lefaivre |
| | Belleisle | 31-Jul-63 | 20-Sep-63 | 63002 | | Farquharson and Bailey (1966) |
| | | 07-Jan-75 | 22-Jun-75 | 75001 | | Petrie, Toulany and Garrett (1988), Forrester |
| | | 26-Jul-80 | 26-Dec-80 | 80021 | | Lively (1984) |

## 3.0 Data

We used data from instrumented moorings from 1963 to 1997, downloaded from the Bedford Institute of Oceanography archive of moored current meters, thermographs and tide gauges (Gregory, 2004). The arrays chosen allow the assessment of variability on the Newfoundland Grand Banks (Fig. 2) and in the Gulf of St. Lawrence (Fig. 3). Positions of regularly sampled AZMP stations and sections are superimposed. The dataset origins are described in Table 1.

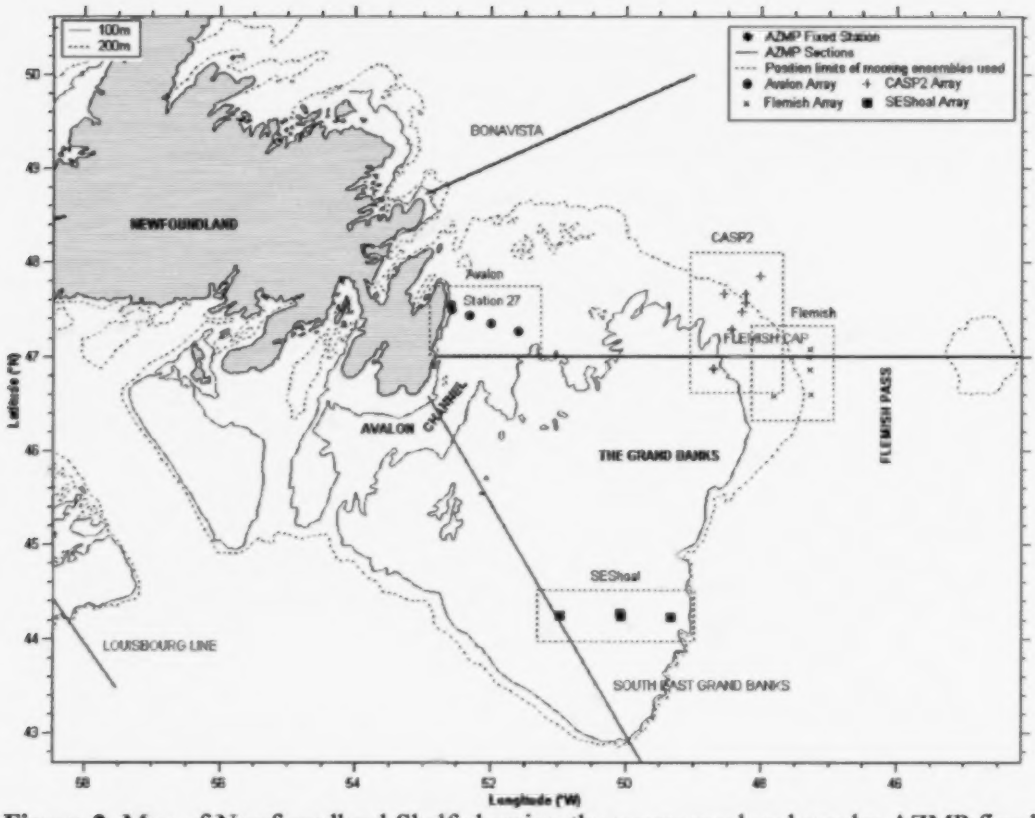


**Figure 2.** Map of Newfoundland Shelf showing the arrays used and nearby AZMP fixed stations and sections (black fonts designate place names, red upper case fonts designate names of AZMP sections, normal case red fonts designate names of AZMP stations, blue fonts designate names of current meter arrays).

3.1 Resampling

The series originally had sampling intervals ranging from 1 hour to 5 minutes. For consistency, all series were standardized to hourly intervals after filtering with a 1-hour moving average boxcar filter. For time series with an original sampling interval less than 1 hour, this smoothing process reduces the potential for aliasing of frequencies higher than 0.5 cph to frequencies lower than 0.5 cph in the decimated time series.

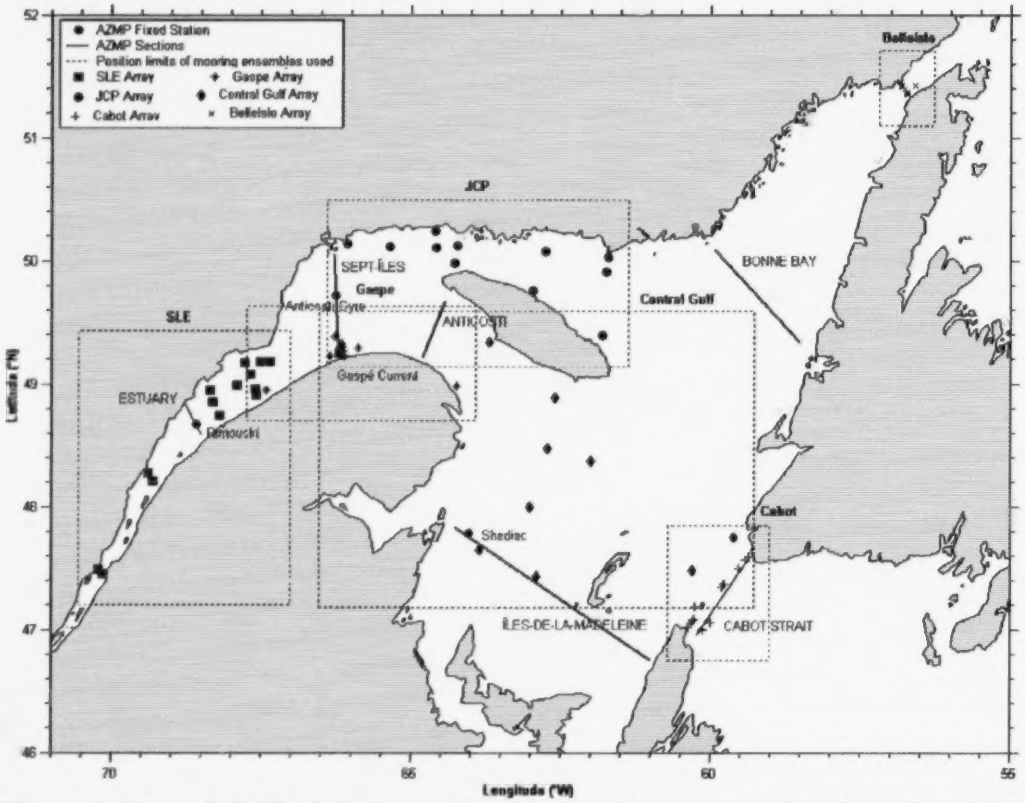


**Figure 3.** Map of Gulf of St. Lawrence showing the arrays used and nearby AZMP stations and sections (red upper case fonts designate names of AZMP sections, normal case red fonts designate names of AZMP stations, blue fonts designate names of current meter arrays).

## 3.2 Subsequent filtering

### *3.2.1 Temperature and salinity data*

Because of the dominant annual, seasonal and monthly cycles in atmospheric temperature, wind, precipitation and river runoff, temperature and salinity usually show substantial low-frequency variability with periods from 2 weeks to 1 year. Our records are generally too short to separate the contribution of the annual cycle from higher frequencies. The variance contained in the low frequencies could produce high correlation coefficients that decrease slowly with distance. The information on the representativity of phenomena at higher frequencies could be contaminated by such low frequency variance. In addition, most of the mooring arrays are of limited duration and do not allow examination of low frequency coherence. The focus of this study is therefore on the higher frequency variability; consequently, the temperature and salinity data were filtered in order to remove the low frequency variability. The observations were first low-passed using a boxcar filter with a cut-off period of 14 days; then the filtered series were subtracted from the original series.

This is equivalent to a high pass filter. The resulting series, used for correlation coefficient computations, are thus expected to have variability in the frequency band ranging from 0.003 to 1 cph. We thus have a more modest goal of examining the scales of variability in this limited frequency range.

The proportion of the total variance examined in the analysis varies according to the site, depth and time of year. We calculated the percentage of the total variance captured within periods 14 d and less (or frequencies 0.003 to 1 cph). The detailed results are shown in Table 2. On average, the proportion of total variance contained in the filtered series tends to increase with depth and is higher (~7%) for salinity than for temperature. The filtered series of the SouthEast Shoal array contain less variance on average, in proportion to the total variance, than series from other mooring arrays, while in the Gaspé Current and Flemish Pass arrays contain more. There is no clear relation between record duration and the proportion of variance accounted for by the filtered series, but the averaged proportion of the filtered variances of the 26 longest series (>200 days, all of which are located in the Gulf), though on average lower than that of the 211 other series (<200 days), is still significant at 29% (temperature) and 32% (salinity).

*3.2.2 Velocity data*

In the regions under study, energy at the diurnal and semi-diurnal tidal frequencies and the inertial frequency usually dominate the kinetic energy spectrum. In order to remove these contributions so that the correlation coefficients represent non-tidal phenomena, we filtered the data using a low-pass boxcar filter with a length of 24 hours. The filtered current velocity series are thus expected to have variability in the frequencies ranging from 0.0014 cph to 0.042 cph (the lower value depends on the duration of simultaneous sampling, which is required to be at least 1 month, ~0.0014 cph).

For each array, the average variance spectra of all instruments (all depths, all moorings), before and after filtering, are shown in Appendix I and will be referred to when needed in our text.

3.3 Coordinate axes rotation

For some arrays, the currents had a dominant flow direction dictated, e.g., by local bathymetry or nearby coastlines. These directions were determined either by examining the original reports that displayed the data and/or by determining the principal axes of variance associated with individual records. The currents were rotated along and across the principal axes. The angles and descriptions are summarized in Table 3 and in Fig. 4 (Newfoundland Shelf) and Fig. 5 (Gulf of St. Lawrence).

**Table 2**. Proportion of total variance accounted for by the filtered series

| Array Name | # of records | Temperature Variance (%) | | | | Salinity Variance (%) | | | |
|---|---|---|---|---|---|---|---|---|---|
| | | Median | Min | Max | Std.Dev | Median | Min | Max | Std.Dev |
| Avalon | 23 | 27 | 2 | 57 | 13 | 28 | 7 | 70 | 23 |
| Flemish | 12 | 57 | 15 | 82 | 20 | 65 | 35 | 76 | 14 |
| CASP2 | 15 | 38 | 2 | 88 | 26 | 45 | 13 | 81 | 21 |
| SEShoal | 19 | 23 | 1 | 37 | 10 | 11 | 7 | 51 | 16 |
| Cabot | 46 | 37 | 1 | 99 | 25 | 49 | 2 | 87 | 18 |
| SLE | 25 | 39 | 6 | 71 | 15 | 38 | 8 | 79 | 19 |
| Central Gulf | 11 | 48 | 27 | 73 | 15 | 42 | 13 | 65 | 15 |
| Gaspé | 20 | 60 | 26 | 98 | 18 | 57 | 47 | 80 | 10 |
| JCP | 54 | 20 | 1 | 96 | 21 | 33 | 4 | 90 | 22 |
| Belleisle | 12 | 37 | 16 | 78 | 21 | 34 | 18 | 63 | 13 |

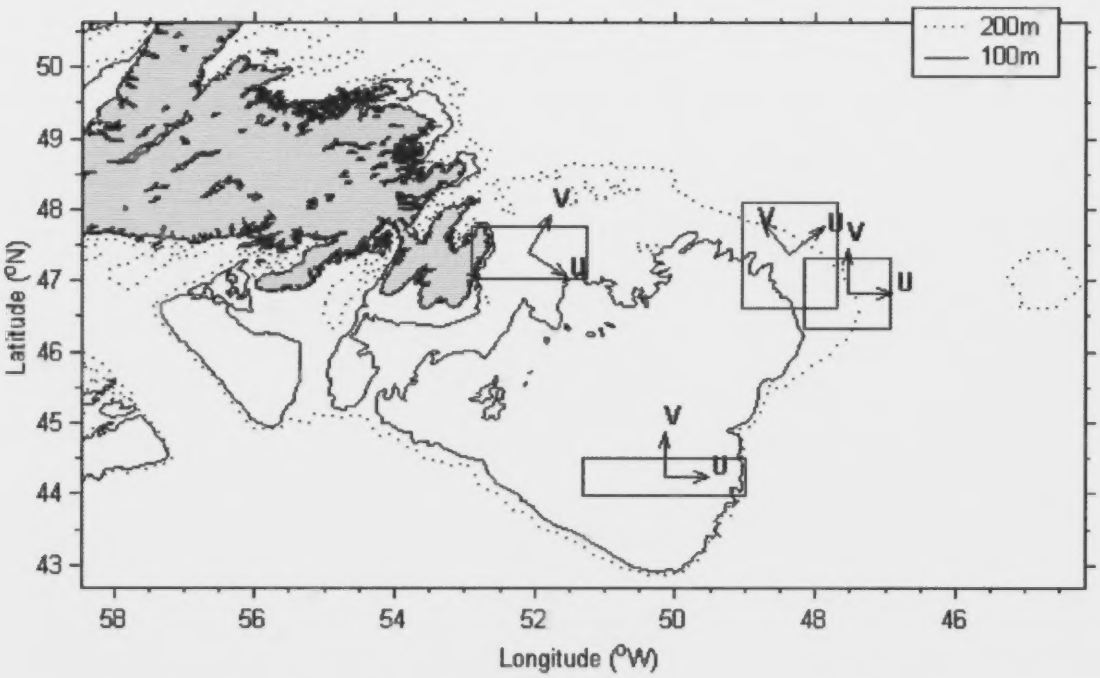


**Figure 4.** Newfoundland Shelf velocity decomposition axes

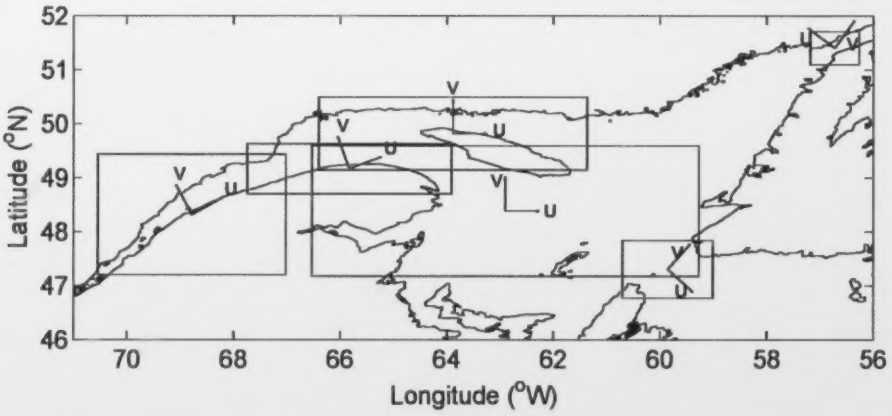


**Figure 5**. Gulf of St. Lawrence velocity decomposition axes

**Table 3.** Velocity coordinates. Angle is clockwise from true north.

| Dataset | U Angle (°T) | Name | V Angle (°T) | Name | Reason |
|---|---|---|---|---|---|
| Avalon | 120 | Across-Channel | 30 | Along-Channel | The inshore branch of Labrador Current flows along Avalon Channel and is strongly influenced by the coastline. |
| Flemish | 90 | Across-Pass | 0 | Along-Pass | Flemish Pass is roughly oriented north-south. The Labrador Current flows mainly along the bathymetric contours, with some intrusions onto the shelf. |
| CASP2 | 50 | Across-Shelf | 320 | Along-Shelf | The Labrador Current generally follows local bathymetry. |
| SEShoal | 90 | Across-Shelf | 0 | Along-Shelf | No strong local depth gradients. |
| Cabot | 132 | Across-Strait | 42 | Along-Strait | Strait orientation |
| SLE | 61 | Along-Estuary | 331 | Across-Estuary | Mean Estuary orientation |
| Central Gulf | 90 | East-west | 0 | North-south | No strong local depth gradients. |
| Gaspé | 70<br>136 | Along-shore<br>(mooring 318) | 340<br>46 | Across-shore<br>(mooring 318) | Gaspé Coast orientation, Gaspé Current flows along coast |
| JCP | 90 | Along-Passage | 0 | Across-Passage | No definite current direction, according to variance diagrams in Gregory et al. (1989) |
| BelleIsle | 306 | Across-Strait | 36 | Along-Strait | According to a current variance analysis conducted by Lively (1984) |

## 4.0 Analysis

The correlation scales given in the following paragraphs are summarized in Tables 4 and 5 (section 5).

### 4.1 Newfoundland Shelf and Grand Banks

#### *4.1.1 Avalon Channel Array*

This array (Fig. 6.1) consists of 4 moorings along a 80 km-long line across the Avalon Channel where the bottom depth ranges from 161 to 175 m. Three were deployed from June to October 1980, and the westernmost mooring (393) was maintained until April 1981. The time series plots, statistics, data recovery and accuracy are discussed by Petrie (1991). The correlation coefficients and estimated scales are shown on Fig. 6.2 to 6.4.

*4.1.1.1 Horizontal correlation across Avalon Channel*

Temperature correlation coefficients were estimated at two depths, while salinity and velocity coefficients could be estimated at only one depth. Coherence scales are all shorter than the shortest separation distance between instruments (22 km).

*4.1.1.2. Vertical correlation at Avalon array*

The availability of thermistor chain data provides sufficient data for an adequate resolution of the vertical scale of temperature, which is equal to 22 m. Salinity scales could not be resolved adequately, but an overall upper limit can be fixed at 25 m. Since only one winter pair was available, summer vs. winter comparisons are not possible. The velocity correlation coefficients computed between any two series that are at 54 m and deeper are higher than the rest, and suggest that the vertical current variations are small below that depth. For all series regardless of depth, the vertical scale of across-channel was 90 m, while the correlation scale of along-channel velocity could not be resolved and its lower limit was set to the maximal separation (100 m).

*4.1.1.3 Temporal auto-correlation at Avalon array*

The temperature and salinity correlation coefficients (Fig 6.4) fall quickly to values less than zero and then rise to reach a maximum at roughly 14 d. For periods greater than 14 d, the coefficients cluster tends towards zero, which is not unexpected since filtering has reduced the energy at longer periods. Exponential fits are not ideal to describe these variations. However, we derived two additional exponential curves to contain approximately the upper and lower limits of the correlation coefficients up to 5 d period, by fitting exponential curves to a series consisting of the maximum coefficients (upper limit) and to a series consisting of the minimum coefficients.

The coefficients at lags less than 1 d are high, even though the series were low-pass filtered at 1 d, because some inertial current energy remained after filtering. Exponential curves were fit to encompass most of the velocity coefficients for lags up to 20 d. The upper bound estimate of the scale of the across-channel component is greater (21 d) than that of the along-channel component (15 d).

The upper bound curve follows roughly the correlation coefficients of the shallowest instruments (25 and 30 m depth) at the westernmost mooring location (393).

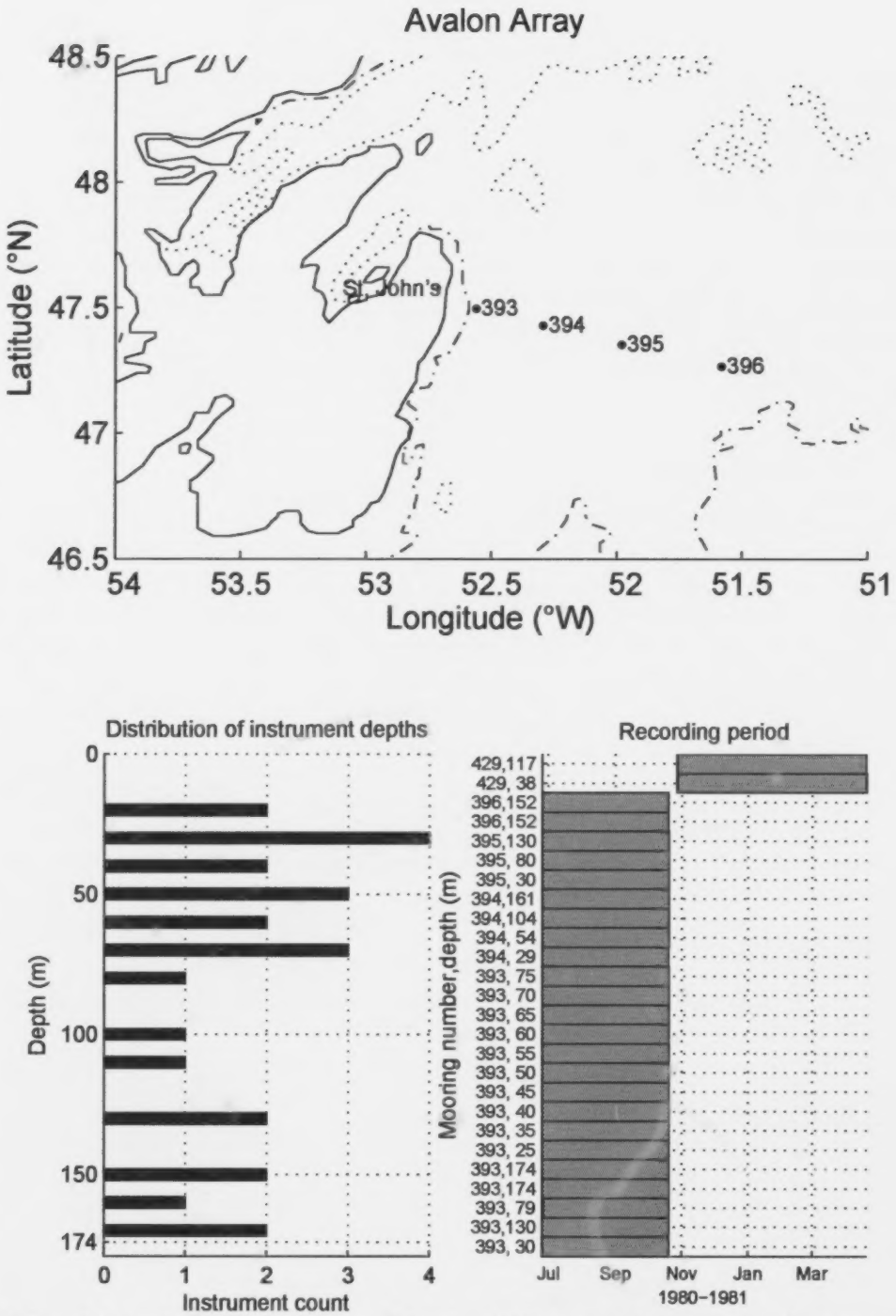


**Figure 6.1** Avalon Channel Array. Mooring 429 was at the same location as mooring 393.

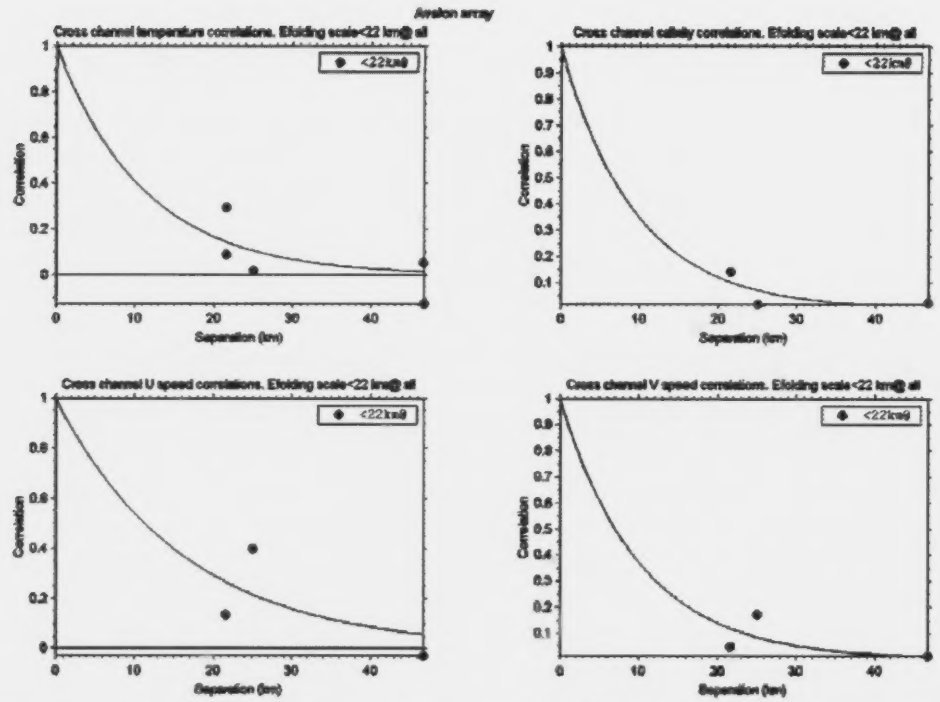
Avalon array
Cross channel temperature correlations. Efolding scale<22 km@ all
Cross channel salinity correlations. Efolding scale<22 km@ all
Cross channel U speed correlations. Efolding scale<22 km@ all
Cross channel V speed correlations. Efolding scale<22 km@ all
Correlation
Separation (km)

**Figure 6.2** Horizontal correlation across Avalon Channel for temperature, salinity, across-channel current (U), along-channel current (V).

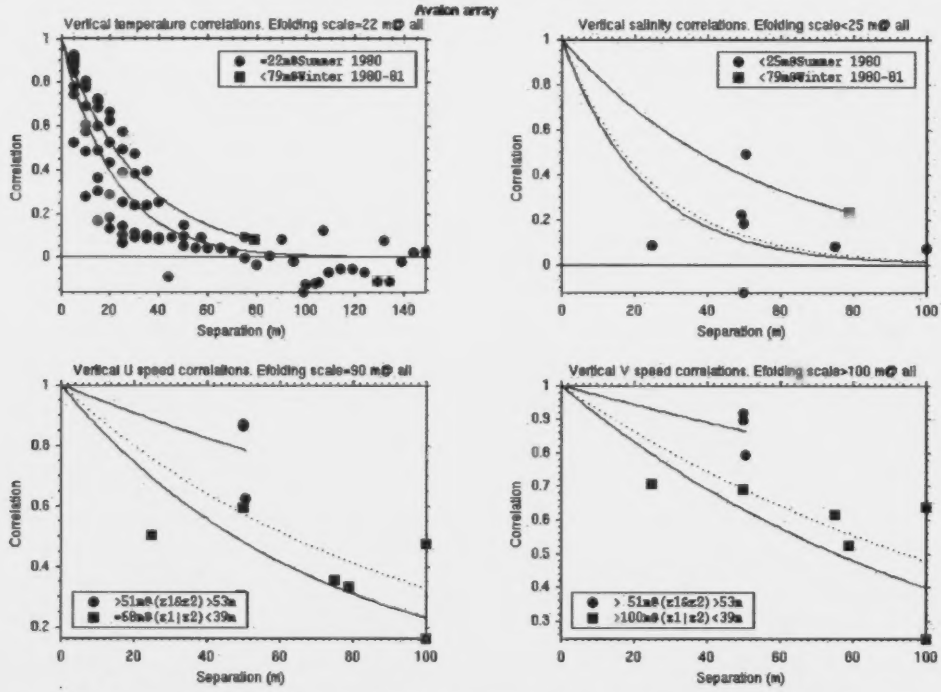


**Figure 6.3**. Vertical correlation at Avalon array for temperature, salinity, across-channel current (U), along-channel current (V). Dotted-line represents fit using all data.

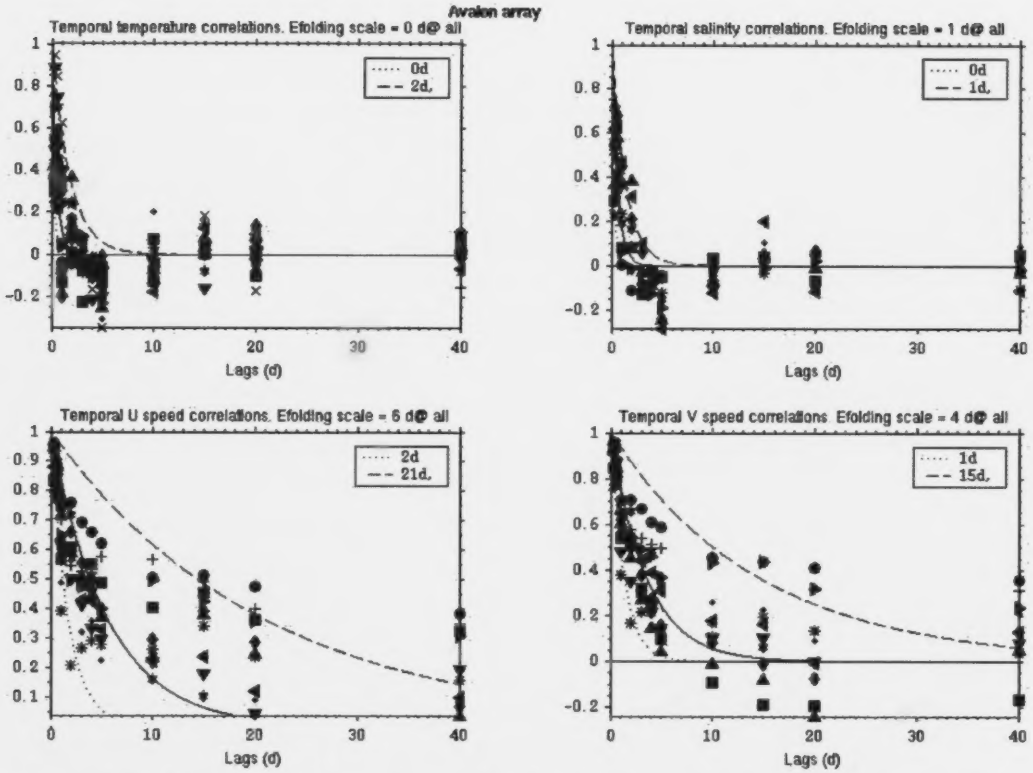


**Figure 6.4**. Temporal auto-correlation for the Avalon array for temperature, salinity, across-channel current (U), along channel current (V). Different symbols are used for different instruments. Solid line represents a fit of all the data.

4.1.2 Flemish Pass Array

This array (Fig. 6.1) consisted of 8 moorings deployed from October 1985 to February 1986 along two lines in a cross pattern, with one of its lines oriented along the 400 m isobath (roughly north-south), along Flemish Pass. The data are discussed in Lively and Petrie (1990). The results from our analyses are shown on Fig. 6.2 to 6.5.

*4.1.2.1. Horizontal correlation scales along Flemish Pass*

On average, the salinity scale could not be adequately resolved and was set to greater than 15 km, while temperature scale was estimated at 14 km (Fig. 6.2). The correlation coefficients of the along-pass component of velocity are very large. The associated correlation scale is greater than the largest separation of instruments (>15 km), while the correlation scale of the across-pass component could be resolved at 13 km on average.

*4.1.2.2 Horizontal correlation scales across Flemish Pass*

For this analysis, only one pair of instruments was available and were offset by 5 m (Fig. 6.3). None of the correlation scales could be resolved. The coefficients are shown for completeness. The correlation scales for temperature, salinity and across-pass velocity

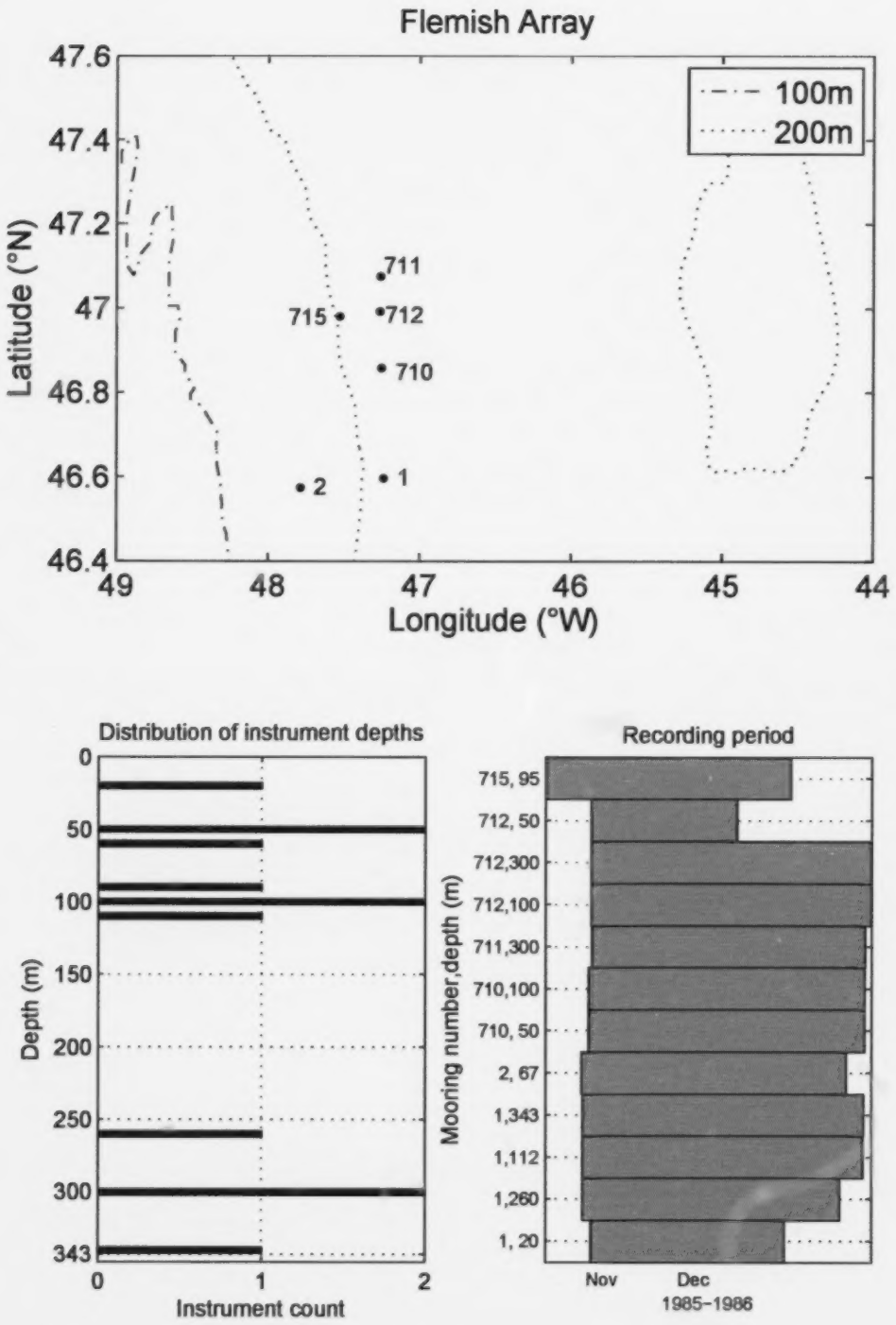


**Figure 7.1**. Flemish Pass Array

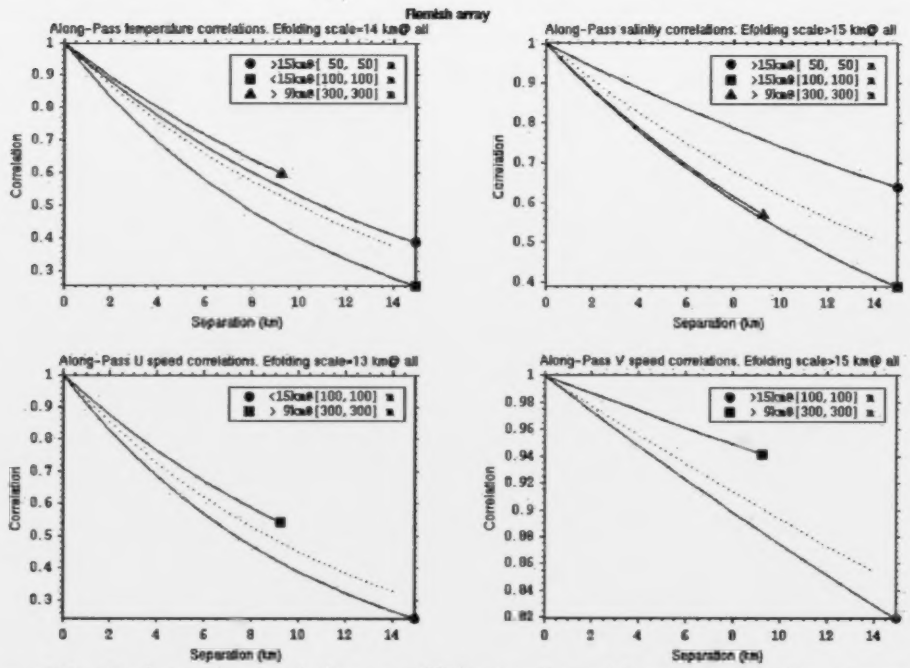


**Figure 7.2**. Horizontal correlation coefficients along Flemish Pass for temperature, salinity, across-pass current (U), along-pass current (V). Dotted-line represents a fit using all data.

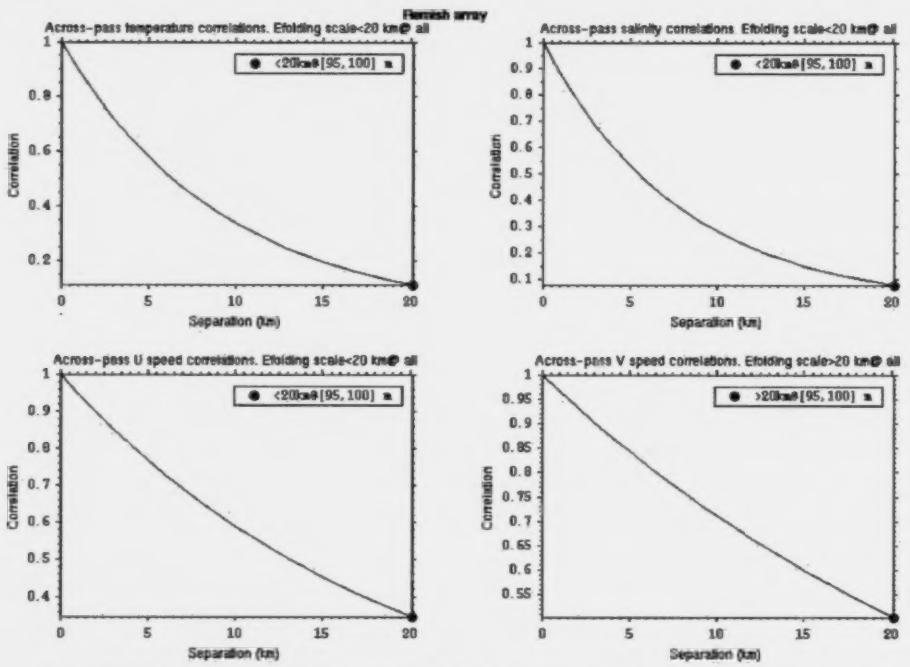


**Figure 7.3.** Horizontal correlation coefficients across Flemish Pass for temperature, salinity, across-pass current (U), along-pass current (V).

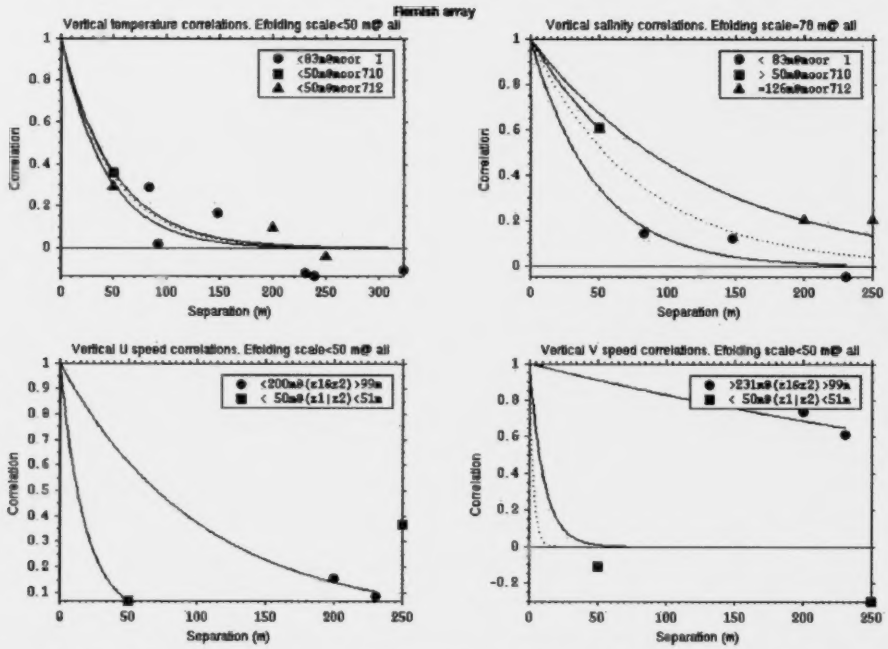
Flemish array
Vertical temperature correlations. Efolding scale<50 m@ all
Vertical salinity correlations. Efolding scale=78 m@ all
Vertical U speed correlations. Efolding scale<50 m@ all
Vertical V speed correlations. Efolding scale<50 m@ all
Correlation
Separation (m)

**Figure 7.4**. Vertical correlation coefficients at the Flemish Pass array for temperature, salinity, across-pass current (U), along-pass current (V). Dotted-line represents fit using all data.

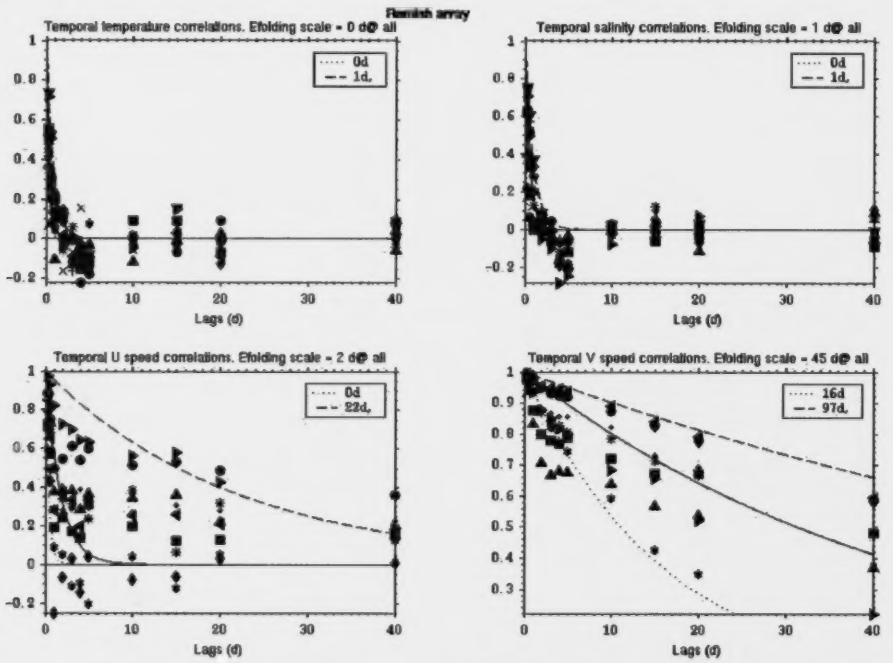
Flemish array
Temporal temperature correlations. Efolding scale = 0 d@ all
Temporal salinity correlations. Efolding scale = 1 d@ all
Temporal U speed correlations. Efolding scale = 2 d@ all
Temporal V speed correlations. Efolding scale = 45 d@ all
Lags (d)

**Figure 7.5.** Temporal auto-correlation coefficients for the Flemish Pass array for temperature, salinity, across-pass current (U), along-pass current (V). Different symbols are used for different instruments. Solid line represents a fit using all data.

are less than 20 km, while the along-pass velocity component shows a larger scale (>20 km).

*4.1.2.3 Vertical correlation scales at Flemish Pass array*

The average vertical temperature scale is less than 50 m, and also smaller than the average salinity scale, which is estimated to be 78 m (Fig. 7.4). The salinity scales increase progressively from mooring 1 to moorings 710 and 712, that is, northward along the 400 m isobath. It should be noted that fewer pairs were available for salinity and velocity than temperature, since some instruments returned good temperature data, but bad salinity and current direction data (Lively and Petrie, 1990). A surprisingly high correlation coefficient (0.8) of along-pass component of velocity is observed at a separation of 200 m. The series giving rise to this coefficient were from deeper than 100 m and the correlation coefficient of the across-pass component of velocity between same instruments is very low (0.15). The ratios of along-pass to across-pass current variances for these two time series are 5.4 (mooring 712 at 100 m) and 34.2 (mooring 712 at 300 m) indicating the dominance of the along-pass component. Furthermore, the across-pass velocity variances were low (17.6 and 4 $cm^2s^{-2}$), thus increasing the potential for low correlation coefficients (assuming the noise levels would be the same in both directions). Trying to evaluate the correlation scale above a depth of 100 m, by involving a series recorded at 50 m, yields a scale shorter than 50 m. On average, vertical correlation scales are shorter than 50 m.

*4.1.2.4 Temporal auto-correlation scales at Flemish Pass array*

Temperature and salinity scales are low (< 1d, Fig. 7.5). Correlation coefficients decrease substantially after a lag of 1 d. The "bump" at 15 d is an effect of high variance in low frequencies combined with high-pass filtering. Along-pass velocity correlation coefficients are bounded by an exponential curve of scales 16 and 97 d, while across-pass velocity scale is < 22 days.

4.1.3 CASP2 Array

This array (Figure 8.1) was deployed in a cross-pattern from December 1991 to May 1992, allowing for the determination of both across-shelf and along-shelf correlation coefficients. The data are discussed in Lively (1994). The data return was greatly affected by the collapsing of three (3) mooring lines and the failure of one current meter. Results from our analyses are presented on Fig. 8.2 to 8.5, making use of series from 14 instruments, of which only 11 had valid salinity and velocity data. Confidence in horizontal scales is small because of the limited number of pairs of series.

*4.1.3.1 Horizontal correlation scales across Newfoundland Shelf at CASP2 Array*

The temperature correlation scale was determined to be 19 km, while the salinity correlation scale was estimated to be shorter than 52 km (Fig. 8.2). The correlation scales of both velocity components could be resolved and are similar (52 and 53 km).

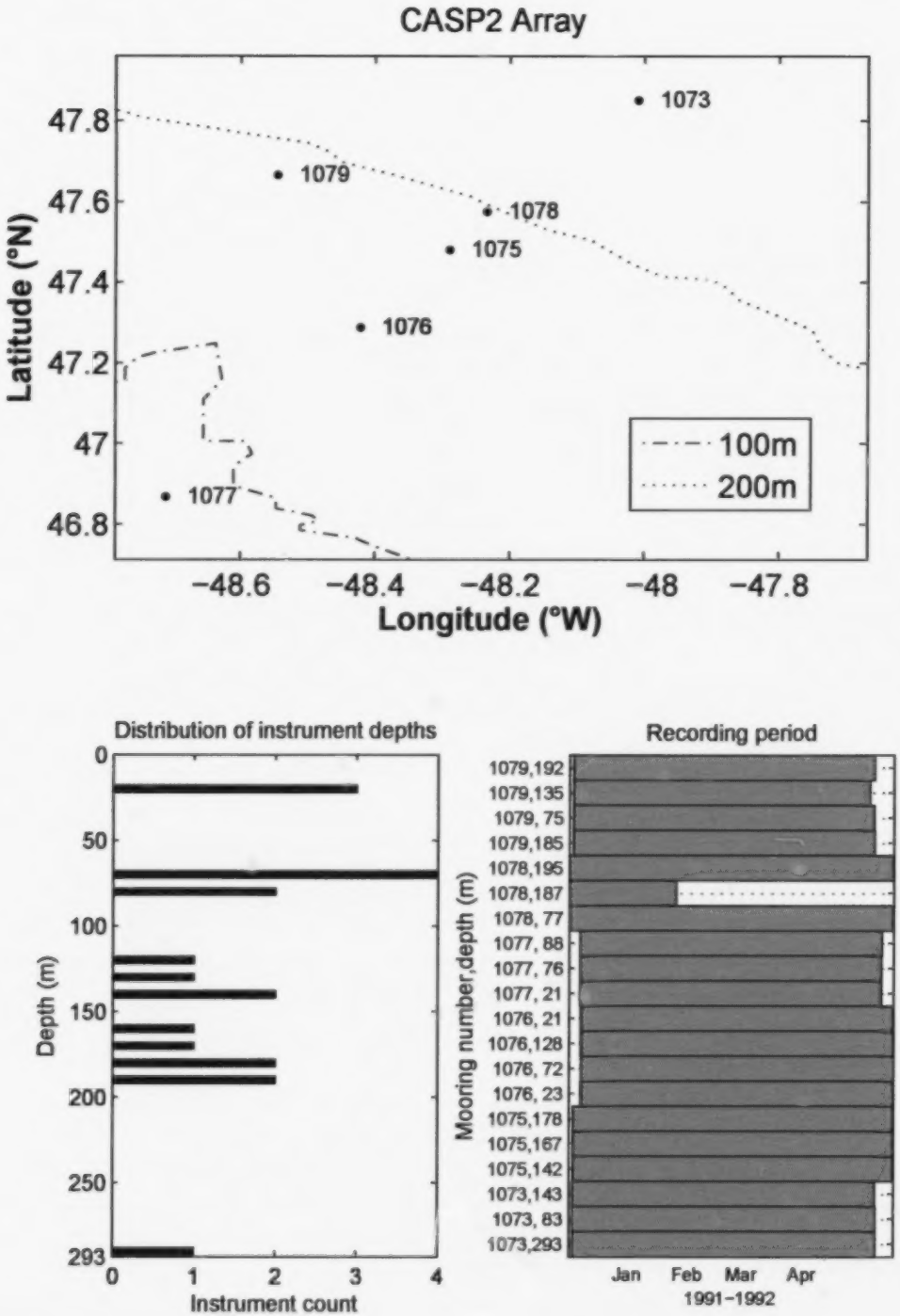


**Figure 8.1.** CASP2 Array.

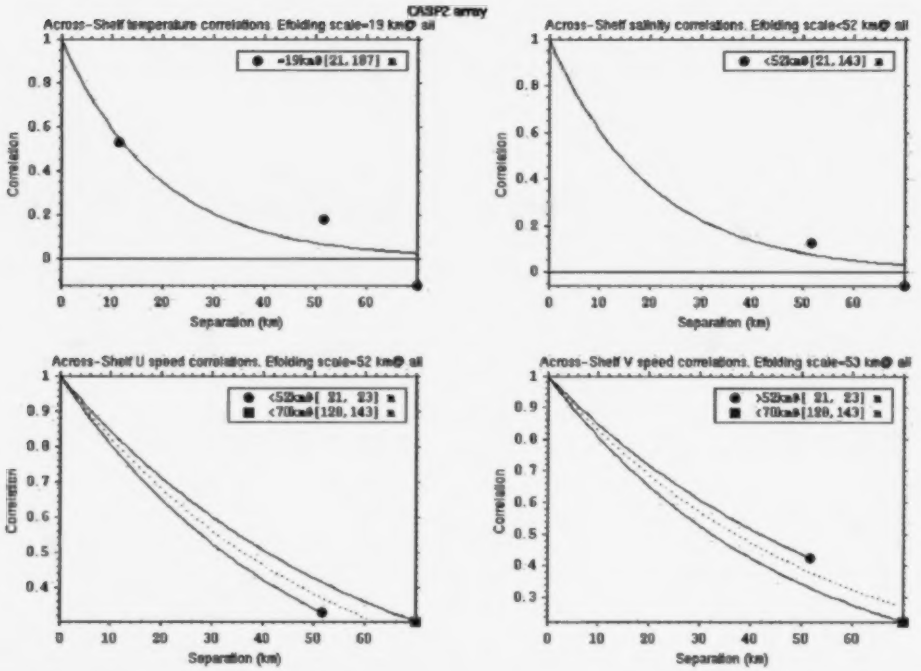
CASP2 array
Across-Shelf temperature correlations. Efolding scale=19 km@ all
Across-Shelf salinity correlations. Efolding scale<52 km@ all
Across-Shelf U speed correlations. Efolding scale=52 km@ all
Across-Shelf V speed correlations. Efolding scale=53 km@ all
Correlation
Separation (km)

**Figure 8.2**. Horizontal correlation coefficients across Newfoundland Shelf from the CASP2 array for temperature, salinity, across-shelf current (U), along-shelf current (V). Dotted-line represents fit using all data.

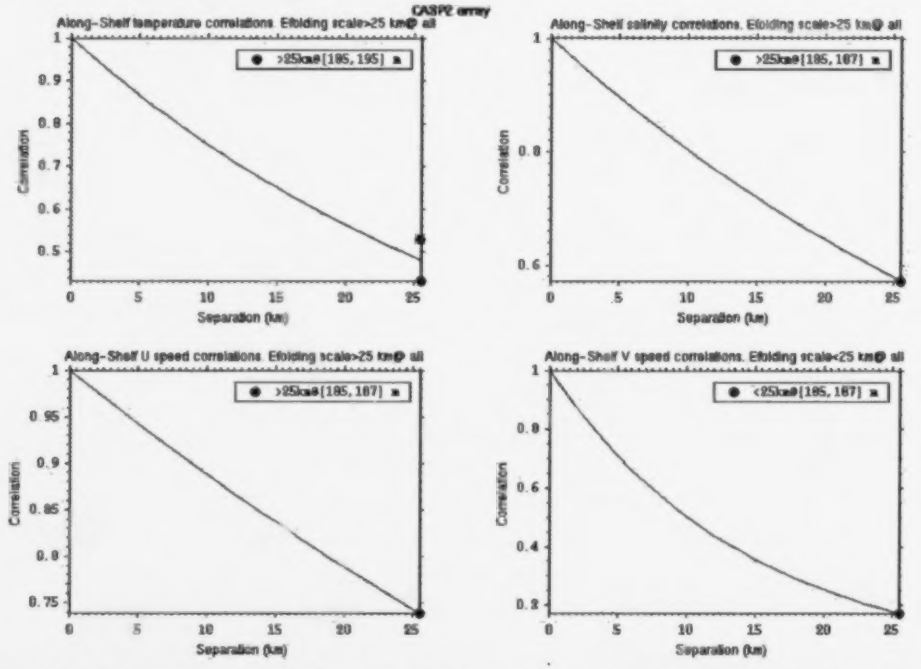
CASP2 array
Along-Shelf temperature correlations. Efolding scale>25 km@ all
Along-Shelf salinity correlations. Efolding scale>25 km@ all
Along-Shelf U speed correlations. Efolding scale>25 km@ all
Along-Shelf V speed correlations. Efolding scale<25 km@ all
Correlation
Separation (km)

**Figure 8.3.** Horizontal correlation coefficients along Newfoundland Shelf at CASP2 array for temperature, salinity, across shelf-current (U), along-shelf current (V).

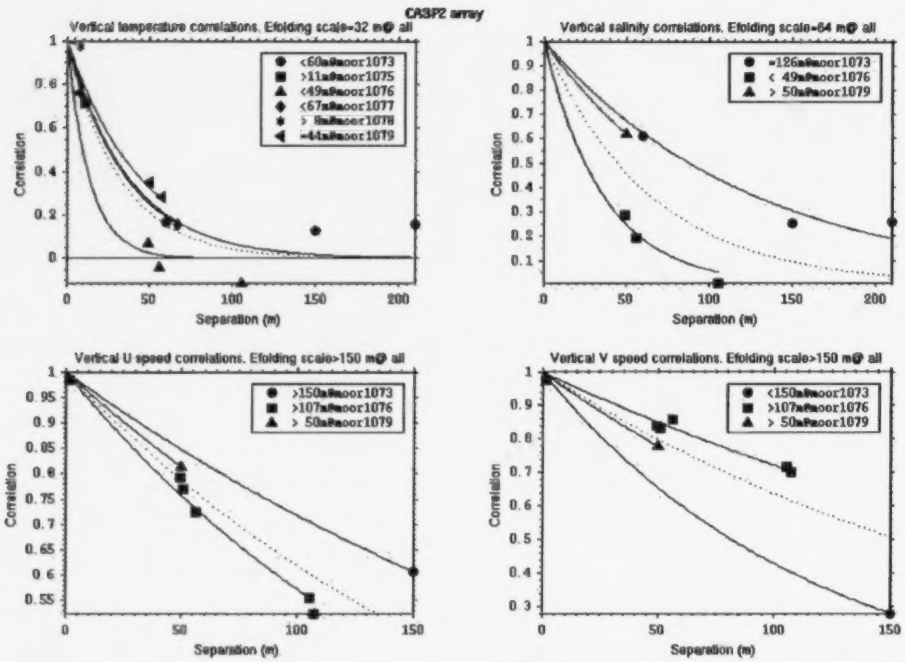
CASP2 array
Vertical temperature correlations. Efolding scale=32 m@ all
Vertical salinity correlations. Efolding scale=64 m@ all
Vertical U speed correlations. Efolding scale>150 m@ all
Vertical V speed correlations. Efolding scale>150 m@ all
Correlation
Separation (m)

**Figure 8.4**. Vertical correlation coefficients at CASP2 array for temperature, salinity, across-shelf current (U), along-shelf current (V). Dotted-line represents fit using all data.

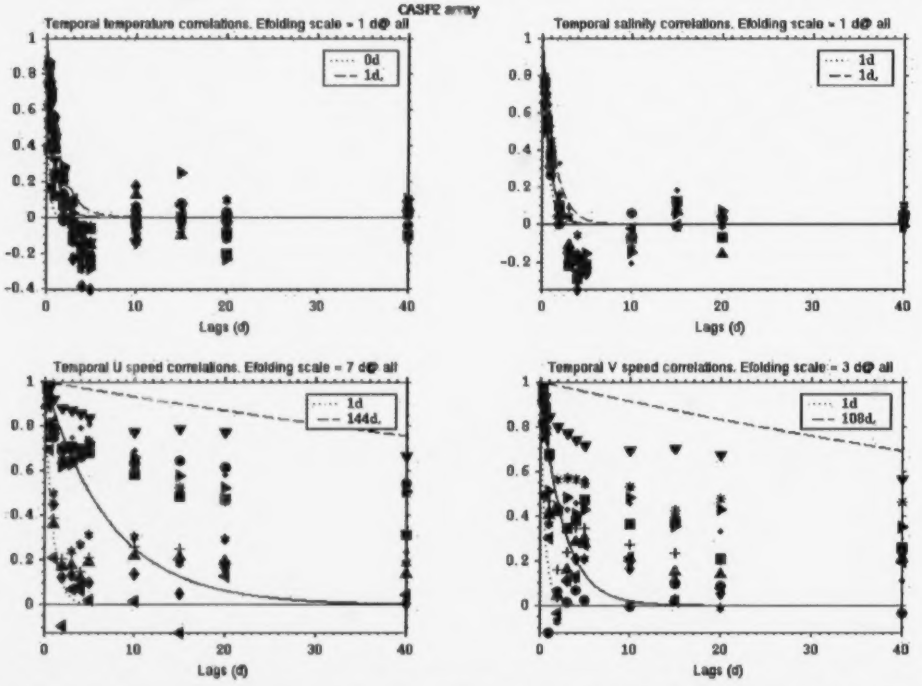
CASP2 array
Temporal temperature correlations. Efolding scale = 1 d@ all
Temporal salinity correlations. Efolding scale = 1 d@ all
Temporal U speed correlations. Efolding scale = 7 d@ all
Temporal V speed correlations. Efolding scale = 3 d@ all
Lags (d)

**Figure 8.5.** Temporal auto-correlation coefficients at the CASP2 array for temperature, salinity, across-shelf current (U), along-shelf current (V). Different symbols are used for different instruments. Solid line represents a fit using all data.

*4.1.3.2 Horizontal correlation scales along Newfoundland Shelf and slope at CASP2 Array*
Only one pair of time series was available to calculate correlation coefficients, so any derived scales are very uncertain. Temperature and salinity correlation scales are estimated to be longer than 25 km (Fig. 8.3). At a separation of 25 km, the correlation coefficient of the across-shelf component of velocity is much higher (0.7) than that of the along-shelf component (0.2). The results indicate that the correlation scale of the across-shelf component is likely greater than 25 km, while that of the along-shelf component is less than 25 km.

*4.1.3.3 Vertical correlation scales at CASP2 array*
On average, vertical temperature correlation scale (32 m) is shorter than the salinity correlation scale (64 m, Fig. 8.4). The lone pair recorded at mooring 1078, located on the 200 m isobath, have very high temperature correlation coefficient, but they were short records (55 days), going from December to January only, while other series end in May. The salinity scale at mooring 1073 is higher (126 m) than that of temperature at same mooring (less than 60 m). At mooring 1073, the across-shelf velocity correlation scale (greater than 150 m) is greater than that of along-shelf component (less than 150 m) and is the most notable difference between the correlation scales of these components among all moorings. Average velocity correlation scales are estimated to be greater than 150 m.

*4.1.3.4 Temporal auto-correlation scales at CASP2 array*
Temperature and salinity auto-correlation functions approach zero after about 2.5 days (Fig. 8.5). Low frequency variance from 10 d to 15 d causes correlations to increase with some coefficients reaching ~0.2. The filter cuts off any high temperature and salinity variability at lags greater than 15 days. Velocity scales are broadly distributed between scales ranging from 1 to 144 d; the average scale for the across-shelf velocity is 7 d, while that of the along-shelf velocity is 3 d. For both components, the largest temporal scale occurs at a depth of 143 m (mooring 1073).

4.1.4 Southeast Shoal Array
Time series from 1986 and 1987 were available from this array, which was located on the Grand Bank, shallower than previously discussed arrays (Fig. 9.1). Most of the 1986 series start in April and end in October, but some end in early August. Most of the 1987 series extend from May to October, but one ends in July. Moorings with numbers in the 700s indicate 1986 sites, while moorings with numbers in the 800s indicate 1987 sites. The data are discussed in Ross, Loder and Graca (1988). Results from our analyses are shown in Fig. 8.2 to 8.5.

*4.1.4.1 Horizontal correlation scales along the East-West axis for the Southeast Shoal array*
The correlation coefficients computed at 12 m are from series ending in July, while the coefficients computed at 45 m are from series ending in October. The correlation scale of the 12 m temperature series is longer (94 km) than the one for the series at 45 m (<61 km, Fig. 8.2). This analysis cannot reveal whether this is due to depth of instruments relative to the mixed layer, and/or seasonal differences. Salinity scales could not be resolved

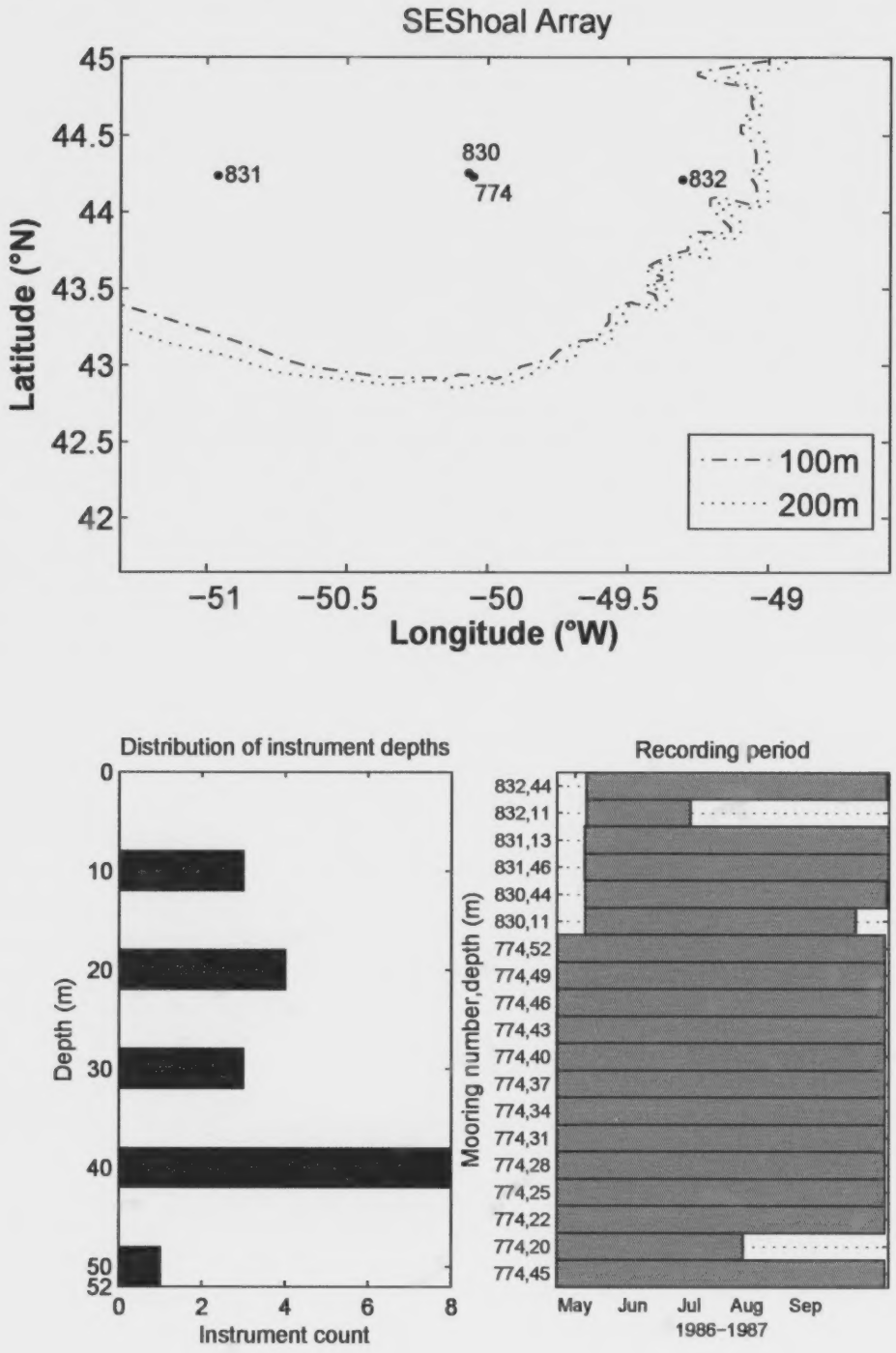


**Figure 9.1**. Southeast Shoal Array.

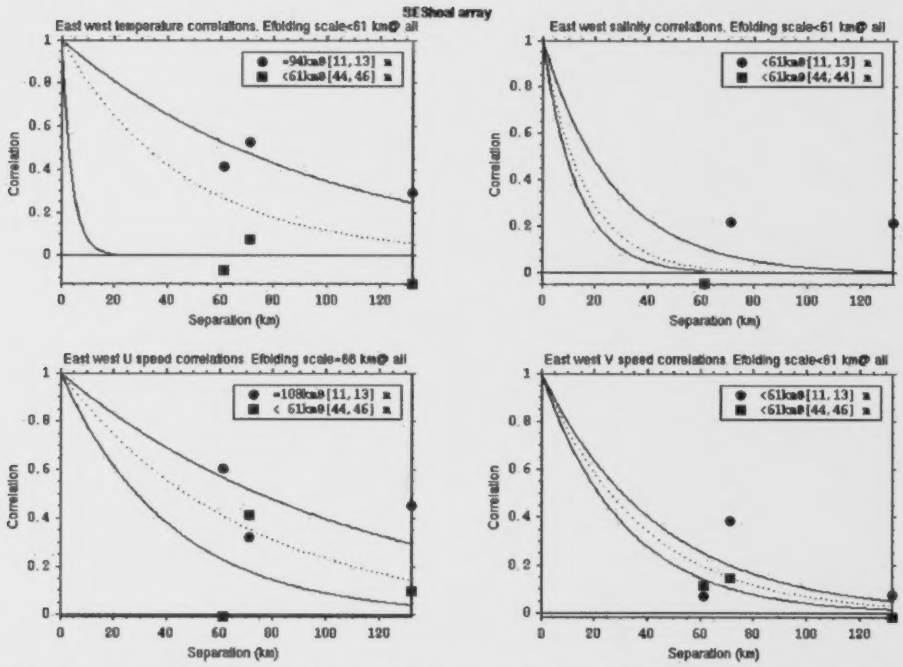


**Figure 9.2**. Horizontal correlation coefficients along the east-west axis for the Southeast Shoal array for temperature, salinity, across-shelf current (U), along-shelf current (V). Dotted-line represents fit using all data.

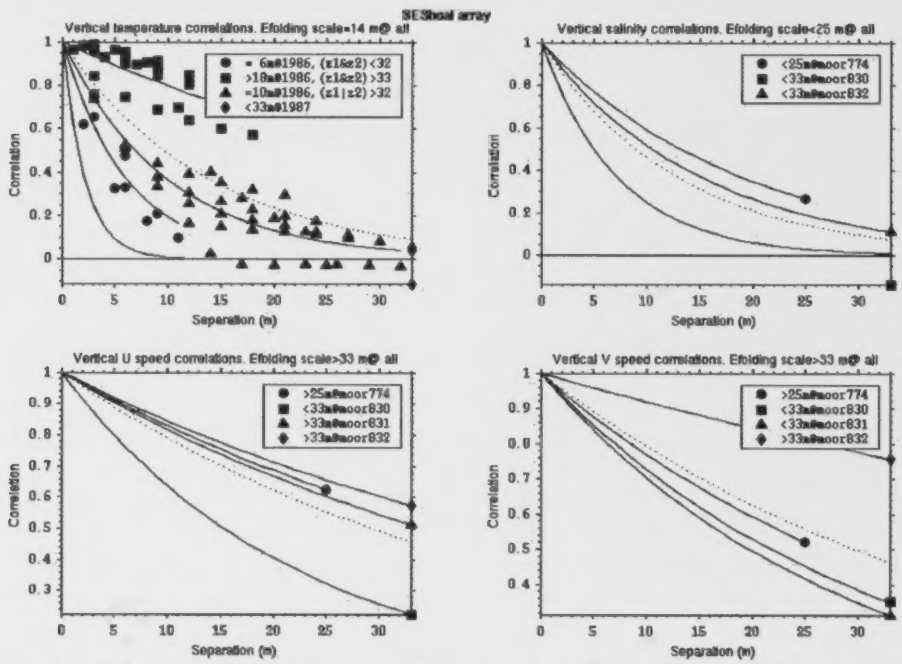


**Figure 9.3.** Vertical correlation coefficients for the Southeast Shoal array for temperature, salinity, across-shelf current (U), along-shelf current (V). Dotted-line represents fit using all data.

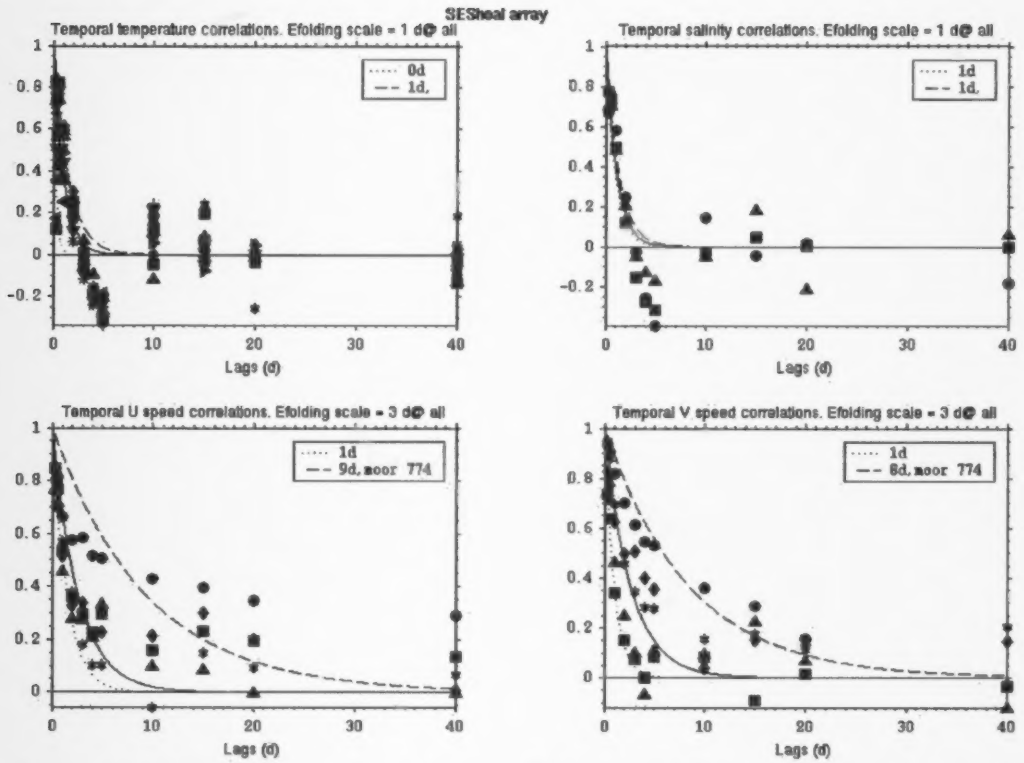


**Figure 9.4.** Temporal auto-correlation coefficients at the Southeast Shoal array for temperature, salinity, across-shelf current (U), along-shelf current (V). Different symbols are used for different instruments.

because all of the correlation coefficients are less than $e^{-1}$; the available values indicate that an upper limit would be <61 km. Both temperature and salinity average correlation scales are <61 km. At a depth of 12 m, the correlation scale of the across-shelf component velocity was 108 km, while that of the along-shelf component was estimated to be <61 km. On average, the across-shelf velocity correlation scale is higher (68 km on average) than the along-shelf velocity scale (~35 km).

*4.1.4.2 Vertical correlation scales for the Southeast Shoal Array*

Among instruments at mooring 774 (a thermistor chain plus a current meter moored in 1986), the distribution of correlation coefficients with separation depends on the depth range of instruments used. The coefficients at this mooring were separated in three groups: 1) pairs with both instruments with depths ≤ 31 m; 2) pairs with both instruments with depths ≥ 33 m ; and, 3) pairs with one instrument shallower than 32 m and one deeper than 32 m. The correlation coefficients between series ≥33 m are all 0.6 or greater, yielding a correlation scale of 44 m, which exceeds the maximum separation, 18 m, for this group (Fig. 9.3). The coefficients from series in the layer shallower than 32 m have a scale of 10 m. Finally, the coefficients from series with one instrument < and one >32 m have the smallest scale (6 m). Among the moorings from 1987 (three pairs), the

correlation scale could not be adequately resolved because it appears shorter than the minimum separation of instruments (33 m). The 1987 points fit within the range of the correlation coefficients from 1986. All salinity correlation coefficients were less than $e^{-1}$ and the minimum separation between instruments was 25 m. Consequently an estimate of the vertical scale is ≤25 m. Both scales of velocity could not be resolved adequately; both are estimated as 42 m for all of the data, which is greater than 33 m, the largest separation of any pair.

*4.1.4.3 Temporal auto-correlation scales for the Southeast Shoal Array*

Both temperature and salinity auto-correlation coefficients are weak at lags from 3 to 10 d (Fig. 9.4). Variance at low frequencies is visible from the increased correlation coefficients at lags of 10 and 15 d. Scales of both components of velocity are similar to one another (3 d). The variance spectra (Appendix I) indicate that the current is dominated by semi-diurnal tide (~5 cm $s^{-1}$ amplitude) and inertial oscillations (period 17.7h, amplitude of ~3 cm $s^{-1}$). Some of that energy remains after the filtering and is responsible for the high correlation of velocity at lags shorter than 1 d. The only 1986 mooring, 774, marks the upper bound of correlation coefficients. Its temporal correlation scales (8 and 9 d) are higher than moorings from year 1987 (on average, 3 d).

## 4.2 Gulf of St. Lawrence and St. Lawrence Estuary

### *4.2.1 Cabot Strait Array*

This array consists of a number of moorings deployed across Cabot Strait (Figure 10.1) for varying periods in different years (1967, 1993 and 1996). Horizontal spacings varied from O(1 km) on the western side of Cabot Strait to O(10 km) in the deep portion, i.e., Laurentian Channel (from 60°W to 59.81°W and from 59.7°W to 59.6°W). Results from our analyses are presented on Fig. 10.2 to 10.5.

#### *4.2.1.1 Horizontal correlation scales across Cabot Strait*

Data sets from 1993 to 1996 alone were used for this analysis because the overlap of observations from 1967 was insufficient (< 1 month). Series were separated according to the duration of simultaneous records. Temperature and salinity correlation coefficients lie in what is likely a "noise" band (i.e. not significantly different from 0) between -0.2 and 0.2 beyond 20 km (Fig. 10.2). The average scales are 9 km for temperature, 6 km for salinity, 11 km and 14 km for the across-strait and along-strait components of velocity respectively.

#### *4.2.1.2 Vertical correlation scales at Cabot Strait*

The vertical scales were computed for ensembles consisting of moorings 1 to 4, mooring 8 (center of the Strait) and moorings 10 to 12 (Fig. 10.3). On average, the salinity scale (36 m) is greater than temperature scale (23 m). The salinity correlation scales in the center of the Strait (mooring 8, <35 m) than at the extremities (36 m and 39 m) are not statistically different. On the other hand, velocity scales are larger (>222 m) at the center mooring (8) than at the extremities (<100 m). A pattern of negative correlation coefficients is found at the easternmost moorings (10 and 11) at separations from 200 to 350 m, suggesting a reversal in the vertical current structure. Scales of both velocity components are quite similar (89 m and 81 m for across-strait and along-strait respectively).

#### *4.2.1.3 Temporal auto-correlation scales at Cabot Strait*

The auto-correlation coefficients of temperature and salinity (Fig. 10.4) show increased correlation coefficients at lags shorter than one (1) day, then weaker correlation coefficients at 10, 15 and 20 days. The raw series (see spectra in Appendix I) in fact contain a lot of variance at diurnal and semi-diurnal periods (tides) and periods of 10 days and longer. Velocity correlation coefficients have a wide range which on average is 10 d for the across-strait component and 4 d for along-strait component. The series at 15 m at mooring 6 has the largest velocity correlation scales for both components (75 and 60 d).

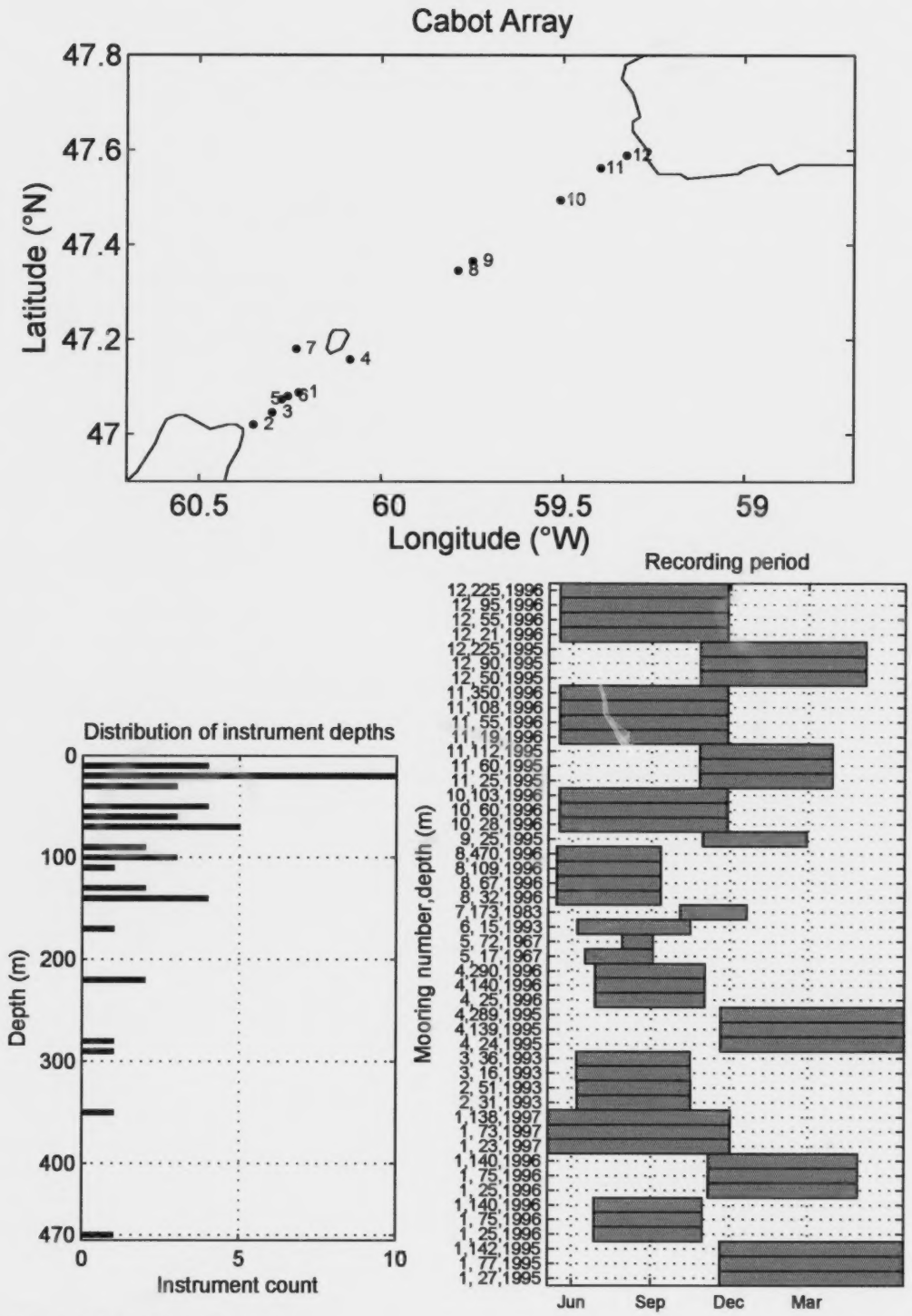


**Figure 10.1.** Cabot Strait Array.

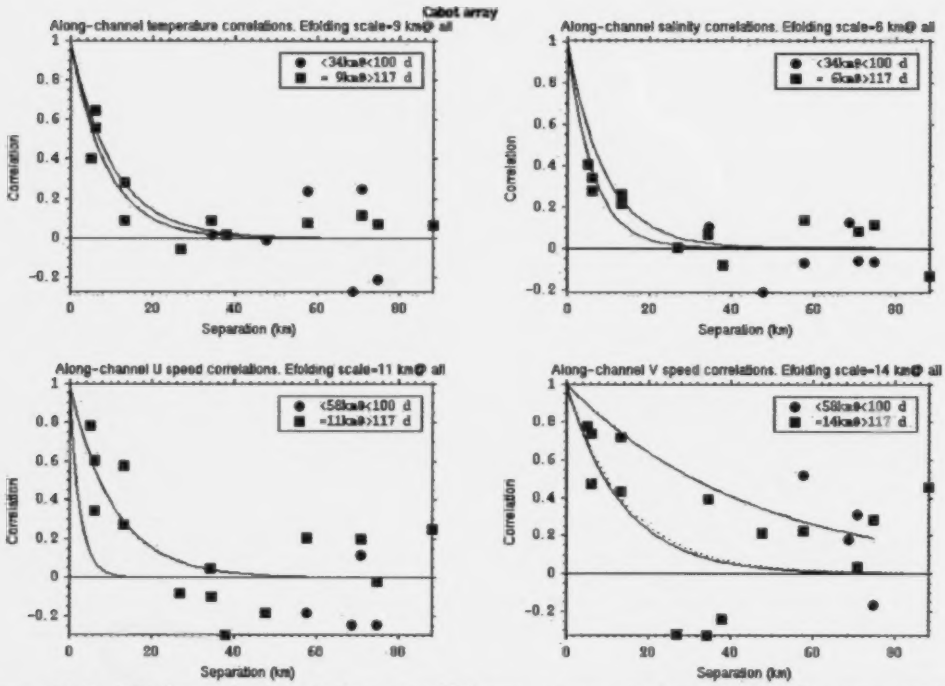
Cabot array
Along-channel temperature correlations. Efolding scale=9 km@ all
Along-channel salinity correlations. Efolding scale=6 km@ all
Along-channel U speed correlations. Efolding scale=11 km@ all
Along-channel V speed correlations. Efolding scale=14 km@ all
Correlation
Separation (km)

**Figure 10.2.** Horizontal correlation coefficients across Cabot Strait for temperature, salinity, across- strait current (U), along-strait current (V).

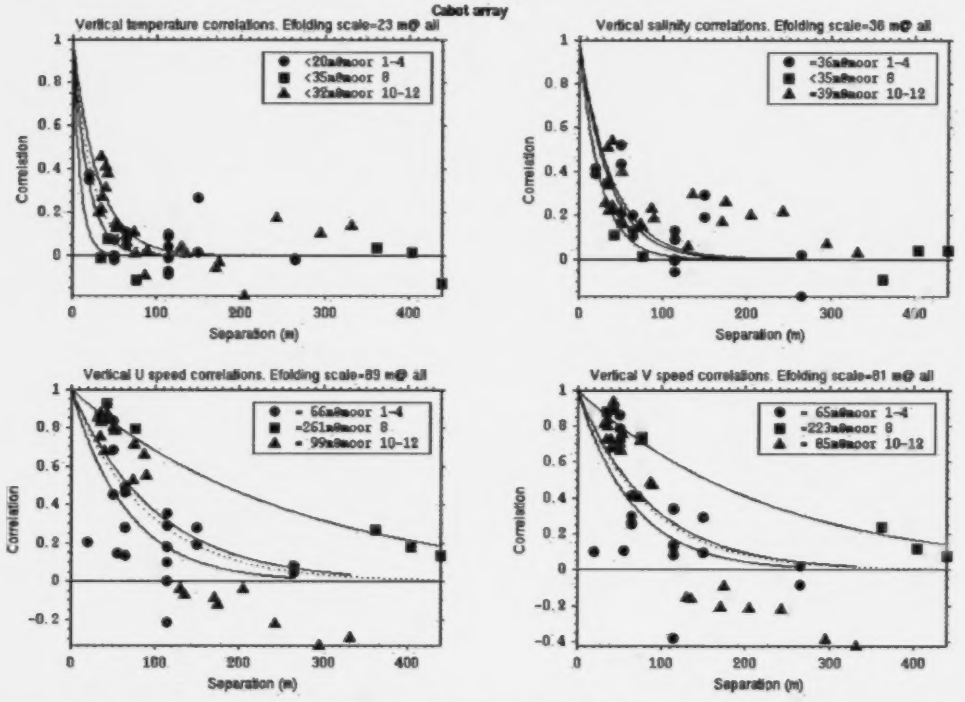
Cabot array
Vertical temperature correlations. Efolding scale=23 m@ all
Vertical salinity correlations. Efolding scale=36 m@ all
Vertical U speed correlations. Efolding scale=89 m@ all
Vertical V speed correlations. Efolding scale=81 m@ all
Correlation
Separation (m)

**Figure 10.3.** Vertical correlation coefficients at Cabot Strait for temperature, salinity, across-strait current (U), along-strait current (V). Dotted-line represents fit using all data.

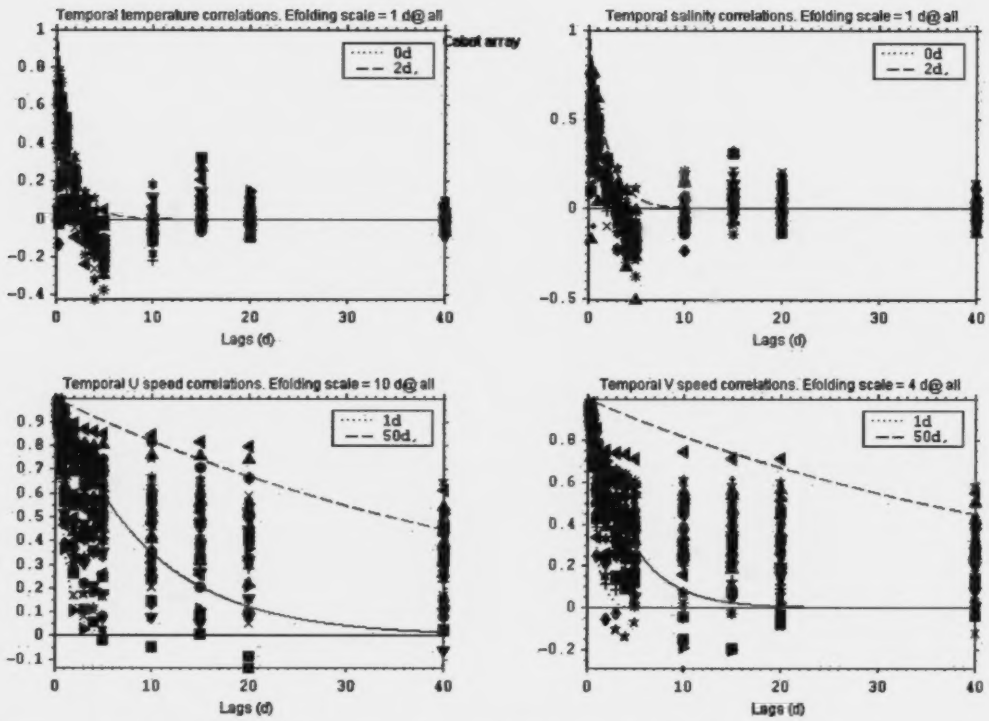


**Figure 10.4.** Temporal auto-correlation coefficients for Cabot Strait for temperature, salinity, across- strait current (U), along-strait current (V). Different symbols are used for different instruments. Solid line represents a fit using all data.

4.2.2 St. Lawrence Estuary Array

Data from 1979 and 1982 summers were used. In the along-estuary direction (Figure 11.1), series were divided in three lines labeled as: southernmost, mid-estuary and northernmost, but only one pair of simultaneous series per line was available. In the cross-estuary direction, two simultaneous pairs along a line at Matane were available. Results are presented on Fig. 11.2 through 11.5.

*4.2.2.1 Horizontal correlation scales across St. Lawrence Estuary*

At all depths sampled, correlation coefficients are low and negative (Fig. 11.2). The horizontal distances between instruments (15 km and more) are thus, in all cases, greater than all fitted e-folding scales. Negative correlation coefficients of the across-estuary velocity are observed along the Matane line, near the Estuary-Gulf boundary where wind-driven transverse currents are presumably known to influence the strength of the eddy found between Pointe-des-Monts and Rimouski (El-Sabh, 1979, Mertz et al., 1988). Since all correlation coefficients are negative, the e-folding scales were set to less than the distance of separation between instruments, i.e., <15 km. They must be interpreted as upper limits (hence the "lesser than" inequality sign in the legend boxes). The curves are shown for completeness, they too must be interpreted as upper limits since they were derived by positing that the correlation coefficient at the shortest separation distance was equal to zero.

*4.2.2.2 Horizontal correlation scales along the St. Lawrence Estuary*

Only one pair of series was available for each line, and the instruments were at depths 8 to 20 m (Fig. 11.3). The correlation coefficients are either small or negative, showing that the e-folding scale is shorter than the separation between instruments (46 km). The exponential curves are shown for completeness, but the results are not statistically significant.

*4.2.2.3 Vertical correlation scales in the St. Lawrence Estuary*

Coefficients involving upper instruments have temperature and salinity correlation scales of 27 m and 29 m (Fig. 11.4). One temperature and salinity correlation coefficient is the result of two series below 100 m depth. This coefficient was calculated between two instruments at mooring 12, located at the deepest point of the array in mid-Estuary, and yields a correlation scale larger than 150 m. This suggests that the temperature and salinity variability structure is more coherent below 100 m than above (unfortunately, no other simultaneous pair of instruments below 100 m was available to compare at other horizontal positions). Along-estuary velocity correlation coefficients give a scale of 10 m, except for the ones calculated at mooring 12 (mid-estuary where the correlation scale is much higher: 100 m). Across-estuary velocity correlation coefficients yield an average scale of 82 m. The difference between the across-estuary scales at mooring 12 (85 m) and the scales at other moorings (78 m on average) is not as important as in the along-estuary direction.

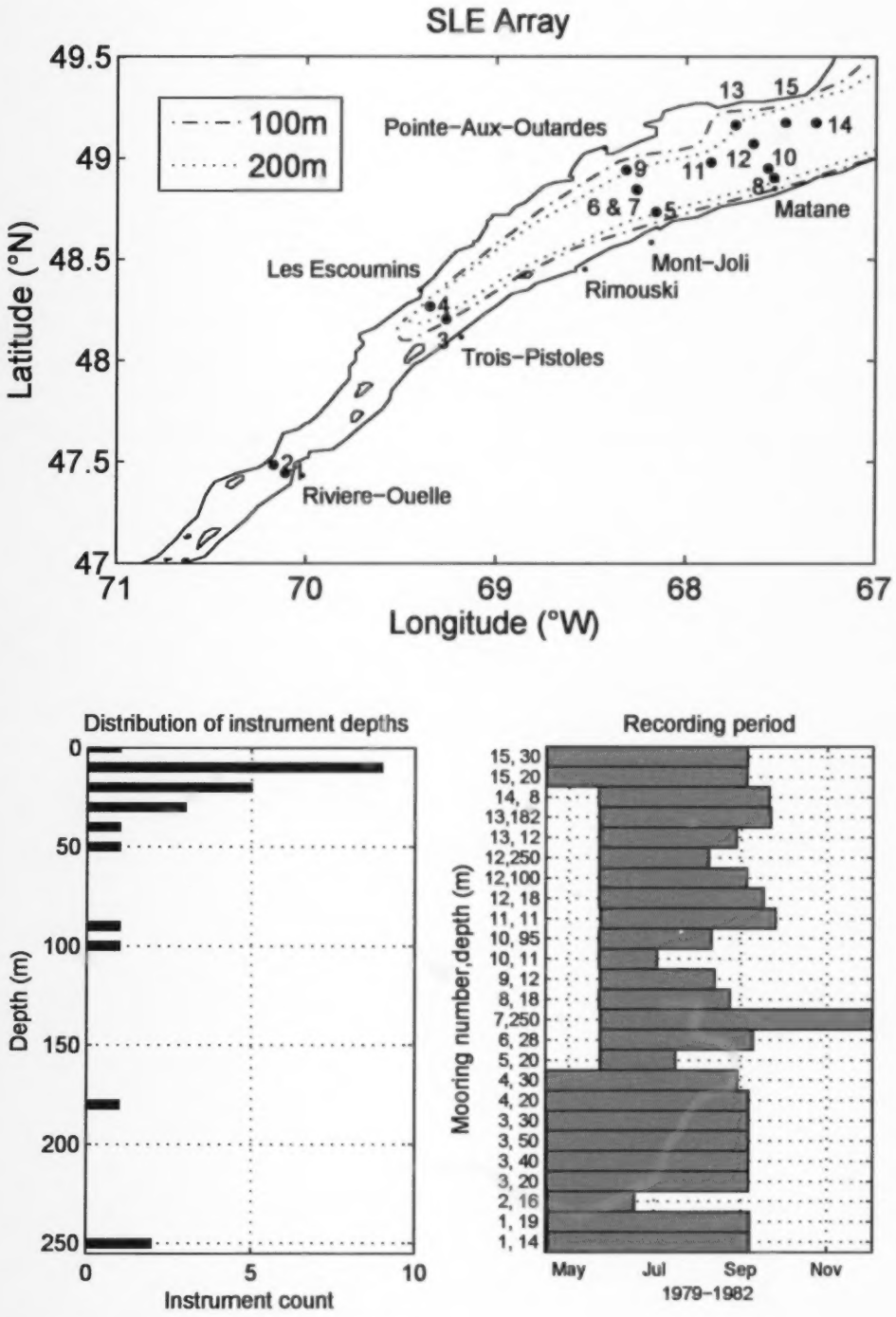


**Figure 11.1.** St. Lawrence Estuary array.

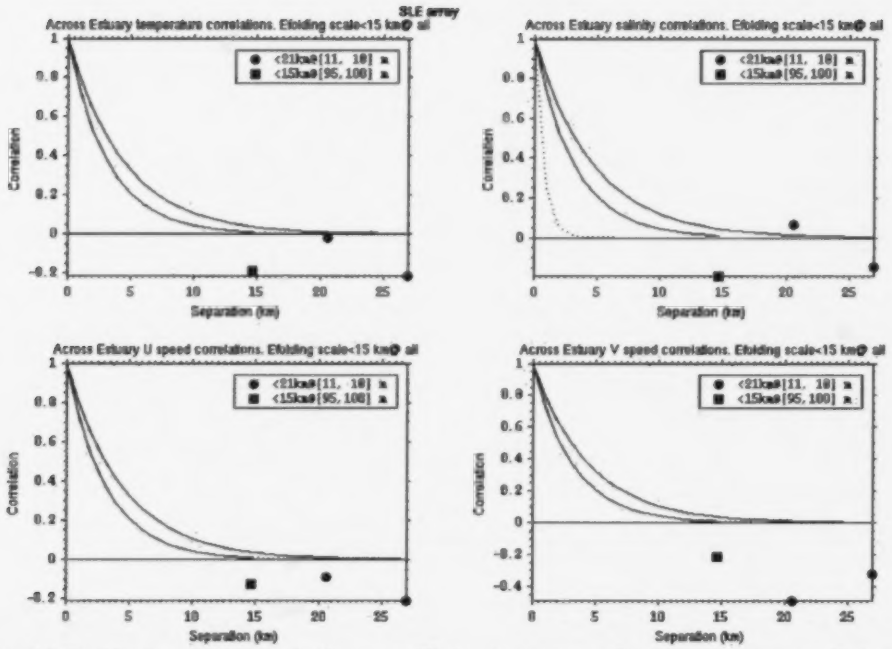
SLE array
Across Estuary temperature correlations. Efolding scale<15 km@ all
Across Estuary salinity correlations. Efolding scale<15 km@ all
Across Estuary U speed correlations. Efolding scale<15 km@ all
Across Estuary V speed correlations. Efolding scale<15 km@ all
Correlation
Separation (km)

**Figure 11.2**. Horizontal correlation coefficients across the St. Lawrence Estuary for temperature, salinity, along-estuary current (U), across-estuary current (V). Dotted-line represents fit using all data.

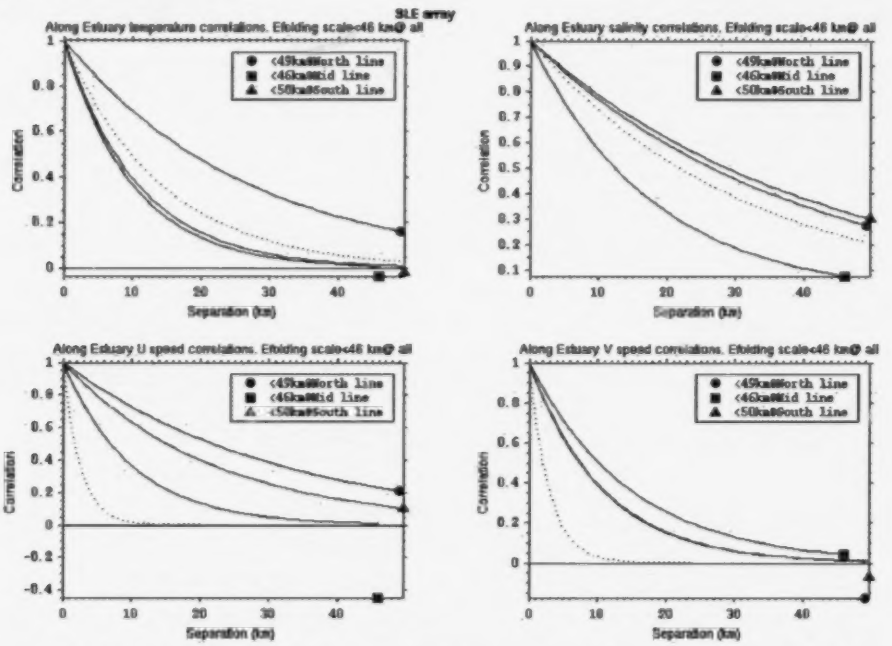
SLE array
Along Estuary temperature correlations. Efolding scale<46 km@ all
Along Estuary salinity correlations. Efolding scale<46 km@ all
Along Estuary U speed correlations. Efolding scale<46 km@ all
Along Estuary V speed correlations. Efolding scale<46 km@ all
Correlation
Separation (km)

**Figure 11.3.** Horizontal correlation coefficients along the St. Lawrence Estuary for temperature, salinity, along-estuary current (U), across-estuary current (V). Dotted-line represents fit using all data.

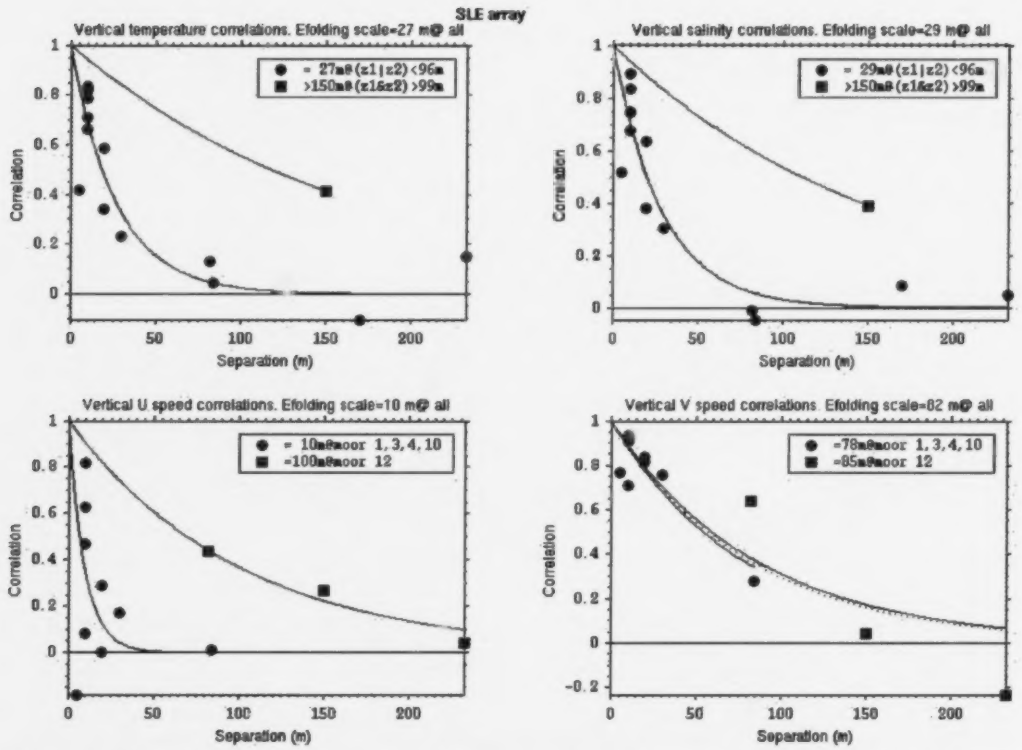
SLE array
Vertical temperature correlations. Efolding scale=27 m@ all
Vertical salinity correlations. Efolding scale=29 m@ all
Vertical U speed correlations. Efolding scale=10 m@ all
Vertical V speed correlations. Efolding scale=82 m@ all
Correlation
Separation (m)

**Figure 11.4.** Vertical correlation coefficients in the St. Lawrence Estuary for temperature, salinity, along-estuary current (U), across-estuary current (V).

*4.2.2.4 Temporal auto-correlation scales in the St. Lawrence Estuary*

Temperature and salinity correlation coefficients are high at lags of 1 d and less (Fig. 11.5). A second correlation maximum is found at a lag of 15 d, where the series recorded at the westernmost mooring (1, depths of 14 and 19 m) have the highest temperature and salinity auto-correlation coefficients (>0.7). This behavior can be interpreted as the result of the high-pass filtering of a series containing energetic low frequency variability. The correlation scales of velocity coefficients are comparable and extend over a wide range for any given lag. They are bound at their upper limits by exponential curves of 144 and 140 d. The average across-estuary correlation coefficients have a longer scale (11 d) than the average along-estuary correlation coefficients (6 d).

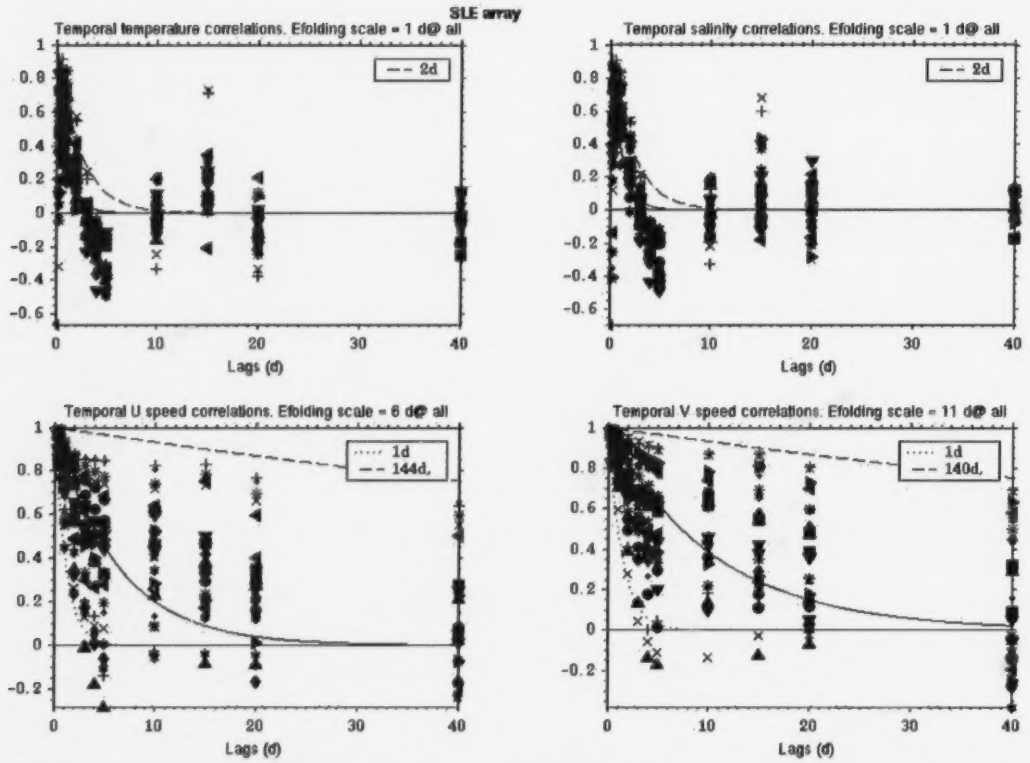
SLE array
Temporal temperature correlations. Efolding scale = 1 d@ all
-- 2d
Lags (d)
Temporal salinity correlations. Efolding scale = 1 d@ all
-- 2d
Lags (d)
Temporal U speed correlations. Efolding scale = 6 d@ all
..... 1d
-- 144d,
Lags (d)
Temporal V speed correlations. Efolding scale = 11 d@ all
..... 1d
-- 140d,
Lags (d)

**Figure 11.5.** Temporal auto-correlation coefficients in the St. Lawrence Estuary for temperature, salinity, along-estuary current (U), across-estuary current (V). Different symbols are used for different instruments. Solid line represents a fit using all data.

*4.2.3 Central Gulf*

Series from different seasons in 1967, 1970, 1979 and 1980 were used for this analysis. Correlation coefficients were computed for two axes, one across and one along the Laurentian Channel (Fig. 12.1). Results are presented at Fig. 12.2 through 12.5.

*4.2.3.1 Horizontal correlation scales across the Laurentian Channel*

The current meter series available for calculation of across channel correlation coefficients were from moorings 328, 389, 373 and 387 (Fig. 12.1). Correlation coefficients were thus obtained for simultaneous series separated by 47 km and greater; all low (< 0.3), some are negative (Fig. 12.2). The correlation scales are thus estimated to be much less than 47 km and the exponential curves that are shown indicate the upper limit of correlation scales.

*4.2.3.2 Horizontal correlation scales along the Laurentian Channel*

The only current meter series available for calculation of across channel correlation coefficients were from moorings 387 and 389 (Fig. 12.1). The simultaneous series available were thus recorded 245 km apart. Correlation scales could not be resolved at this distance, since all coefficients are < 0.3 (Fig. 12.3).

*4.2.3.3 Vertical correlation scales in Central Gulf*

Only simultaneous series of velocity were available for analysis of the vertical scales (Fig. 11.4). Except at mooring 702, correlation coefficients suggest scales shorter than instrument separation (<42 m). There are high correlation coefficients at mooring 702 between instruments at 13 m and 75 m, but the coefficients obtained at the same mooring for larger distances are small (<42 m).

*4.2.3.4 Temporal auto-correlation scales in Central Gulf*

The behaviour of the auto-correlation estimates for these time series is similar to the earlier ones in this report. The estimates decrease rapidly at lags shorter than 5 d, then increase at 10-20 d. A strong correlation of temperature and salinity at a lag of 15 d is observed for an instrument at 300 m, located in the easternmost mooring of our array (eastern edge of the Laurentian Channel). Omitting these "outliers", the average correlation scales are 2 d for both temperature and salinity. East-west and north-south components of velocity have correlation coefficients that are bounded at their upper limits by exponential curves of 34 d and 60 d.

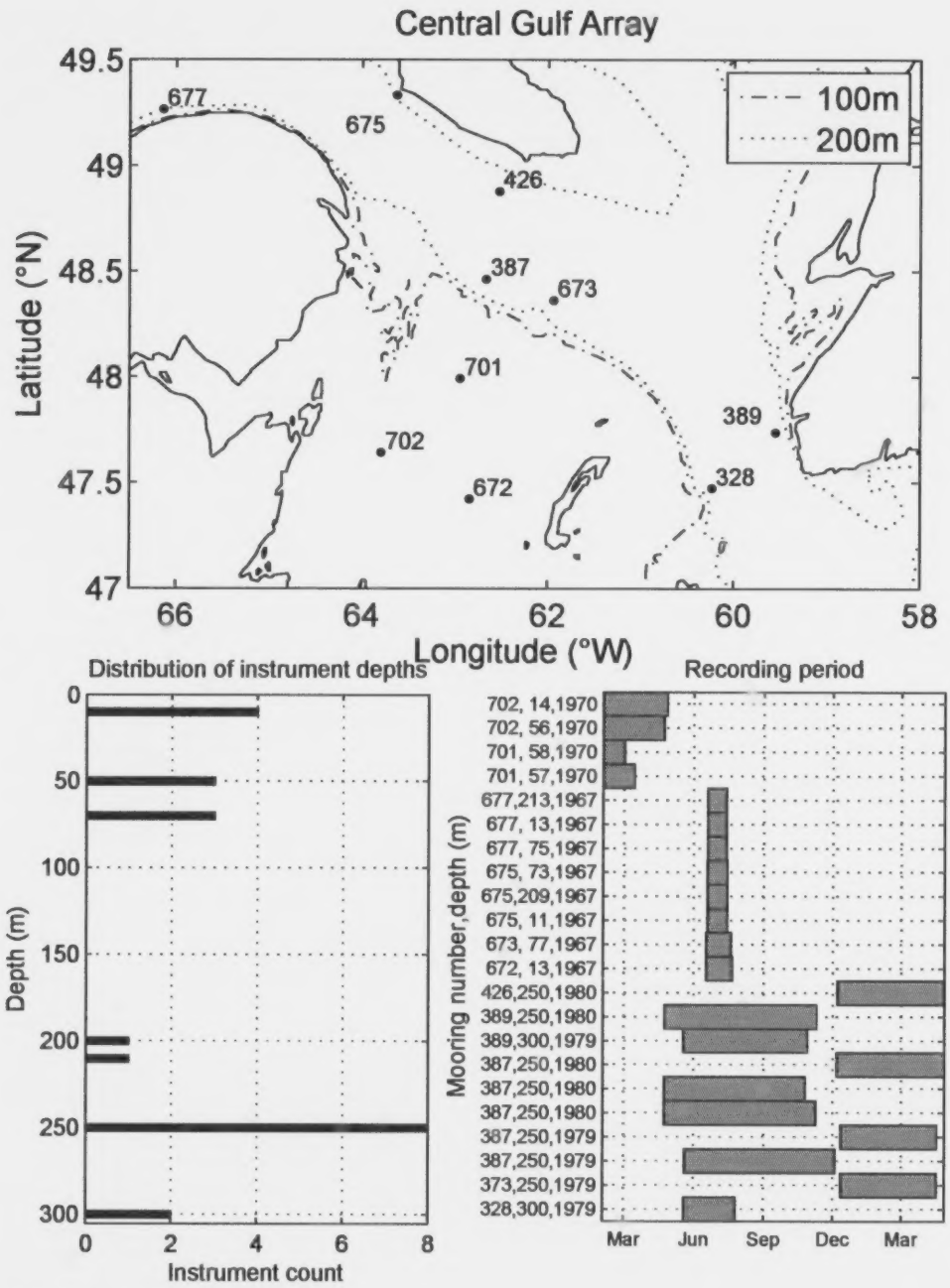


**Figure 12.1** Central Gulf Array

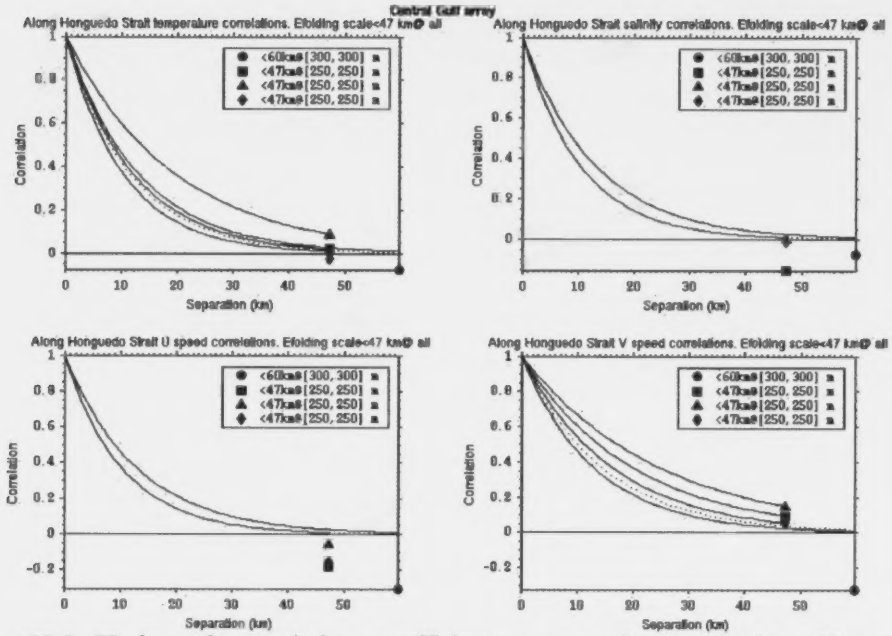
Central Gulf array
Along Honguedo Strait temperature correlations. Efolding scale<47 km@ all
Along Honguedo Strait salinity correlations. Efolding scale<47 km@ all
Along Honguedo Strait U speed correlations. Efolding scale<47 km@ all
Along Honguedo Strait V speed correlations. Efolding scale<47 km@ all
Correlation
Separation (km)

**Figure 12.2** Horizontal correlation coefficients across the Laurentian Channel for temperature, salinity, east-west current (U), north-south current (V). Dotted-line represents fit using all data.

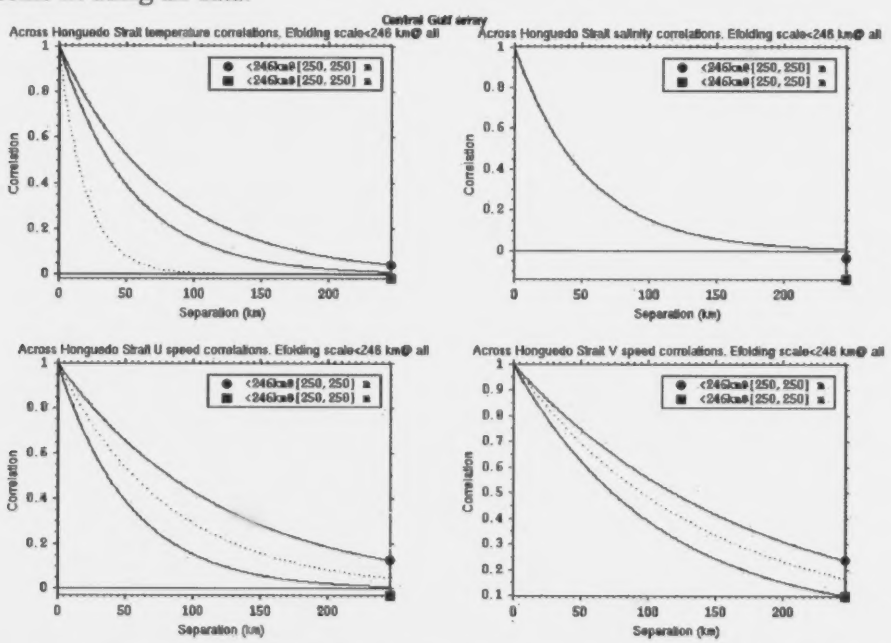
Central Gulf array
Across Honguedo Strait temperature correlations. Efolding scale<246 km@ all
Across Honguedo Strait salinity correlations. Efolding scale<246 km@ all
Across Honguedo Strait U speed correlations. Efolding scale<246 km@ all
Across Honguedo Strait V speed correlations. Efolding scale<246 km@ all
Correlation
Separation (km)

**Figure 12.3** Horizontal correlation coefficients along the Laurentian Channel for temperature, salinity, east-west current (U), north-south current (V). Dotted-line represents fit using all data.

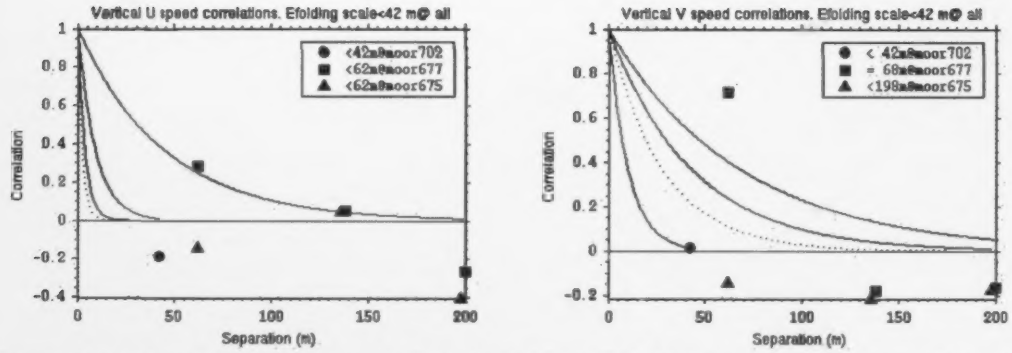


**Figure 12.4** Vertical correlation coefficients in Central Gulf for east-west current (U) and north-south current (V). Dotted-line represents fit using all data.

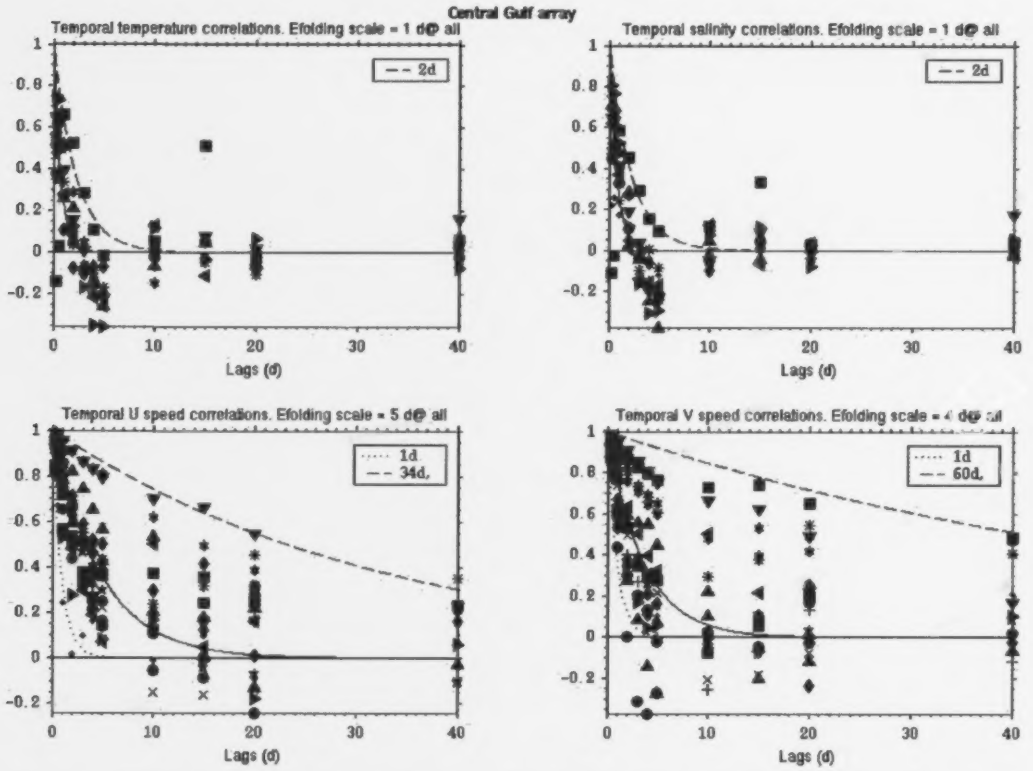


**Figure 12.5** Temporal auto-correlation coefficients in Central Gulf for temperature, salinity, east-west current (U), north-south current (V). Different symbols are used for different instruments. Solid line represents a fit using all data.

4.2.4 Gaspé Current Array

The data for this array were collected from June to September of 1978 with 10 moorings deployed in a cross-pattern (Figure 13.1): one line along the shore (following roughly the 100 m isobath), and two lines across the shore (one in front of La Martre, and the other slightly farther east, towards Sept-Îles). The "La Martre" across-shore line, which had only two moorings, extended beyond the 300 m isobath, while the other line, consisting of five moorings, ended inside the 300 m isobath.

*4.2.4.1 Horizontal correlation scales along 100 m isobath off Gaspé shore*

The scales for temperature and salinity decrease with depth. The correlation coefficients at distances of ≥150 km involve a series at mooring 318 (located near Gaspé Peninsula's easternmost point) and decrease slowly with distance. At depths of 20 m and 60 m, the salinity scales are higher than temperature scales (75 km and 45 km for salinity vs. 51 km and 19 km for temperature). On average, salinity and temperature scales are virtually the same (22 and 23 km). Velocity correlation scales also decrease with depth. On average, the along-isobath component of velocity has a larger correlation scale (38 km) than the across-isobath component (25 km). Along-estuary velocity correlation coefficients greater than 0.3 were observed between the series at mooring 318 (depth 36 m) and any series recorded at separations ≥141 km.

*4.2.4.2 Horizontal correlation scales across the Northwest Gulf of St. Lawrence*

For temperature and salinity, few pairs were available for each line. The correlation scale was determined on average (all lines, all depths) as 11 km for temperature, 15 km for salinity, 11 km for the along-shore component of velocity and 9 km for the across-shore.

*4.2.4.3 Vertical correlation scales in Gaspé Current vicinity*

Correlation coefficients were grouped according to the vertical position of the instruments relative to 100 m depth. Temperature correlation scales are greater than 50 m between series that were recorded at depths >99 m. The temperature correlation scales however decrease when computed between two series in which at least one of them is recorded at 60 m or less. Series at depths ≤60 m are negatively correlated to series from depths ≥100 m. The average temperature correlation scale is <36 m. Salinity correlation scales are greater than temperature scales and vary less with vertical position of series. On average, the salinity correlation scale is 69 m.

Velocity correlation coefficients were not grouped according to depth, but to moorings. Coefficients from instruments at moorings 315 and 318 were separated from the other coefficients. These moorings are located at both westernmost and easternmost points of our dataset, and the correlation scales associated with them are shorter (37 m and less) than the correlation scales at other moorings. The along-shore velocity correlation scale at moorings other than 315 and 318 is 115 m, while across-shore velocity correlation scale is 128 m. On average, the correlation scale of the across-shore component of velocity (92 m) is greater than that of the along-shore component (81 m).

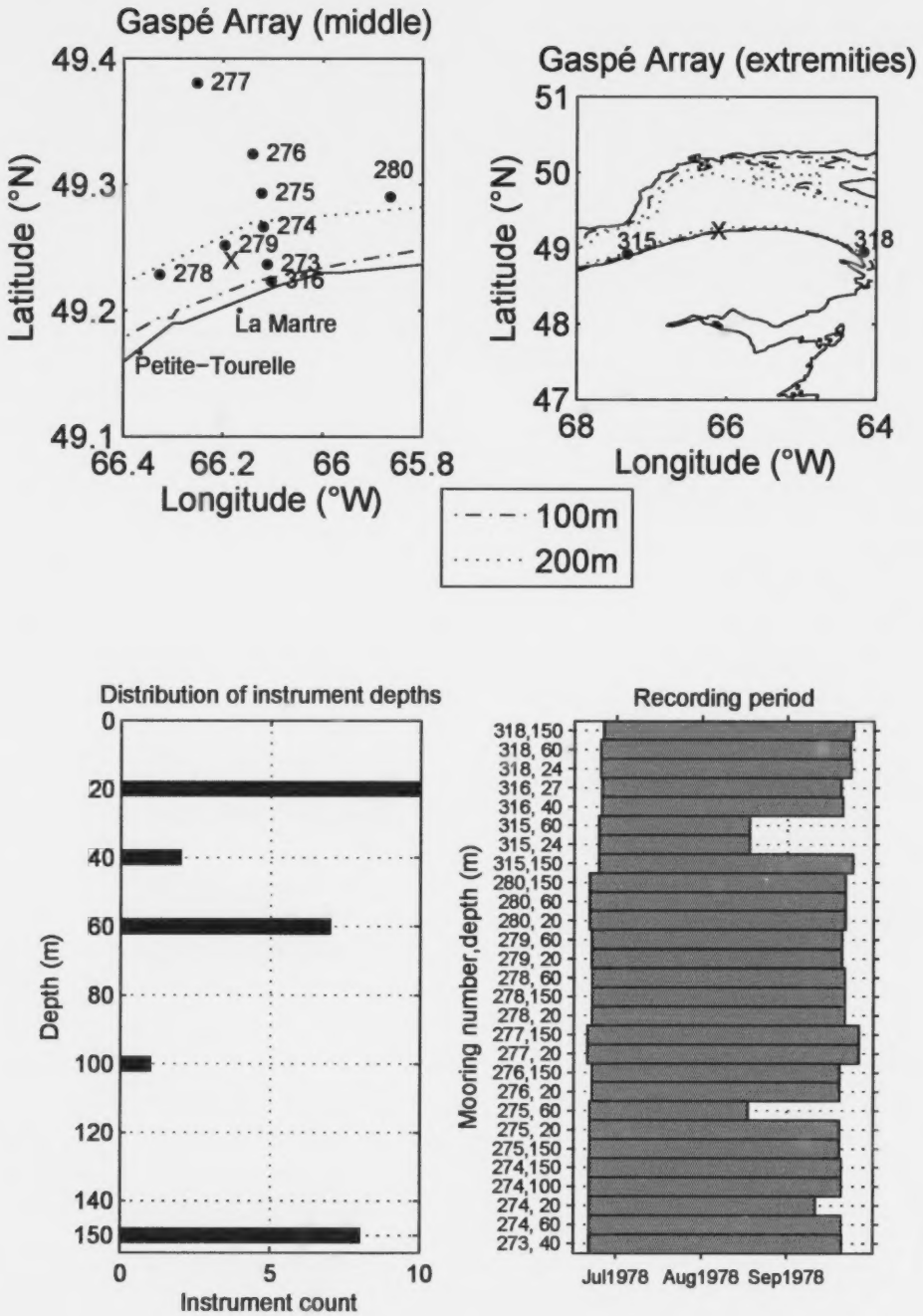


**Figure 13.1** Gaspé Current Array. The X symbol represents the location of the Gaspé Current AZMP fixed station.

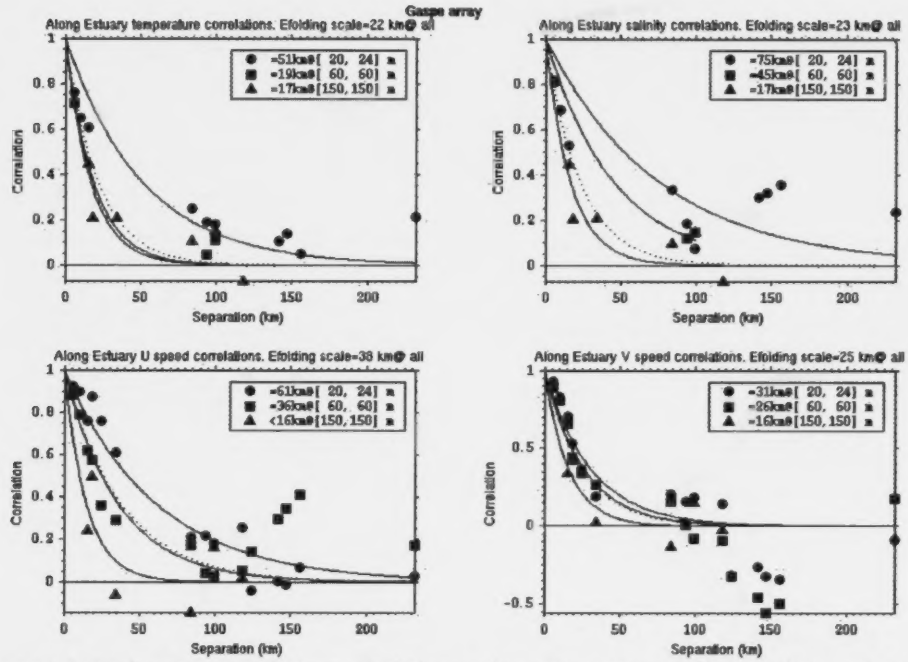
Gaspe array
Along Estuary temperature correlations. Efolding scale=22 km@ all
Along Estuary salinity correlations. Efolding scale=23 km@ all
Along Estuary U speed correlations. Efolding scale=38 km@ all
Along Estuary V speed correlations. Efolding scale=25 km@ all
Correlation
Separation (km)

**Figure 13.2** Horizontal correlation coefficients along the 100 m isobath off Gaspé shore for temperature, salinity, along-shore current (U), across-shore current (V). Dotted-line represents fit using all data.

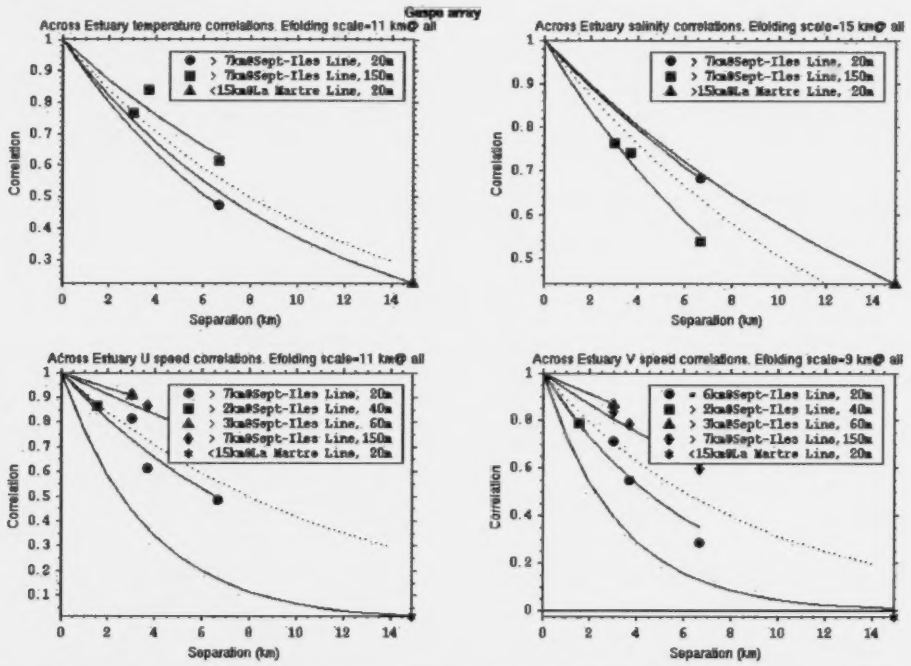
Gaspe array
Across Estuary temperature correlations. Efolding scale=11 km@ all
Across Estuary salinity correlations. Efolding scale=15 km@ all
Across Estuary U speed correlations. Efolding scale=11 km@ all
Across Estuary V speed correlations. Efolding scale=9 km@ all
Correlation
Separation (km)

**Figure 13.3** Horizontal correlation coefficients across the Northwest Gulf of St. Lawrence for temperature, salinity, along-shore current (U), across-shore current (V). Dotted-line represents fit using all data.

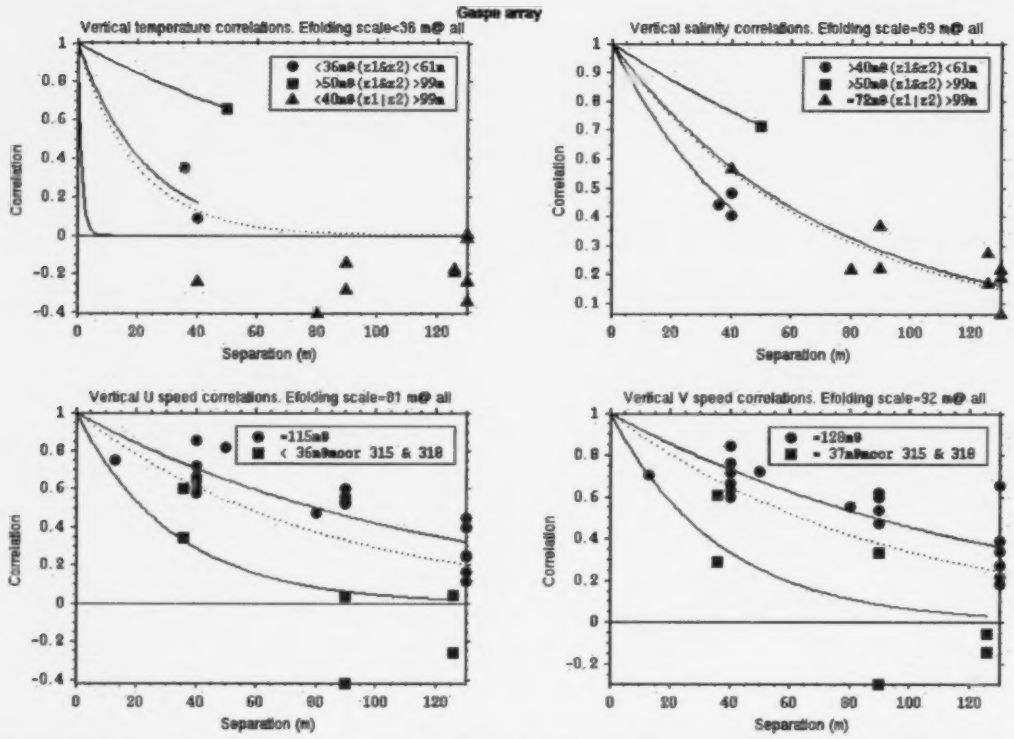
Gaspe array
Vertical temperature correlations. Efolding scale<36 m@ all
Vertical salinity correlations. Efolding scale=69 m@ all
Vertical U speed correlations. Efolding scale=81 m@ all
Vertical V speed correlations. Efolding scale=92 m@ all
Correlation
Separation (m)

**Figure 13.4** Vertical correlation coefficients in Gaspé Current for temperature, salinity, along-shore current (U), across-shore current (V). Dotted-line represents fit using all data.

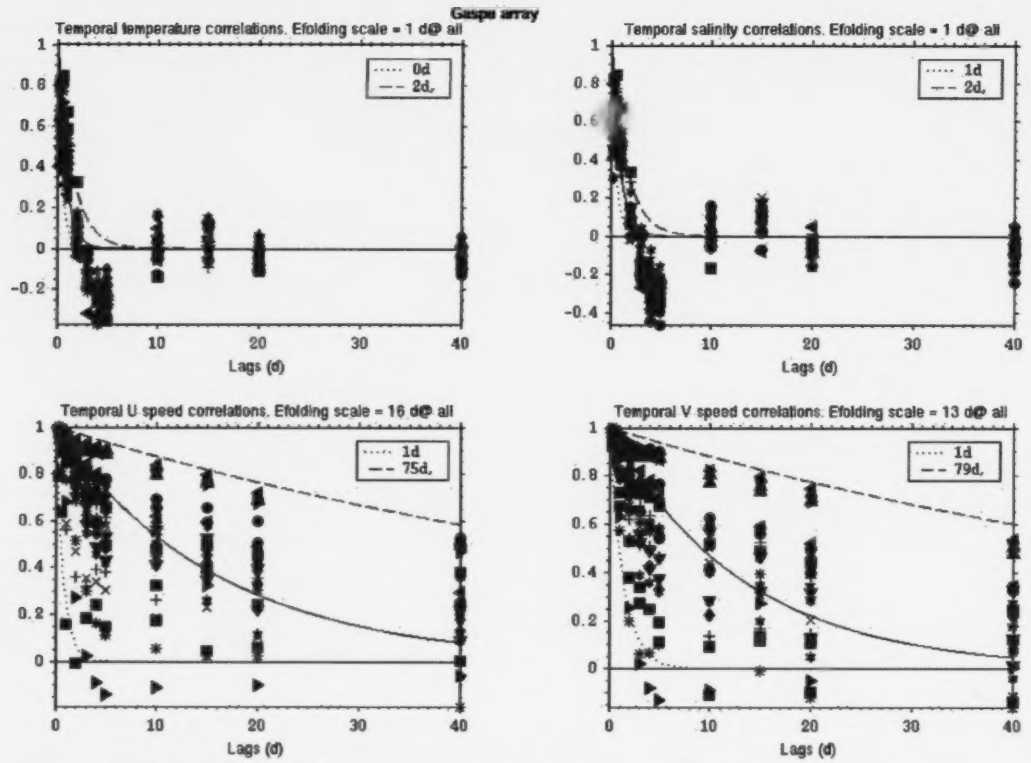


**Figure 13.5** Temporal auto-correlation coefficients in Gaspé Current for temperature, salinity, along-shore current (U), across-shore current (V). Different symbols are used for different instruments. Solid line represents a fit using all data.

*4.2.4.4 Temporal auto-correlation scales in Gaspé Current vicinity*

Temperature and salinity auto-correlation coefficients decrease from lags 6 h to 5 d, then increase at 10 d because of low frequency variance, and decrease again due to filter effects. Their average scales are shorter than 1 d. Auto-correlation coefficients are comparable for both components of velocity, and with an upper bound characterized by exponential curves of 75 and 79 d e-folding scales.

4.2.5 Jacques Cartier Passage Array

This dataset (Fig. 14.1) consists of instruments deployed during four periods:

| Start/End | Season | Moorings |
|---|---|---|
| May 1986 – October 1986 | Summer 1986 | 6, 8 |
| October 1986 -May 1987 | Winter 1986 | 2, 5, 6, 7, 8, 9 |
| Jun 1987 – Sep 1987 | Summer 1987 | 1,3, 4, 5, 7, 8, 9, 12 |
| Sep 1987 – May 1988 | Winter 1987 | 18 |

The moorings are configured in two east-west lines: one close and parallel to the Québec mainland's north shore (along-passage), the other, close and parallel to Anticosti's north shore. Across-shore correlation investigation is also possible along three lines, from west to east, Magpie Line, Baie Johan-Beetz Line and Natashquan Line (moorings 7, 8 and 9, Fig 14.1). Mooring 1 on Fig 14.1, along Québec's north shore, is situated on Boucane Bank, while moorings 3 and 18 are on Mingan Bank. The analyses were broken down by season. Results are presented on Fig. 14.2 to 14.10.

*4.2.5.1 Horizontal correlation scales along Jacques Cartier Passage*

*Summer*

The temperature and salinity correlation scales between any two series recorded above different banks (Boucane Bank vs. Mingan Bank) are <55 km at all depths (Fig. 14.2). On Mingan Bank alone, the correlation scales of temperature and salinity could not be resolved. Averaging coefficients from all pairs, correlation scales of temperature and salinity are less than 55 km, the shortest distance between instruments.

The velocity correlation coefficients were divided according to depth. The series at 20 m had slightly different sampling periods, and the simultaneous period of any two series differs from one pair to another. We calculated two sets of coefficients at that depth: one with maximal period for each pair (May to August, June to September, empty circles), the other with the common period to all three series (June to August, full circles). The along-passage correlation coefficient between series at a depth of 20 m and 261 km apart is much higher (0.6) when data from May to September are used than when data from June to August are used (0.1). The along-passage correlation scale of along-passage velocity is 258 km at a depth of 50 m, but <55 km at all other depths. The average correlation scales of components of velocity are 70 km (along-passage) and less than 55 km (across-passage).

*Winter*

Temperature and salinity scales are less than 75 km, at all depths (Fig. 14.3). For both components of velocity, the correlation scale at 20 m is >131 km. On average, a correlation scale of 206 km was found for along-passage velocity and 101 km for across-passage velocity.

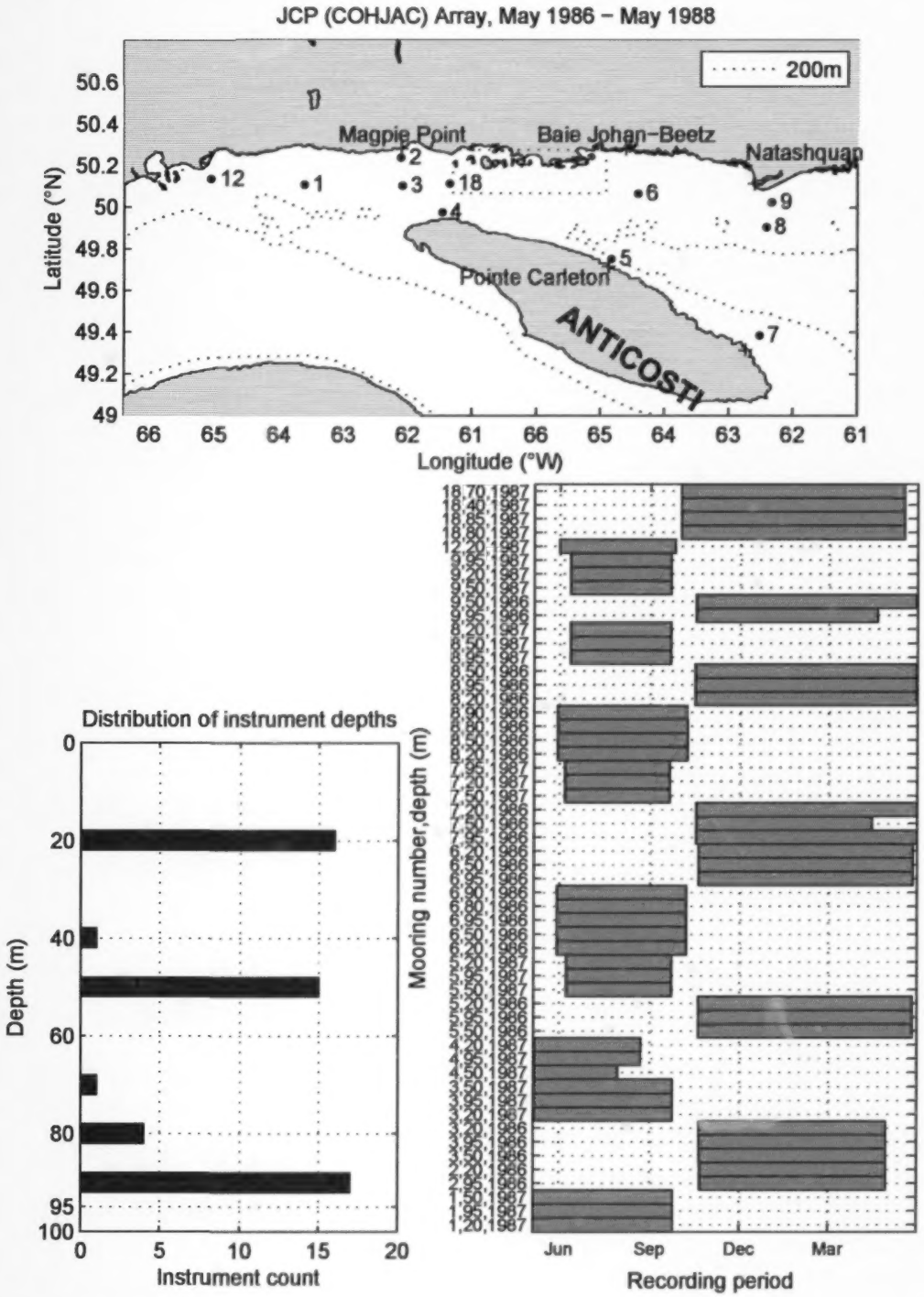


**Figure 14.1** Jacques Cartier Passage Array.

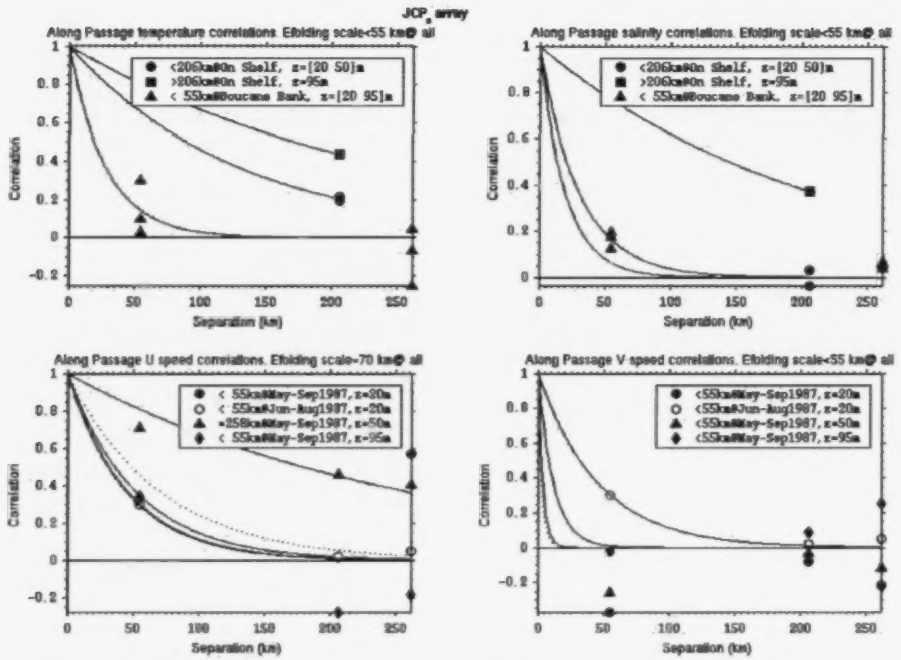
JCP array
Along Passage temperature correlations. Efolding scale<55 km@ all
Along Passage salinity correlations. Efolding scale<55 km@ all
Along Passage U speed correlations. Efolding scale=70 km@ all
Along Passage V speed correlations. Efolding scale<55 km@ all
Correlation
Separation (km)

**Figure 14.2** Summer horizontal correlation coefficients along Jacques Cartier passage for temperature, salinity, along-passage current (U), across- passage current (V). Dotted-line represents fit using all data.

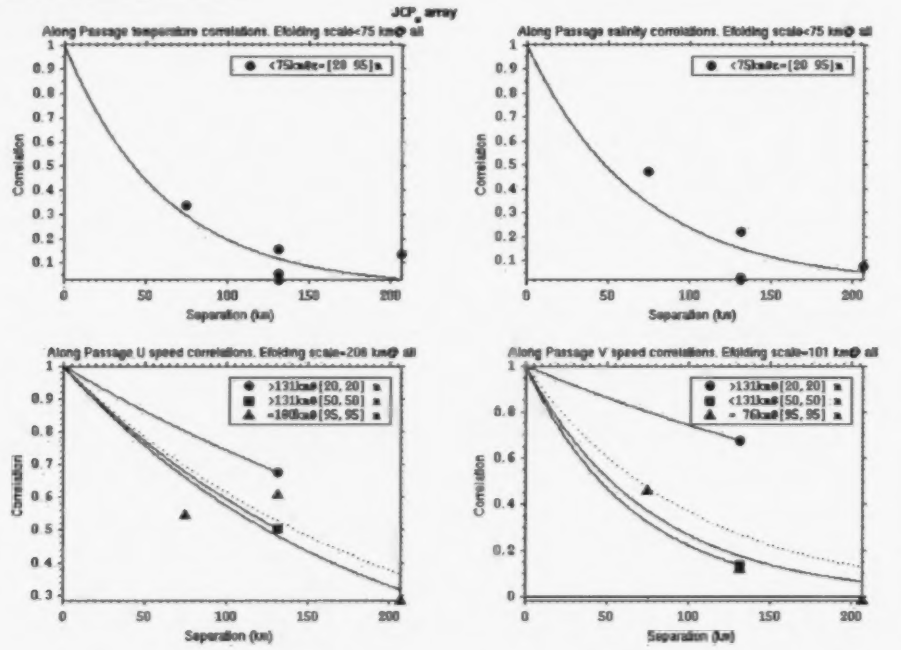
JCP array
Along Passage temperature correlations. Efolding scale<75 km@ all
Along Passage salinity correlations. Efolding scale<75 km@ all
Along Passage U speed correlations. Efolding scale=208 km@ all
Along Passage V speed correlations. Efolding scale=101 km@ all
Correlation
Separation (km)

**Figure 14.3** Winter horizontal correlation coefficients along Jacques Cartier Passage for temperature, salinity, along-passage current (U), across-passage current (V). Dotted-line represents fit using all data.

Overall and on average, the horizontal along-passage correlation scales are larger during winter than during summer.

*4.2.5.2 Horizontal correlation scales along Anticosti north-shore*
*Summer and winter*
The only significant temperature and salinity correlation coefficients (Fig.14.4) are between the two easternmost moorings (5 and 7) at 20 m (r=0.6 at a distance of 93 km). Moorings 4 and 5, 97 km apart, are not as well correlated (0.1), and a time series plot (not shown here) has shown that they are out of phase. Correlation scales are <93 km.

*4.2.5.3 Horizontal correlation scales across Jacques Cartier Passage*
*Summer*
There are significant negative correlation coefficients (-0.54 and –0.40) between temperature and salinity series of moorings 7 and 9 at 20 m (Fig. 14.5). The scales are greater at a depth of 95 m (16 and 15 km) than at depths of 20 and 50 m (less than 14 km). Correlation scales of the along-passage component of velocity decrease with depth (more than 71 km at 20 m, 20 km at 50 m and less than 14 km at 95 m). Correlation scales of the across-passage component of velocity are found to be less than 14 km.

*Winter*
Temperature, salinity and across-passage velocity scales are also found to be less than 14 km (Fig 14.6), while along-passage velocity has a scale of 18 km. At 50 m, correlation scale of along-passage component of velocity is greater along the Natashquan line (60 km) than along other lines (less than 38 km). At 95 m, the correlation scale of along-passage velocity (36 km) is smaller than at 50 m. Across-passage velocity correlation scale could not be resolved, except at a depth of 95 m along Natashquan Line, where it is 20 km.

*4.2.5.4 Vertical correlation scales in Jacques Cartier Passage*
*Summer*
The distribution of correlation coefficients with distance is very scattered (Fig. 14.7). The average correlation scale for temperature is 20 m, less than the average correlation scale of salinity (32 m). For temperature, salinity and along-passage component of velocity, we note that the correlation coefficients at moorings 6 and 9 are significantly higher than at other moorings, yielding larger correlation coefficients than at the other moorings. The along-passage component of velocity has a larger coherence scale (52 m) than the across-passage component (22 m)

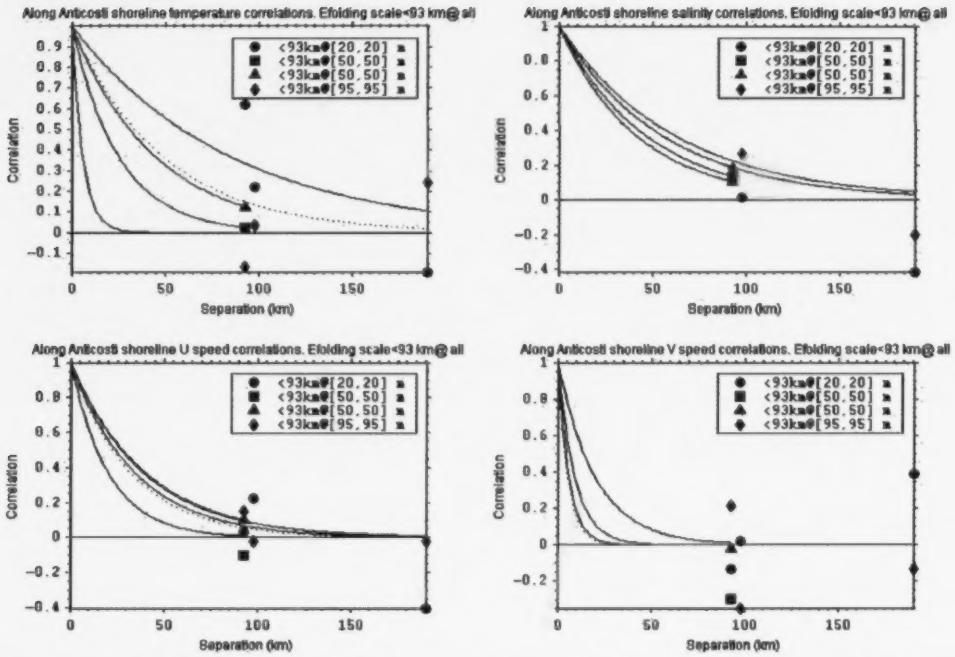
Along Anticosti shoreline temperature correlations. Efolding scale<93 km@ all
Along Anticosti shoreline salinity correlations. Efolding scale<93 km@ all
Along Anticosti shoreline U speed correlations. Efolding scale<93 km@ all
Along Anticosti shoreline V speed correlations. Efolding scale<93 km@ all
Correlation
Separation (km)

**Figure 14.4** Horizontal correlation coefficients along Anticosti north-shore for temperature, salinity, along-passage current (U), across-passage current (V). Dotted-line represents fit using all data.

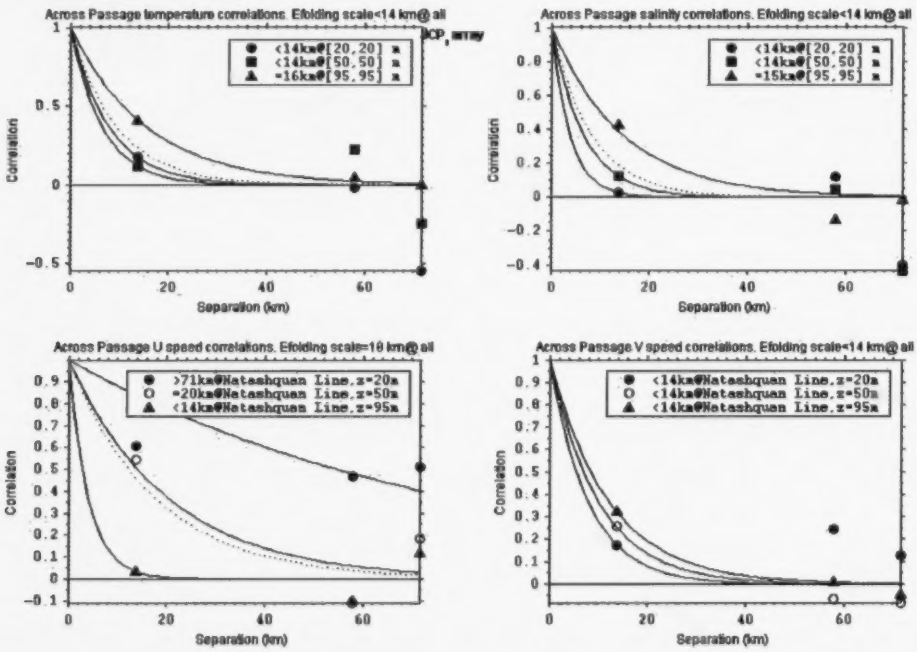
Across Passage temperature correlations. Efolding scale<14 km@ all
Across Passage salinity correlations. Efolding scale<14 km@ all
Across Passage U speed correlations. Efolding scale=18 km@ all
Across Passage V speed correlations. Efolding scale<14 km@ all
Correlation
Separation (km)

**Figure 14.5** Summer horizontal correlation coefficients across Jacques Cartier passage for temperature, salinity, along-passage current (U), across- passage current (V). Dotted-line represents fit using all data.

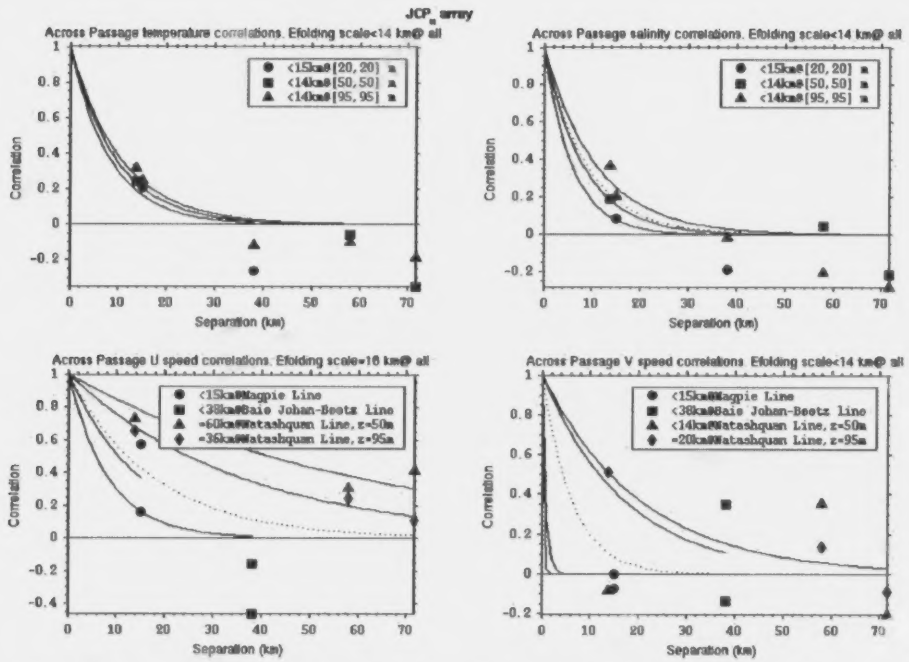
JCP array
Across Passage temperature correlations. Efolding scale<14 km@ all
Across Passage salinity correlations. Efolding scale<14 km@ all
Across Passage U speed correlations. Efolding scale=16 km@ all
Across Passage V speed correlations. Efolding scale<14 km@ all
Correlation
Separation (km)

**Figure 14.6** Winter horizontal correlation coefficients across Jacques Cartier passage for temperature, salinity, along- passage current (U), across- passage current (V). Dotted-line represents fit using all data.

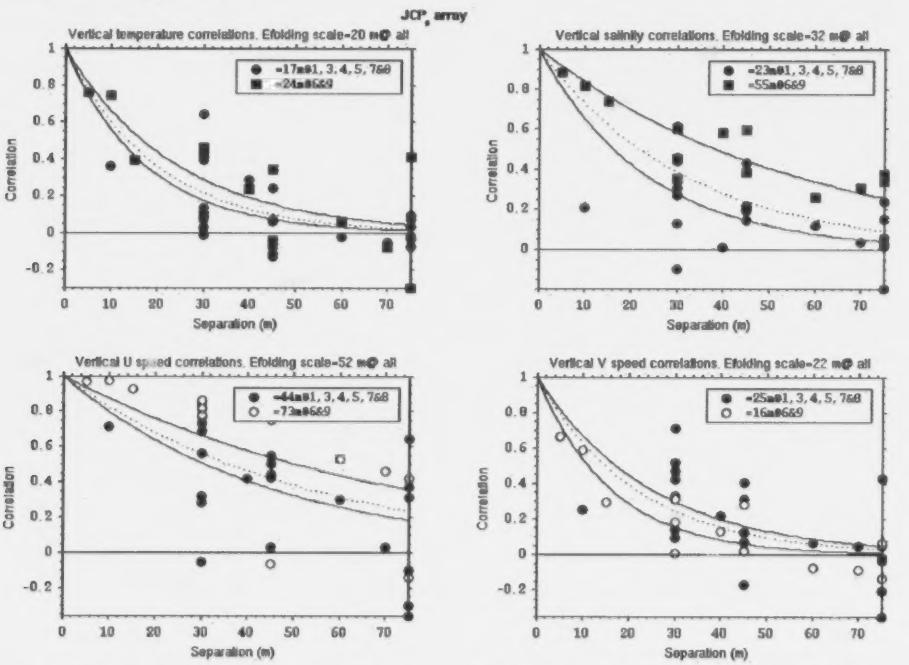
JCP array
Vertical temperature correlations. Efolding scale=20 m@ all
Vertical salinity correlations. Efolding scale=32 m@ all
Vertical U speed correlations. Efolding scale=52 m@ all
Vertical V speed correlations. Efolding scale=22 m@ all
Correlation
Separation (m)

**Figure 14.7** Summer vertical correlation coefficients in Jacques Cartier passage for temperature, salinity, along- passage current (U), across- passage current (V). Dotted-line represents fit using all data.

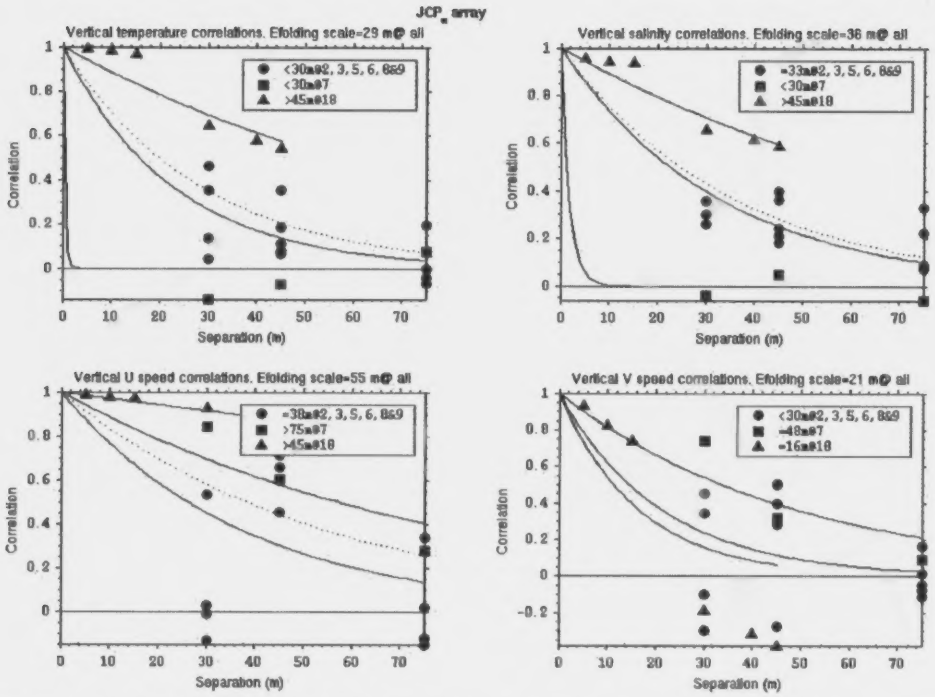
JCP array
Vertical temperature correlations. Efolding scale=29 m@ all
Vertical salinity correlations. Efolding scale=36 m@ all
Vertical U speed correlations. Efolding scale=55 m@ all
Vertical V speed correlations. Efolding scale=21 m@ all
Correlation
Separation (m)

**Figure 14.8** Winter vertical correlation coefficients in Jacques Cartier passage for temperature, salinity, along- passage current (U), across- passage current (V). Dotted-line represents fit using all data.

*Winter*

All variables measured at mooring 18 behave differently than they do at other moorings and, for our dataset, it is the only mooring deployed in winter 1987-1988 (Fig. 14.8). Temperature and salinity correlation scales at mooring 18 were both >45 m), greater than average correlation scales at all moorings (29 m for temperature, 36 m for salinity). At mooring 18, the across-passage velocity correlation function has a sharp cut-off between the correlation coefficients computed between series below 70 m (<15 m separation), and the coefficients computed between a series at 40 m and the other one deeper than 70 m (at 30 m separation and greater). This shows that two very different current regimes are at work above and below a depth between 40 and 70 m. The average correlation scale of across-passage velocity (21 m) is smaller than that of along-passage velocity (55 m). For both components, the correlation coefficients from mooring 18 are among the highest. It is however impossible to conclude from this analysis alone whether this high vertical correlation at mooring 18 is due to its geographical location or to the different period during which it was deployed (winter 1987-1988 as opposed to winter 1986-1987).

From this analysis, we also notice that coherence scales are generally larger during winter than during summer.

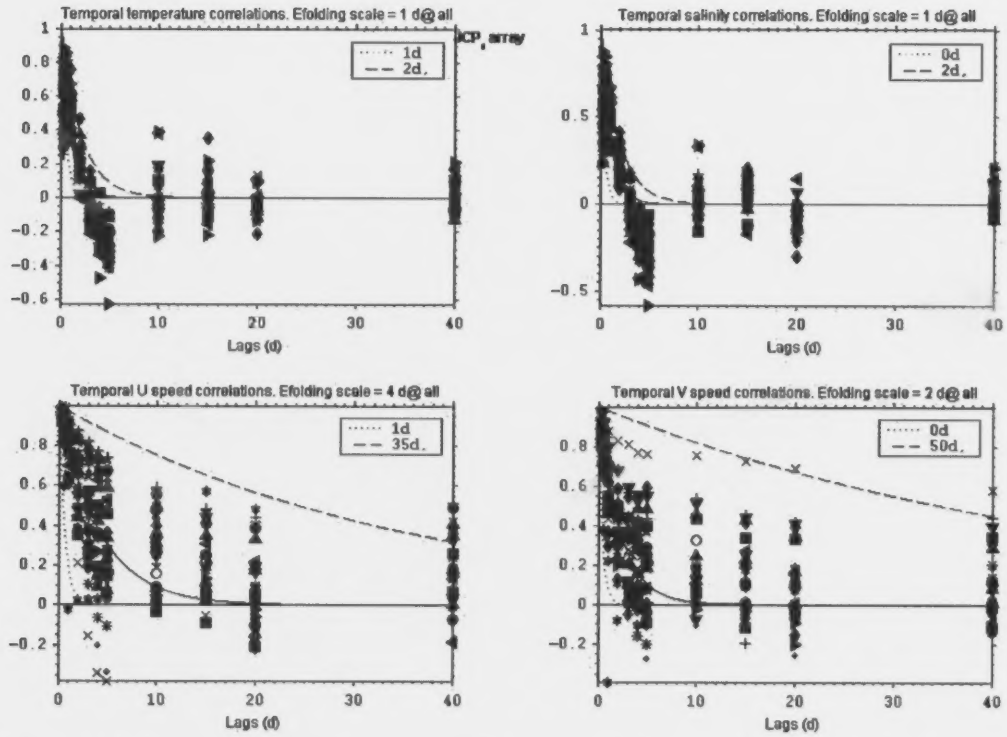


**Figure 14.9** Summer temporal auto-correlation coefficients in Jacques Cartier Passage for temperature, salinity, along- passage current (U), across- passage current (V). Different symbols are used for different instruments. Solid line represents a fit using all data.

*4.2.5.5 Temporal auto-correlation scales in Jacques Cartier Passage*

The auto-correlation coefficients are on average higher during summer than winter. Temperature and salinity auto-correlation coefficients decrease within 2 d lags, then increase at 10 d lag, indicating that there is some energy at low frequency (Fig. 14.9 and 14.10). The upper bound velocity scales are higher during winter (182 and 179 d) than during summer (35 d and 50 d).

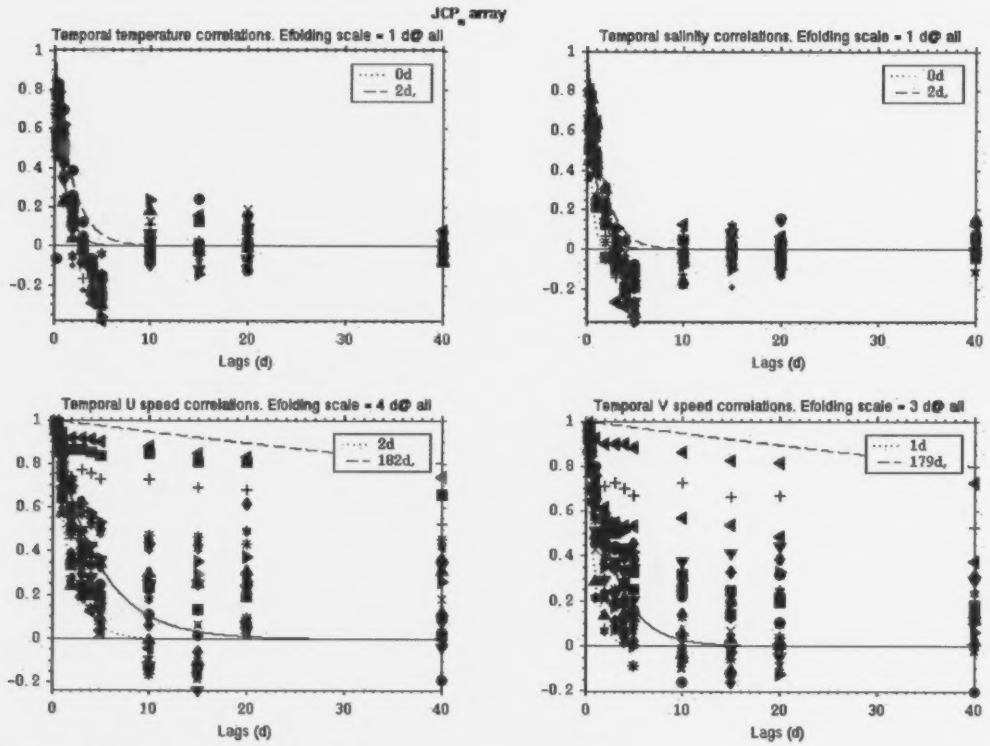


**Figure 14.10** Winter temporal auto-correlation coefficients in Jacques Cartier Passage for temperature, salinity, along- passage current (U), across- passage current (V). Different symbols are used for different instruments. The solid lines represent a fit using all data.

4.2.6 Strait of Belle Isle Array

This array has both summer (1963 and 1980) and winter (1975) moorings deployed across the Strait of Belle Isle at a location where the width is approximately 21.6 km (Figure 15.1). Results are presented in Figures 15.2 to 15.4.

*4.2.6.1 Horizontal correlation scales across Strait of Belle Isle*

Only the summer data allowed for the determination of horizontal correlation coefficients. The results show no significant change of the coherence scales with depth. Coefficients are grouped in two subsets: the pairs involving the southern/easternmost moorings (398 and 399, likely both moorings are within the region of outflow from the Gulf to the Newfoundland shelf), and the pairs involving only moorings from the center (these moorings may include the frontal region between Gulf outflow and Labrador inflow).

Temperature and salinity scales are similar to one another (6 km and 4 km), and are smaller in the mid-channel subset, suggesting a different behavior of temperature and salinity near the Labrador coast than farther southeast near the Newfoundland coast (Figure 15.2). The along-channel components of velocity (V) have the highest coherence scale (>13 km) of all fields. The correlation scale of the across-channel velocity (U) is higher at moorings from mid-channel than at the western extremity, and on average is 2 km.

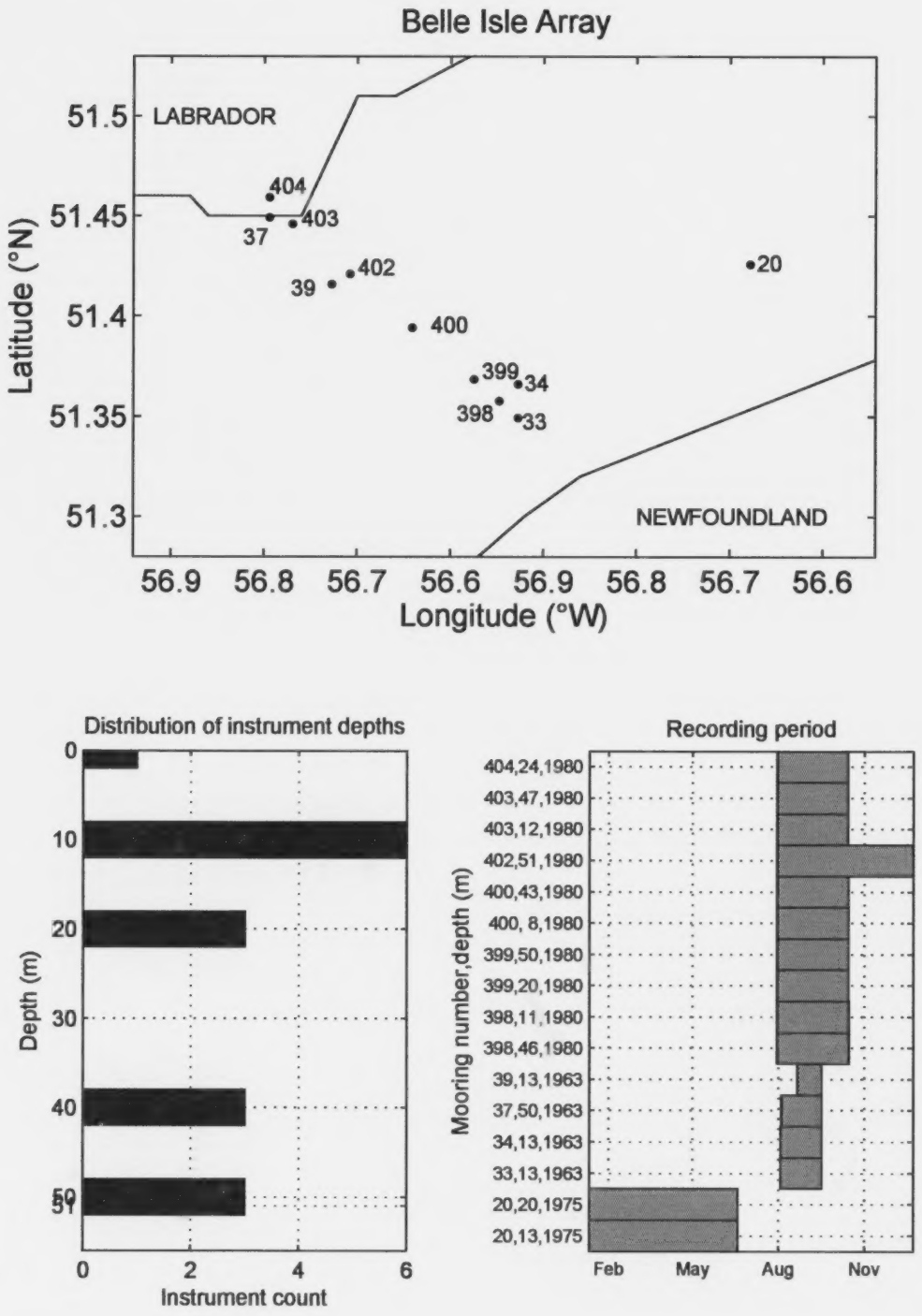


**Figure 15.1** Strait of Belle Isle array

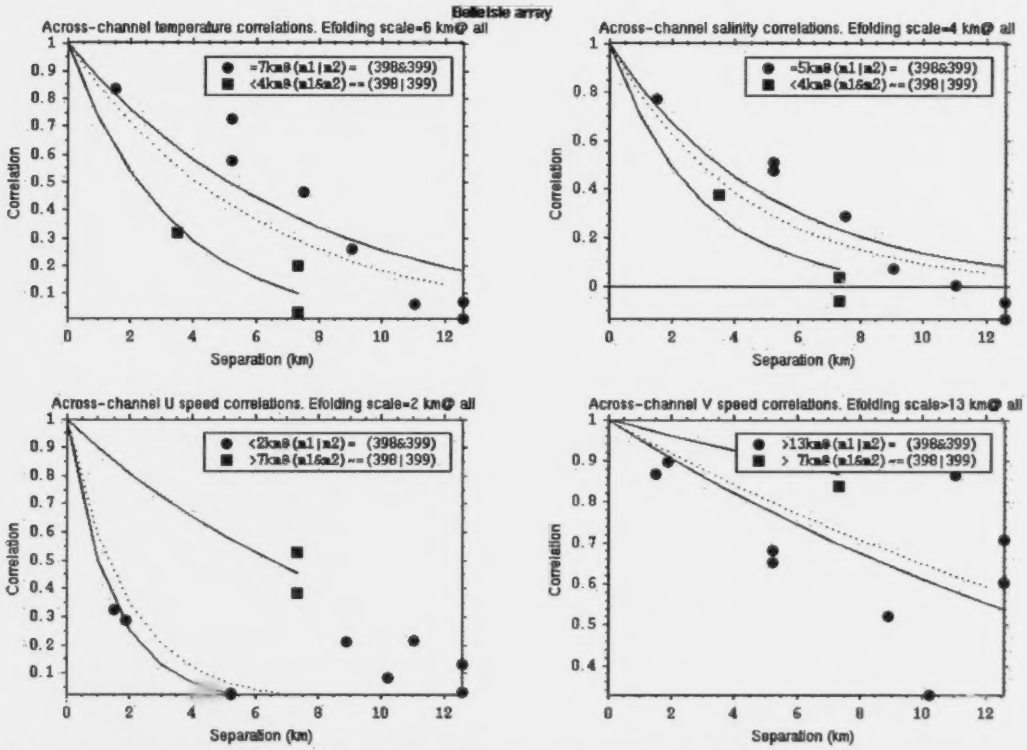
Belle Isle array
Across-channel temperature correlations. Efolding scale=6 km@ all
Across-channel salinity correlations. Efolding scale=4 km@ all
Across-channel U speed correlations. Efolding scale=2 km@ all
Across-channel V speed correlations. Efolding scale>13 km@ all
Correlation
Separation (km)

**Figure 15.2** Horizontal correlation coefficients across Strait of Belle Isle for temperature, salinity, across-strait current (U), along-strait current (V). Dotted-line represents fit using all data.

*4.2.6.2 Vertical correlation scales in Strait of Belle Isle*

Our dataset only allows the computation of one pair of instruments per mooring. The average correlation scale is >35 m for temperature and >28 m for salinity (Fig 15.3). The correlation scale of across-strait velocity (U) is greater than 35 m, while the average scale of the along-strait velocity (V) is equal to 14 m.

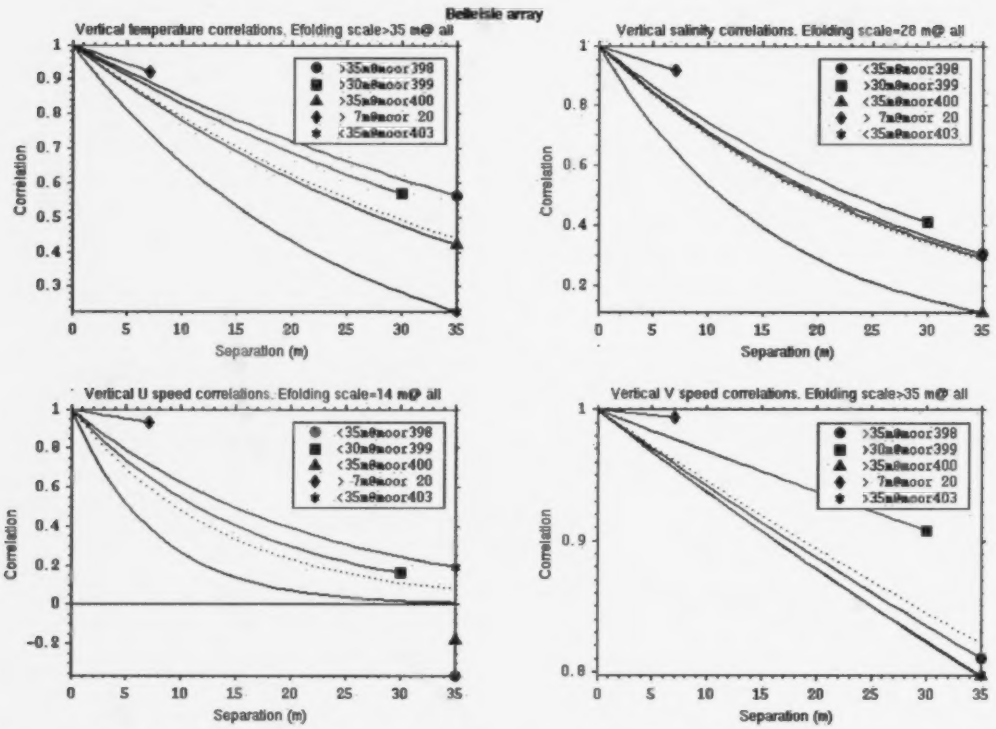
Belleisle array
Vertical temperature correlations. Efolding scale>35 m@ all
Vertical salinity correlations. Efolding scale=28 m@ all
Vertical U speed correlations. Efolding scale=14 m@ all
Vertical V speed correlations. Efolding scale>35 m@ all
Correlation
Separation (m)

**Figure 15.3** Vertical correlation coefficients in Strait of Belle Isle for temperature, salinity, across-strait current (U), along-strait current (V). Dotted-line represents fit using all data.

*4.2.6.3 Temporal auto-correlation in Strait of Belle Isle*

Temperature and salinity auto-correlation coefficients decrease drastically after 2 d lag (Fig 15.4). Higher correlation coefficients occur at lags of 10 d and 15 d, as a result of presence of low frequency energy. At a lag of 15 d, mooring 403 (depth 47 m) has a higher correlation coefficient than the other series.

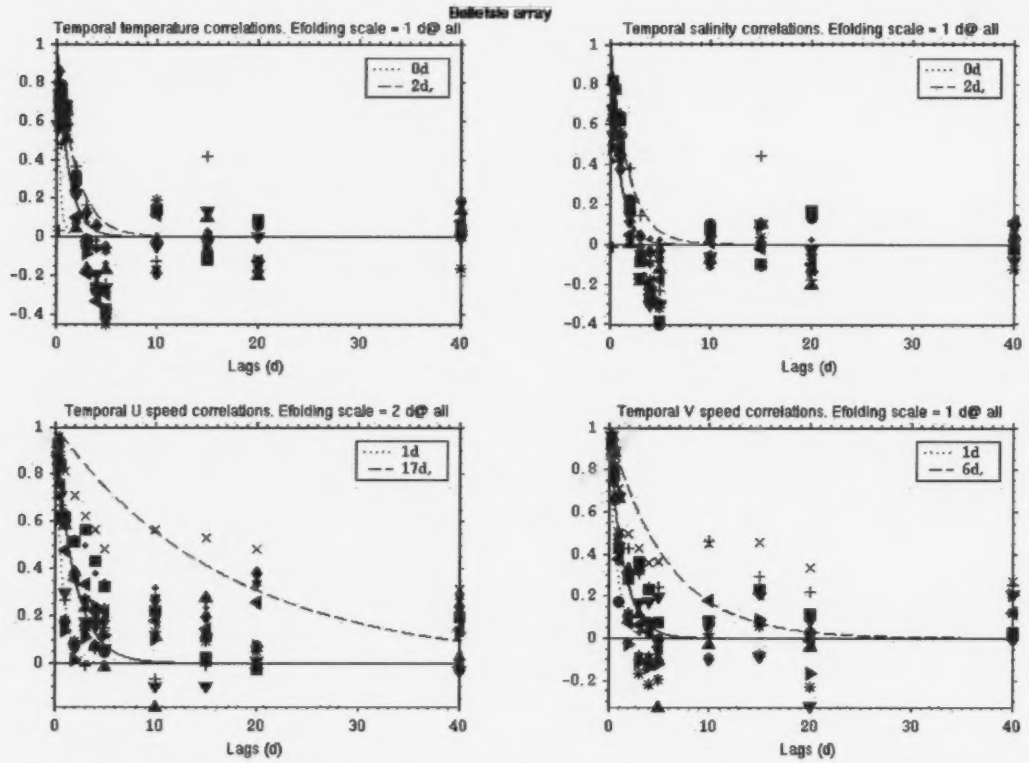


**Figure 15.4** Temporal auto-correlation coefficients in Strait of Belle Isle for temperature, salinity, across-strait current (U), along-strait current (V). Different symbols are used for different instruments. Solid line represents a fit using all data.

## 5.0 Conclusion

### 5.1 Newfoundland Shelf and Grand Banks

The correlation scales of datasets on the Newfoundland Shelf are summarized in Table 4.

#### *5.1.1 Horizontal scales on Newfoundland Shelf*

The horizontal correlation scales of temperature and salinity obtained on Newfoundland Shelf are summarized on Figure 16.1 (temperature) and Figure 16.2 (salinity). The configurations of moorings do not always allow the resolution of horizontal correlation scales, either because of current meter arrays are too sparse (across Avalon Channel, across Flemish Pass, across-slope during CASP2), or too confined (along Flemish Pass, across-slope at Southeast Shoal, along-shelf during CASP2). Typical scales are O(10km). In some areas, the horizontal correlation has vertical structure. For instance on Southeast Shoal, temperature and across-shelf velocity correlation scales are 94 km and 108 km at 12 m depth, and less than 61 km at 45 m depth. Horizontal scales are greater for temperature and across-shelf velocity (U) at Southeast Shoal than elsewhere. Where horizontal velocity scales could be resolved, it was found that they are greater in the direction of the component which is aligned with the mooring

**Table 4**. Correlation scales on Newfoundland Shelf. Numbers in bold italic characters indicate that only one coefficient was available for scale estimation. Note that the temperature and salinity data were high-pass filtered in order to remove the low-frequency variability, while the velocity data were low-pass filtered in order to eliminate the tidal and inertial variability.

| **HORIZONTAL** | **Depth range (m)** | **Season** | **Correlation scales (km)** | | | |
|---|---|---|---|---|---|---|
| | | | **T** | **S** | **Velocity** | |
| | | | | | **Across** | **Along** |
| Across Avalon Channel | [29 80] | Summer | <22 | <22 | <22 | <22 |
| Across Flemish Pass | [95 100] | Winter | ***<20*** | ***<20*** | ***<20*** | ***>20*** |
| Along Flemish Pass | [50 300] | Winter | 14 | >15 | 13 | >15 |
| Across-Shelf during CASP2 | [18.5 132] | Winter | 19 | <52 | 52 | 53 |
| Along-Shelf during CASP2 | [185 195] | Winter | >25 | >25 | ***>25*** | ***<25*** |
| Across-Shelf at SE Shoal | [11 13] | Summer | 94 | <61 | 108 | <61 |
| Across-Shelf at SE Shoal | [11 46] | Summer | <61 | <61 | <61 | <61 |
| Across-Shelf at SE Shoal | [44 46] | Summer | <61 | ***<61*** | <61 | <61 |
| **VERTICAL** | **Depth range (m)** | **Season** | **Correlation scales (m)** | | | |
| | | | **T** | **S** | **Velocity** | |
| | | | | | **Across** | **Along** |
| Avalon Channel | [25 174] | Summer | 22 | <25 | 90 | >100 |
| Avalon Channel | [54 130] | Summer | x | x | >51 | >51 |
| Flemish Pass | [50 300] | Winter | <50 | 78 | <51 | <51 |
| Flemish Pass | [100 300] | Winter | X | x | <200 | >200 |
| CASP2 | [17 293] | Winter | 32 | 64 | >150 | >150 |
| Southeast Shoal | [34 52] | Summer | >18 | x | x | X |
| Southeast Shoal | [20 52] | Summer | 14 | <25 | >33 | >33 |
| **TEMPORAL** | **Depth range (m)** | **Season** | **Average scales (d)** | | | |
| | | | **T** | **S** | **Velocity** | |
| | | | | | **Across** | **Along** |
| Avalon Channel | [25 174] | Summer | <1 | 1 | 6 | 4 |
| Flemish Pass | [20 343] | Winter | <1 | 1 | 2 | 45 |
| CASP2 | [17 293] | Winter | 1 | 1 | 7 | 3 |
| Southeast Shoal | [11 52] | Summer | 1 | 1 | 3 | 3 |

configuration. For instance, at Southeast Shoal, in the across-shelf direction, the across-shelf component of velocity has a greater scale (108 km) than the along-shelf component (61 km). Along Flemish Pass, the along-pass component of velocity has a greater scale (>15 km) than the across-pass component (13 km). However at CASP2, the scales were quite symmetrical for both components of velocity (52 km and 53 km) when both were resolved.

*5.1.2 Vertical scales on Newfoundland Shelf*

Because of the stratification occurring in the summer, winter data sets such as CASP2 and Flemish Pass have higher vertical correlation scales of temperature and salinity than the two other datasets, which were recorded in the summer. Typical vertical scales range from ~10 to ~100 m.

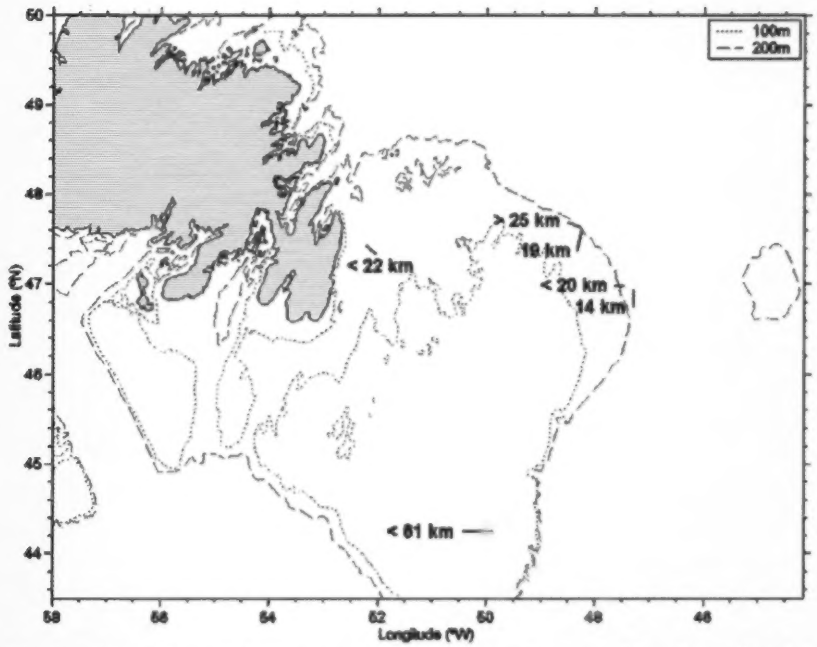


**Figure 16.1**. Horizontal correlation scales of temperature on Newfoundland Shelf. The direction and length of scales is represented by proportional thick solid lines. Scale magnitudes are printed next to each line. Comparative symbols (<, >) are used whenever scales could not be resolved by our method.

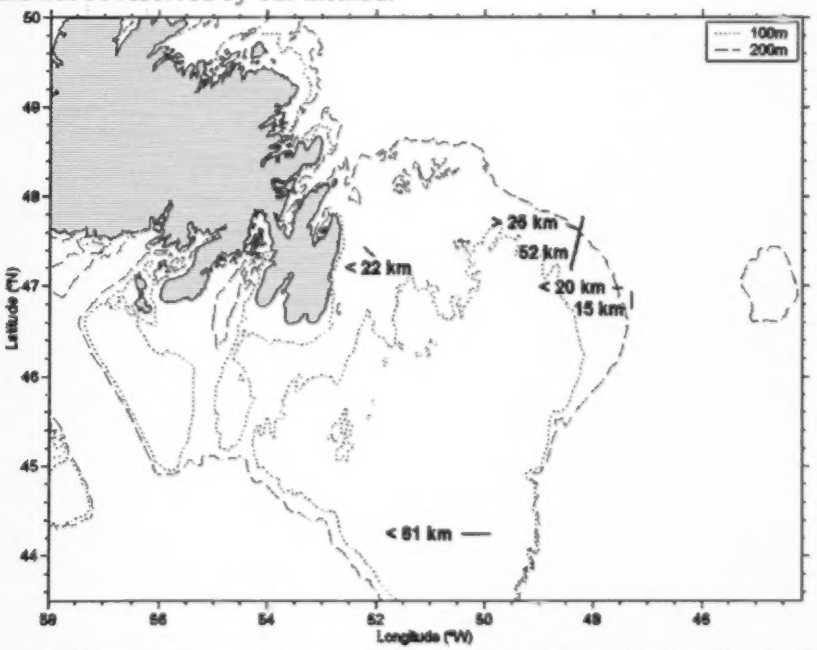


**Figure 16.2** Horizontal correlation scales of salinity on Newfoundland Shelf. The direction and length of scales is represented by proportional thick solid lines. Scale magnitudes are printed next to each line. Comparative symbols (<, >) are used whenever scales could not be resolved by our method.

*5.1.3 Temporal scales on Newfoundland Shelf*

Temperature and salinity temporal scales are similar throughout the region (about 1 d). Because of the different filters applied to velocity data (high pass vs. low pass), their temporal scales as calculated in this report are generally higher (3-45 d) than temperature and salinity scales. The Flemish Pass and CASP2 arrays, both on the edge of the Grand Banks and representing "winter" conditions, had larger velocity temporal scales than Avalon and SE Shoal arrays. It can be seen from that the unfiltered velocity series (Appendix I) have energy at semi-diurnal and diurnal frequencies, but furthermore, series at CASP2 and Flemish Pass contain inertial and low frequency energy (supra-diurnal periods). Some of the energy at periods of 60 h and more was not eliminated by the filtering.

5.2 Gulf of St. Lawrence

The correlation scales of datasets from the Gulf of St. Lawrence are summarized in Table 5.

*5.2.1 Horizontal scales in Gulf of St. Lawrence*

The horizontal correlation scales of temperature and salinity obtained in Gulf of St. Lawrence are summarized on Figure 17.1 and Figure 17.2. There was a large range of scales in the region, but overall values of O(10 km) were generally found.. Across straits (Belle Isle, Cabot), scales are shorter than 15 km. It was impossible to resolve the scales of correlation in the St. Lawrence Estuary and Central Gulf because the current meter arrays were too sparse. Results along the Gaspé Current show that correlation scales along the Current decrease with depth, and are larger than the scales across the Current. In Jacques Cartier Passage, only velocity correlation scales could be resolved, and they are generally larger in the wintertime than during summertime.

*5.2.2 Vertical scales in Gulf of St. Lawrence*

Typical scales range from ~10 to ~100 m. In Cabot Strait and the St. Lawrence Estuary, vertical scales of velocity reach a significantly greater value somewhere in the middle of the channel. Summer and winter correlation scales are quite similar for Jacques Cartier Passage.

*5.2.3 Temporal scales in Gulf of St. Lawrence*

The temperature and salinity average temporal scale were about 1 d, whereas the velocity scales ranged from 1 to 13 d for the along-shore component and 2-16 d for the cross-shore.Velocity auto-correlation scales varied from one dataset to another as indicated by the broad range of correlation values at any given lag.

**Table 5**. Correlation scales in Gulf of St. Lawrence. The temperature and salinity data were high-pass filtered in order to remove the low-frequency variability associated with the annual cycle; the velocity data were low-pass filtered in order to eliminate the tidal and inertial variability which could dominate the overall correlation coefficient.

| HORIZONTAL | Depth (m) | Season | Correlation scales (km) | | | |
|---|---|---|---|---|---|---|
| | | | T | S | Along | Across |
| Across Cabot Strait | [16 109] | Mixed | 9 | 6 | 11 | 14 |
| Across St. Lawrence Estuary | [11 100] | Summer | <15 | <15 | <15 | <15 |
| Along St. Lawrence Estuary | [8 20] | Summer | <46 | <46 | <46 | <46 |
| Central Gulf along Honguedo Strait | [250 300] | Mixed | <47 | <47 | <47 | <47 |
| Central Gulf across Honguedo Strait | 250 | Mixed | <246 | <246 | <246 | <246 |
| Along Gaspé Current (parallel to 100 m isobath) | [20 24] | Summer | 51 | 75 | 61 | 31 |
| Along Gaspé Current (parallel to 100 m isobath) | 60 | Summer | 19 | 45 | 36 | 26 |
| Along Gaspé Current (parallel to 100 m isobath) | 150 | Summer | 17 | 17 | <16 | 16 |
| Along Gaspé Current (parallel to 100 m isobath, all depths) | [60 150] | Summer | 22 | 23 | 38 | 25 |
| Across the northwest Gulf of St. Lawrence (La Martre) | [20 150] | Summer | 11 | 15 | 11 | 9 |
| Jacques Cartier Passage along North-shore | [20 95] | Summer | <55 | <55 | 55 | 70 |
| Jacques Cartier Passage along North-shore | 50 | Summer | X | X | <55 | 258 |
| Jacques Cartier Passage along North-shore | [20 95] | Winter | <75 | <75 | 206 | 101 |
| Jacques Cartier Passage along Anticosti shore | [20 95] | Mixed | <93 | <93 | <93 | <93 |
| Across Jacques Cartier Passage | [20 95] | Mixed | <14 | <14 | <15 | <15 |
| Across Natashquan Line at Jacques Cartier Passage | 20 | Summer | X | X | >71 | 14 |
| Across Natashquan Line at Jacques Cartier Passage | 50 | Winter | X | X | 60 | <14 |
| Across Strait of Belle Isle, within 5 km from NFLD | [8 51] | Summer | 7 | 5 | >13 | <2 |
| Across Strait of Belle Isle, farther than 5 km from Nfld (moorings 398 and 399) | [8 51] | Summer | <4 | <4 | >7 | >7 |
| **VERTICAL** | **Depth (m)** | **Season** | **Correlation scales (m)** | | | |
| | | | T | S | Along | Across |
| Cabot Strait at extremities | [16 470] | Mixed | 23 | 36 | 81 | 89 |
| Cabot Strait center (mooring 8) | [32 470] | Mixed | <35 | <35 | 223 | 261 |
| St. Lawrence Estuary | [11 250] | Summer | 27 | 29 | 10 | 78 |
| St. Lawrence Estuary, center (mooring 12) | [100 250] | Summer | X | X | 100 | 85 |
| Central Gulf | [11 209] | Mixed | X | X | <42 | <42 |
| Gaspé Current (middle) | [20 150] | Summer | <36 | 69 | 115 | 128 |
| Gaspé Current, moorings 315 and 318 (extremities) | [24 150] | Summer | <36 | 69 | <36 | 37 |
| Gaspé Current (all) | | Summer | <36 | 69 | 81 | 92 |
| Jacques Cartier Passage | [20 95] | Summer | 20 | 32 | 52 | 22 |
| Jacques Cartier Passage | [20 95] | Winter | 29 | 36 | 55 | 21 |
| Jacques Cartier Passage, mooring 18 | [40 85] | Winter | >45 | >45 | >45 | 16 |
| Strait of Belle Isle | [8 50] | Mixed | >35 | 28 | >35 | 14 |
| **TEMPORAL** | **Depth (m)** | **Season** | **Average scales (d)** | | | |
| | | | T | S | Along | Across |
| Cabot Strait | [15 470] | Mixed | 1 | 1 | 4 | 10 |
| St. Lawrence Estuary | [8 250] | Summer | 1 | 1 | 11 | 6 |
| Central Gulf | [11 300] | Mixed | 1 | 1 | 4 | 5 |
| Gaspé Current | [20 150] | Summer | 1 | 1 | 13 | 16 |
| Jacques Cartier Passage | [20 95] | Summer | 1 | 1 | 2 | 4 |
| Jacques Cartier Passage | [20 95] | Winter | 1 | 1 | 3 | 4 |
| Strait of Belle Isle | [8 51] | Mixed | 1 | 1 | 2 | 1 |

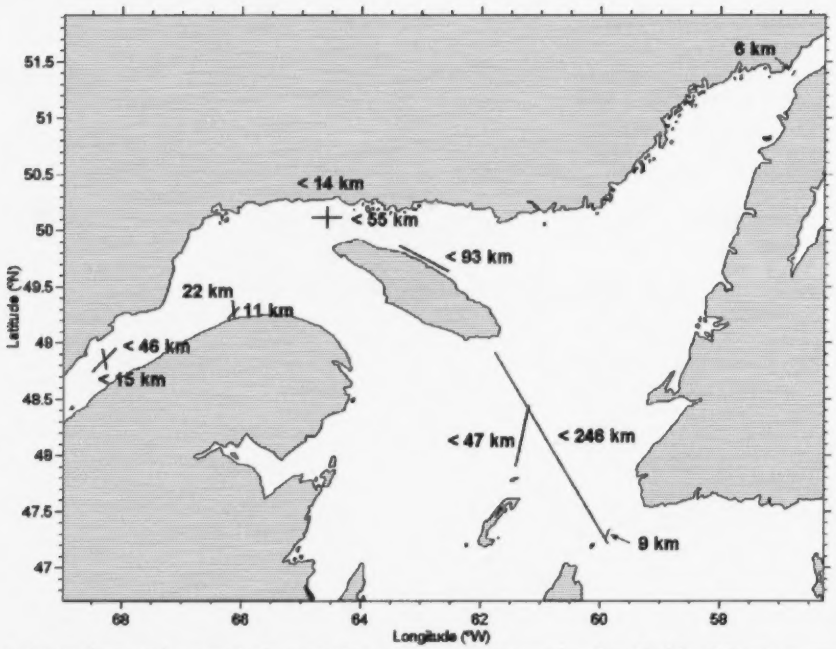


**Figure 17.1** Horizontal correlation scales of temperature in the Gulf of St. Lawrence. The direction and length of scales is represented by proportional thick solid lines. Scale magnitudes are printed next to each line. The "lesser than" symbol (<) is used when the scale could not be resolved by our method. Arrows are used to link values to short lines.

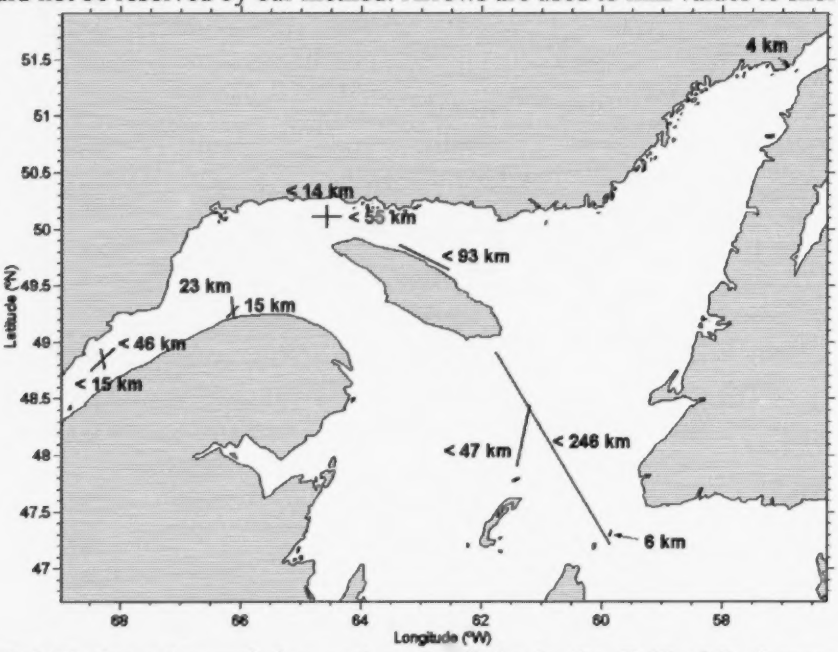


**Figure 17.2** Horizontal correlation scales of salinity in the Gulf of St. Lawrence. The direction and length of scales is represented by proportional thick solid lines. Scale magnitudes are printed next to each line. The "lesser than" symbol (<) is used when the scale could not be resolved by our method. Arrows are used to link values to short lines.

**Table 6**: AZMP Sections with names of corresponding current meter arrays. The distances between stations were calculated from the coordinates established at the beginning of the program (Plourde, 1999) for the Gulf sections. Distance statistics were also calculated using the positions of the actual sampling which took place from 1999-2010, taken from the AZMP website, which is generated from the ISDM Archives

| AZMP Section | Average Distance Between Stations ± 1 std.dev. (km) (Plourde, 1999) | Average Distance Between Stations ± 1 std.dev. (km) (AZMP website, 1999-2010) | Current meter Array |
|---|---|---|---|
| Estuary | 5.7 ± 0.8 | 6.1 ± 1.8 | SLE Array (Mont-Joli Line) |
| Sept-Iles (southern portion, <=49.4°N) | 17.6 ± 0.0 | 11.2 ± 6.5 | Gaspé Current |
| Cabot Strait | 19.2 ± 7.0 | 19.9 ± 7.0 | Cabot Strait |
| Flemish Cap | -------- | 22 ± 13.0 | Avalon Channel and Flemish Pass |

5.3 Representativity of sampling along AZMP sections

One aspect of the representativity of the AZMP network of sections can be evaluated by assessing whether the distances between individual stations which comprise the sections are short enough to allow for the resolution of horizontal variability.

From Figures 2 and 3 it can be seen that the Estuary, Sept-Îles, Cabot Strait and Flemish Cap AZMP sections have corresponding instrumented arrays closely aligned with them. The average distances between the stations that constitute those AZMP sections were calculated and are shown in Table 6.

*5.3.1 Estuary Section vs. SLE Array (Mont-Joli line)*

On average, this section has 7 stations spaced ~5.7 km apart from each other. Since the horizontal coherence scale across Estuary was determined as <21 km, i.e. only an upper bound because of limitations due to the array separations, we cannot conclude that the AZMP section is adequately sampled.

*5.3.2 Sept-Îles Section (southern portion) vs. Gaspé Current Array*

This section has 6 stations spaced ~18 km apart, but the two stations located south of 49.4°N are located 17.6 km apart. However, during years 1999-2010 of AZMP, this section of the line was sampled with an average distance of 11.2 km between samples. In the southern part of the Estuary, our analysis determined temperature and salinity scales of 11 km and 15 km respectively. This suggests that it might be beneficial in terms of variability resolution to keep sampling this part of the Estuary section at 11 km.

*5.3.3 Cabot Strait Section vs. Cabot Strait Array*

The temperature and salinity scales across Cabot Strait are 9 and 6 km respectively, while the average distance between stations is 19.2 km (the line comprises 6 stations). This analysis suggests the section is undersampled and that up to 6 or 7 extra stations would be required in order to better resolve the horizontal variability of temperature and salinity along Cabot Strait.

*5.3.4 Flemish Cap Section vs. Flemish Pass/Avalon Channel Arrays*

The temperature and salinity scales across Flemish Pass were less than 20 km, based upon only one pair of instruments over Flemish Pass. Similarly, the horizontal length scale was <20 km in Avalon Channel. The Flemish Cap section extends from Avalon Peninsula to Flemish Cap, comprising on average of 33 stations extending over >700 km long and with a mean separation of ~22 km. However, the station spacing varies from 9 km near the coast to a maximum of 67 km over the central Grand Bank to as short as 6 km on the upper slope of Flemish Pass off Grand Bank. While definitive conclusions about the sampling along Flemish Cap section based on our analysis alone cannot be made (we found that the scales of variability were <20 km but cannot firmly set a value), it is likely that the section is capturing the variability in the frequency bands of our analysis in the near shore region of the Avalon Channel array and the offshore region of the Flemish Pass array, where AZMP sampling is at spacings much less than 20 km. Data analysis from a larger array would be needed to assess the entire section.

## 6.0 Acknowledgements

The work underlying this report was funded by the Science Strategic Fund. Current meter data were extracted from the Ocean Data Inventory (ODI[1]) maintained by Ocean Sciences Division, Bedford Institute of Oceanography (Gregory, 2004). Information pertaining to sampling of AZMP sections was extracted from the AZMP website[2] maintained by Integrated Science Data Management (formerly MEDS), Ottawa. We thank Fraser Davidson and Peter Galbraith whose reviews led to clarifications and improvements in the report.

[1]http://www2.mar.dfo-mpo.gc.ca/science/ocean/database/data_query.html
[2]http://www.meds-sdmm.dfo-mpo.gc.ca/isdm-gdsi/azmp-pmza/index-eng.html

## 7.0 References

Bourque, M.-C. and Kelley, D. 1995. Evidence of Wind-Driven Upwelling in Jacques-Cartier Strait. Atmosphere-Ocean. **33 (4)** : 621-637.

Castonguay, M. and Gilbert, D. 1995. Effects of tidal streams on migrating Atlantic mackerel, *Scomber scombrus*. *ICES J. Mar. Sci.*, **52:** 941-954.

Desruisseaux, M. 1996. Structure spatio-temporelle des courants dans le sud-ouest du détroit de Cabot. Université du Québec à Rimouski, Mémoire de maîtrise. **405** : ix, 181 p.

El-Sabh, M.I. 1979. The lower St. Lawrence estuary as a physical oceanographic system. *Naturaliste Can.*, **106** : 55-73

El-Sabh, M.I., Lie and Koutitonsky, V. 1982. Variability of the Near-Surface Residual Current in the Lower St. Lawrence Estuary. *Journal of Geophysical Research.* **(87)**: 9589-9600.

Farquharson, W., 1970. Tides, tidal streams and currents in the Gulf of St. Lawrence. *Report (Atlantic Oceanographic Laboratory).* **1970-5** : 145 p.

Farquharson, W. and Bailey, W. 1966. Oceanographic study of Belle Isle Strait. *Report (Bedford Institute of Oceanography).* **66-9** : iv, 78 p

Dennis, J.E. 1977. Nonlinear Least Squares, *State of the Art in Numerical Analysis*, ed. D. Jacobs, Academic Press, pp. 269-312.

Gandin, LS. 1967. Objective analysis of meteorological fields. *NTIS.* vi, 242p.

Gregory, D.N. 2004. Ocean Data Inventory (ODI): A Database of Ocean Current, Temperature and Salinity Time Series for the Northwest Atlantic. *Can. Sci. Advis. Sec. Res. Doc. 2004/097*

Gregory, D., Nadeau, O. and Lefaivre, D. 1989. Current statistics of the Gulf of St. Lawrence and estuary. *Can. Tech. Rep. Hydrogr. Ocean Sci.* **120** : vi, 178 p.

Lawrence, D. 1968. Current meter data from Cabot Strait. *Data series (Bedford Institute of Oceanography).* **68-10** : 34 p.

Lively, R. 1984. Current meter and tide gauge observations for the Strait of Belle Isle. *Can. Tech. Rep. Hydrogr. Ocean Sci.* **46** : vi, 166 p.

Lively, R. 1994. Current meter tide gauge, MINIMET meteorological buoy and hydrographic observations for the CASP II experiment on the northern Grand Banks and N.E. Newfoundland Shelf, December 1991 to May 1992. *Can. Data Rep. Hydrogr. Ocean Sci.* **131**; v, 258 p.

Lively, R. and Petrie, B. 1990. Labrador Current variability study : current meter observations October 1985 to January 1986. *Can. Data Rep. Hydrogr. Ocean Sci.* **91**; v, 146 p.

Lomas, P. and Lawrence, D.J. 1973. An inventory of current meter records at the Bedford Institute of Oceanography 1958-1972. *Data series (Bedford Institute of Oceanography).* BI-D-**73-7** : 96 p.

Mertz, G., El-Sabh, M. and Koutitonsky, V. 1988. Wind-driven currents at the mouth of the St. Lawrence estuary. *Atmos.-Ocean.* **26** : 509-523.

Milewska, E. and Hogg, W.D. 2001. Spatial representativeness of a Long-Term Climate Network in Canada. *Atmos.-Ocean.* **39 (2)** : 145-161

Ouellet, M., Petrie, B. and Chassé, J., 2003. Temporal and spatial scales of sea-surface temperature variability in Canadian Atlantic waters. *Can. Tech. Rep. Hydrogr. Ocean Sci.* **228:** v + 30 p.

Petrie, B. 1991. Current meter and tide gauge observations from Avalon Channel, 1980-1981. *Can. Data Rep. Hydrogr. Ocean Sci.* **102** : v, 89 p.

Petrie, B. and Dean-Moore, J. 1996. Temporal and spatial scales of temperature and salinity on the Scotian Shelf. *Can. Tech. Rep. Hydrogr. Ocean Sci.* **177**: viii, 45 p.

Petrie, B., Toulany, B. and Garrett, C. 1988. The transport of water, heat and salt through the Strait of Belle Isle. *Atmos.-Ocean.* **26**: 234-251.

Plourde, J. 1999. Official positions of stations on the standard AZMP sections *in* ZMP Second Annual Meeting Minutes, Annex VI. (unpublished, available on-line http://www/isdm-gdsi/azmp-pmza/docs/ZMP_Meeting_minutes00_e.pdf )

Ross, C., Loder, J. and Graça, M.-J. 1988. Moored current and hydrographic measurements on the southeast shoal of the Grand Bank 1986 and 1987. *Can. Data Rep. Hydrogr. Ocean Sci.* **71** : 132 p.

Tang, C. and Bennett, A. 1981. Physical oceanographic observations in the northwestern Gulf of St. Lawrence. *Data series (Bedford Institute of Oceanography).* **BI-D-81-6** : 127 p.

Tee, K.-T. and Lim, T.-H. 1987. The freshwater pulse - a numerical model with application to the St. Lawrence Estuary. *J. Mar. Res.*, **45:** 871-909.

Therriault, J.-C., Petrie B., Pepin, P., Gagnon, J., Gregory, D., Helbig, J., Herman, A., Lefaivre, D., Mitchell, M., Pelchat, B., Runge, J., and Sameoto, D.1998. Proposal for a northwest Atlantic zonal monitoring program. *Can. Tech. Rep. Hydrogr. Ocean Sci.* **194**: vii+57 p.

## Appendix I

Variance spectra of temperature, salinity, and components of velocity averaged over all series are presented on the following figures. For a given series, spectral estimates were computed with 2 degrees of freedom, then averaged on frequency bands of 1/30 $d^{-1}$. Then for a given array, all series (all depth, all moorings, all periods of recording) were averaged to yield two spectra: one of the filtered data (high-pass for T and S, low-pass for U and V, see section 3.2 – solid line), the other of unfiltered data (dashed line).

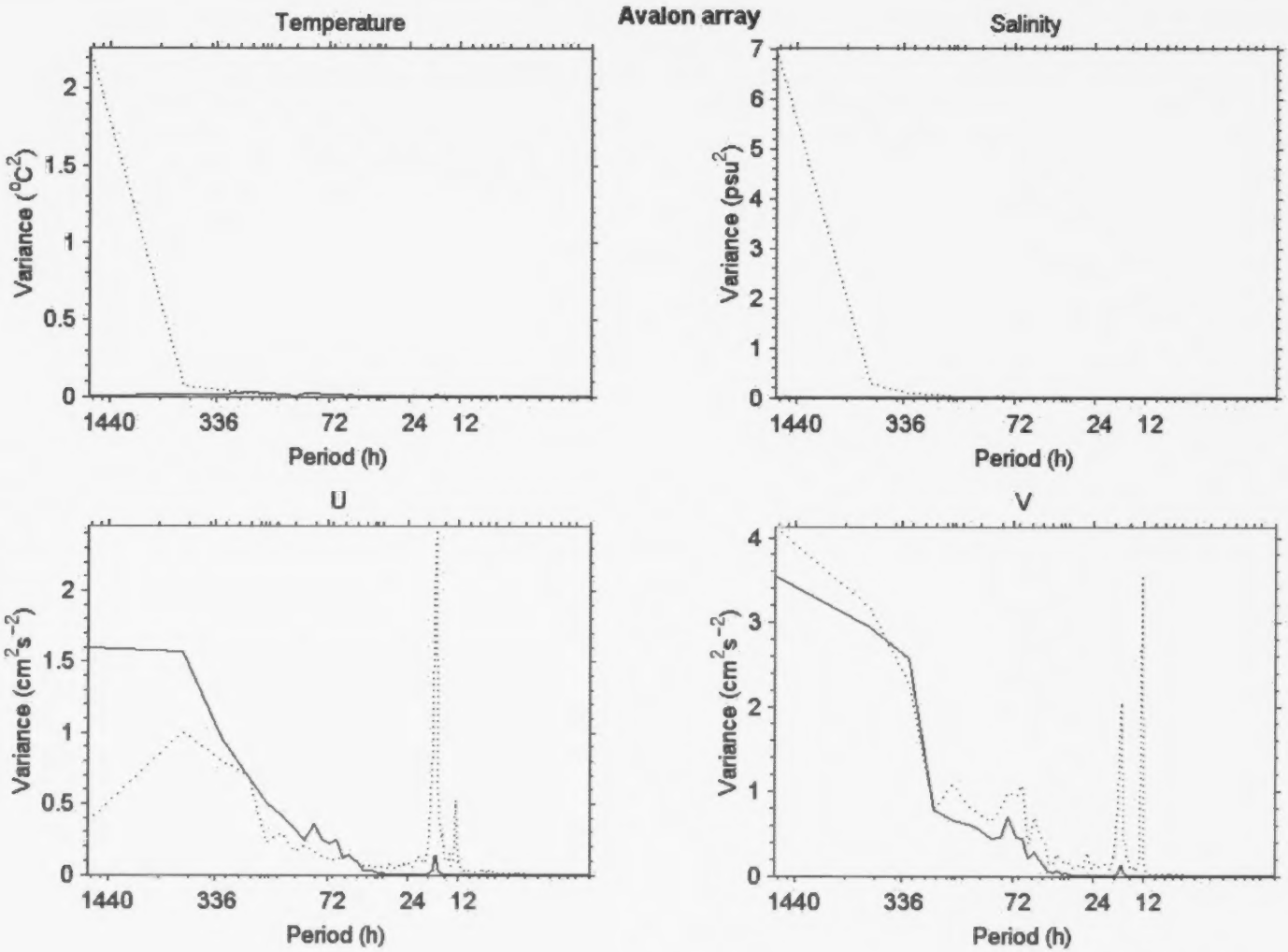
Avalon array
Temperature
Variance ($^0C^2$)
Period (h)
1440
336
72
24
12
Salinity
Variance (psu$^2$)
U
Variance (cm$^2$s$^{-2}$)
V

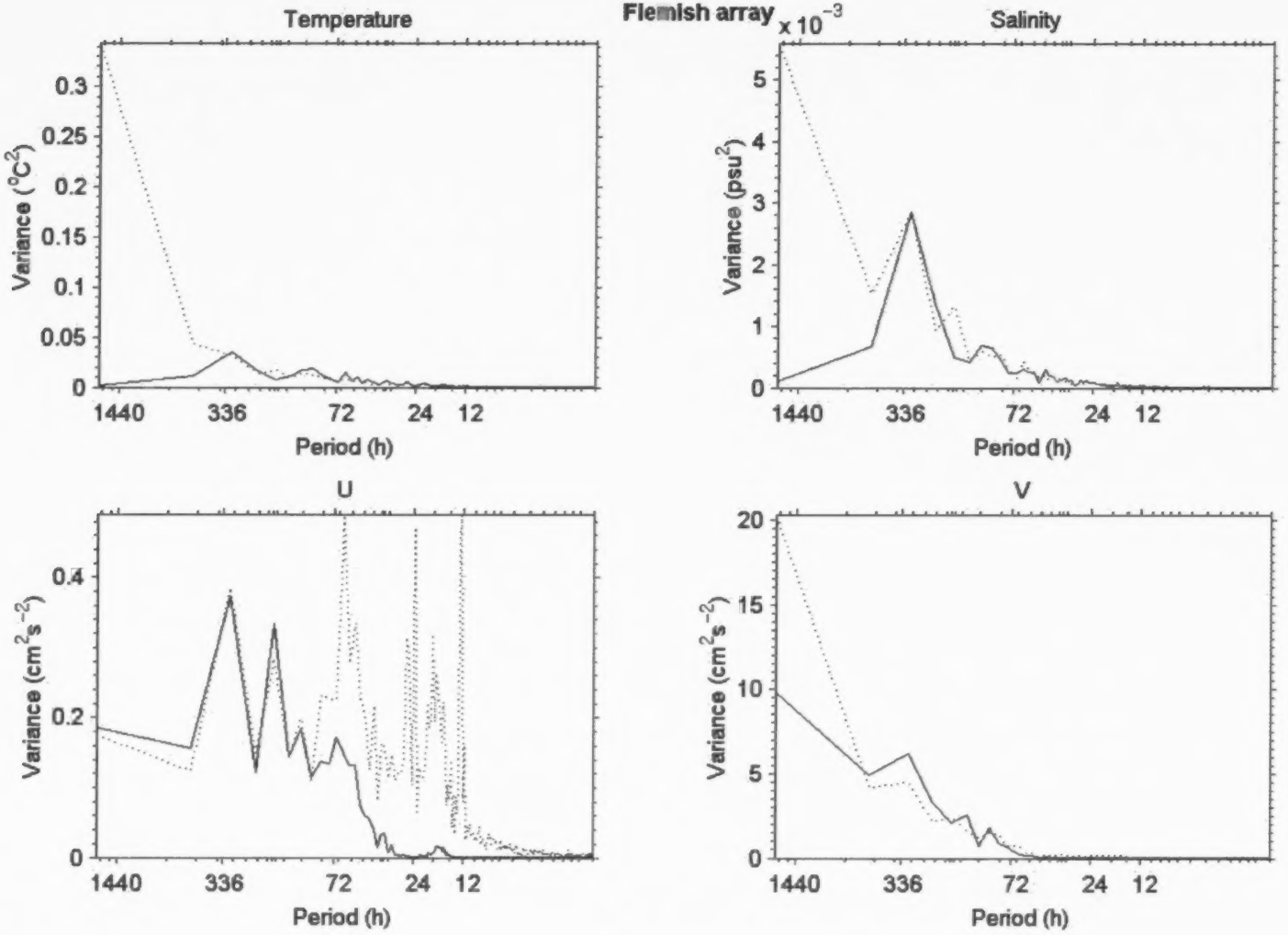
Flemish array
Temperature
Variance (°C²)
0.3
0.25
0.2
0.15
0.1
0.05
0
1440
336
72
24
12
Period (h)
Salinity
x 10⁻³
Variance (psu²)
5
4
3
2
1
0
1440
336
72
24
12
Period (h)
U
Variance (cm²s⁻²)
0.4
0.2
0
1440
336
72
24
12
Period (h)
V
Variance (cm²s⁻²)
20
15
10
5
0
1440
336
72
24
12
Period (h)

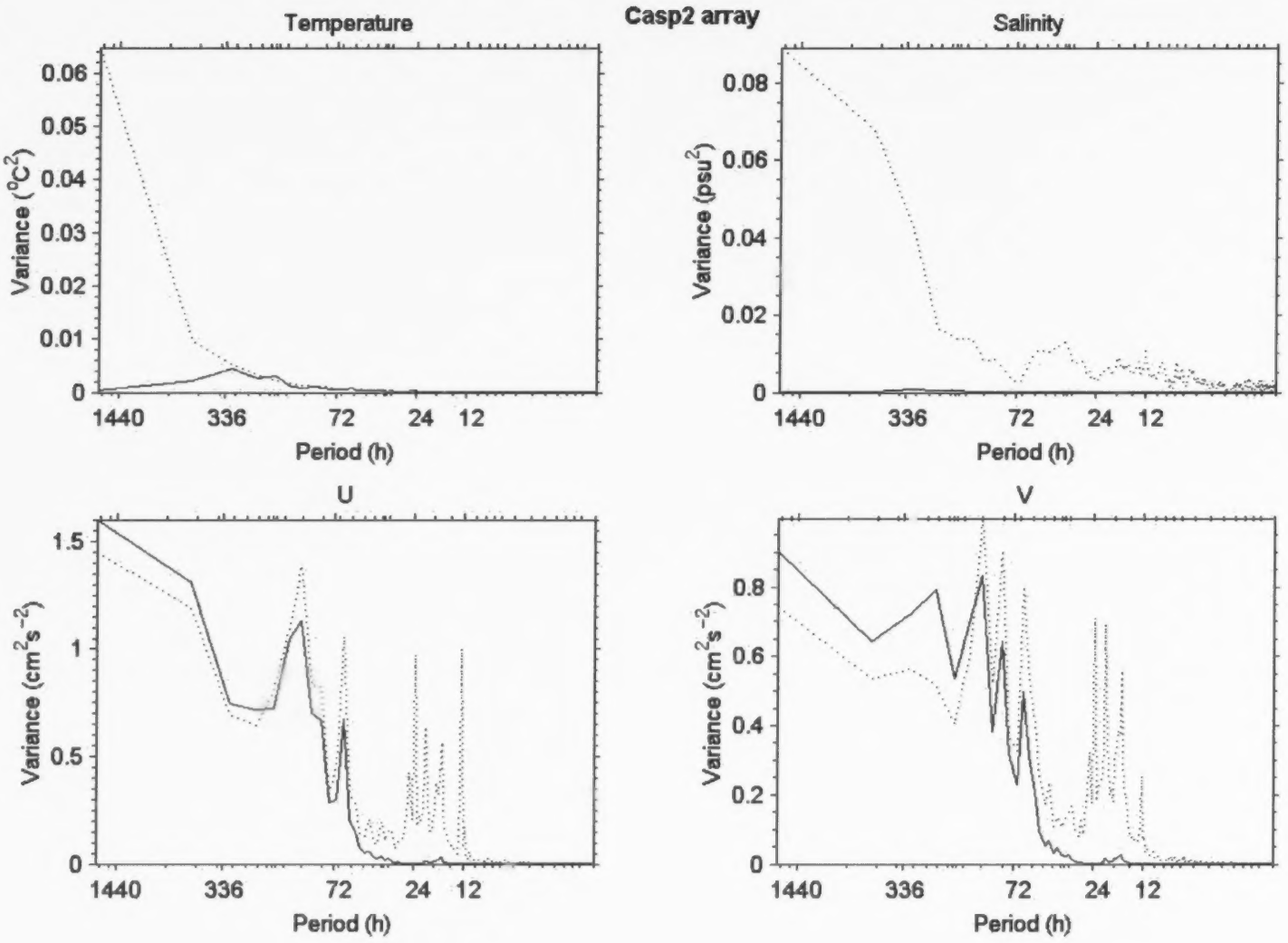
Casp2 array
Temperature
Variance (°C²)
0.06
0.05
0.04
0.03
0.02
0.01
0
1440
336
72
24
12
Period (h)
Salinity
Variance (psu²)
0.08
0.06
0.04
0.02
0
1440
336
72
24
12
Period (h)
U
Variance (cm²s⁻²)
1.5
1
0.5
0
1440
336
72
24
12
Period (h)
V
Variance (cm²s⁻²)
0.8
0.6
0.4
0.2
0
1440
336
72
24
12
Period (h)

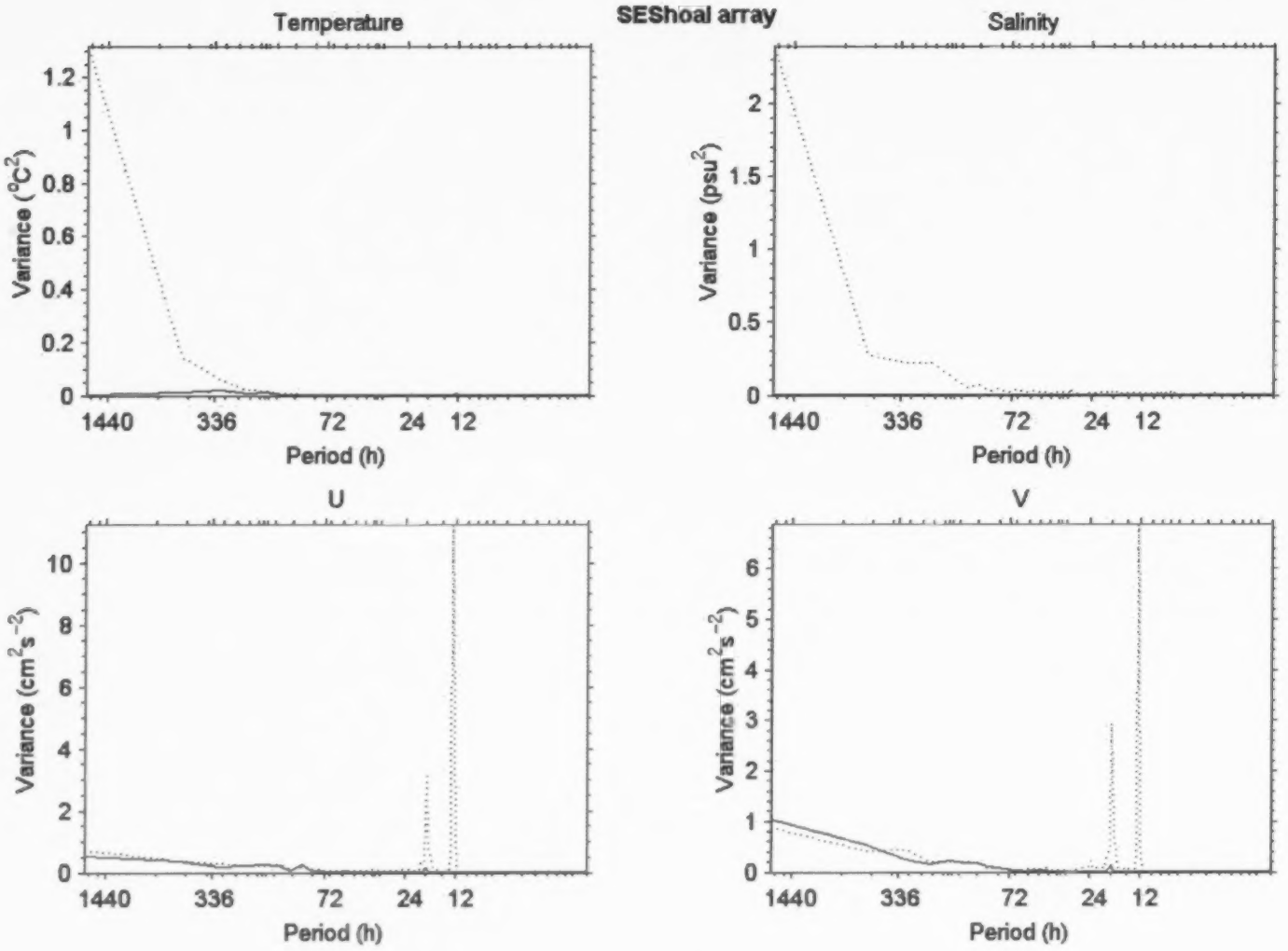
SEShoal array
Temperature
Variance (°C²)
1.2
1
0.8
0.6
0.4
0.2
0
1440
336
72
24
12
Period (h)
Salinity
Variance (psu²)
2
1.5
1
0.5
0
1440
336
72
24
12
Period (h)
U
Variance (cm²s⁻²)
10
8
6
4
2
0
1440
336
72
24
12
Period (h)
V
Variance (cm²s⁻²)
6
5
4
3
2
1
0
1440
336
72
24
12
Period (h)

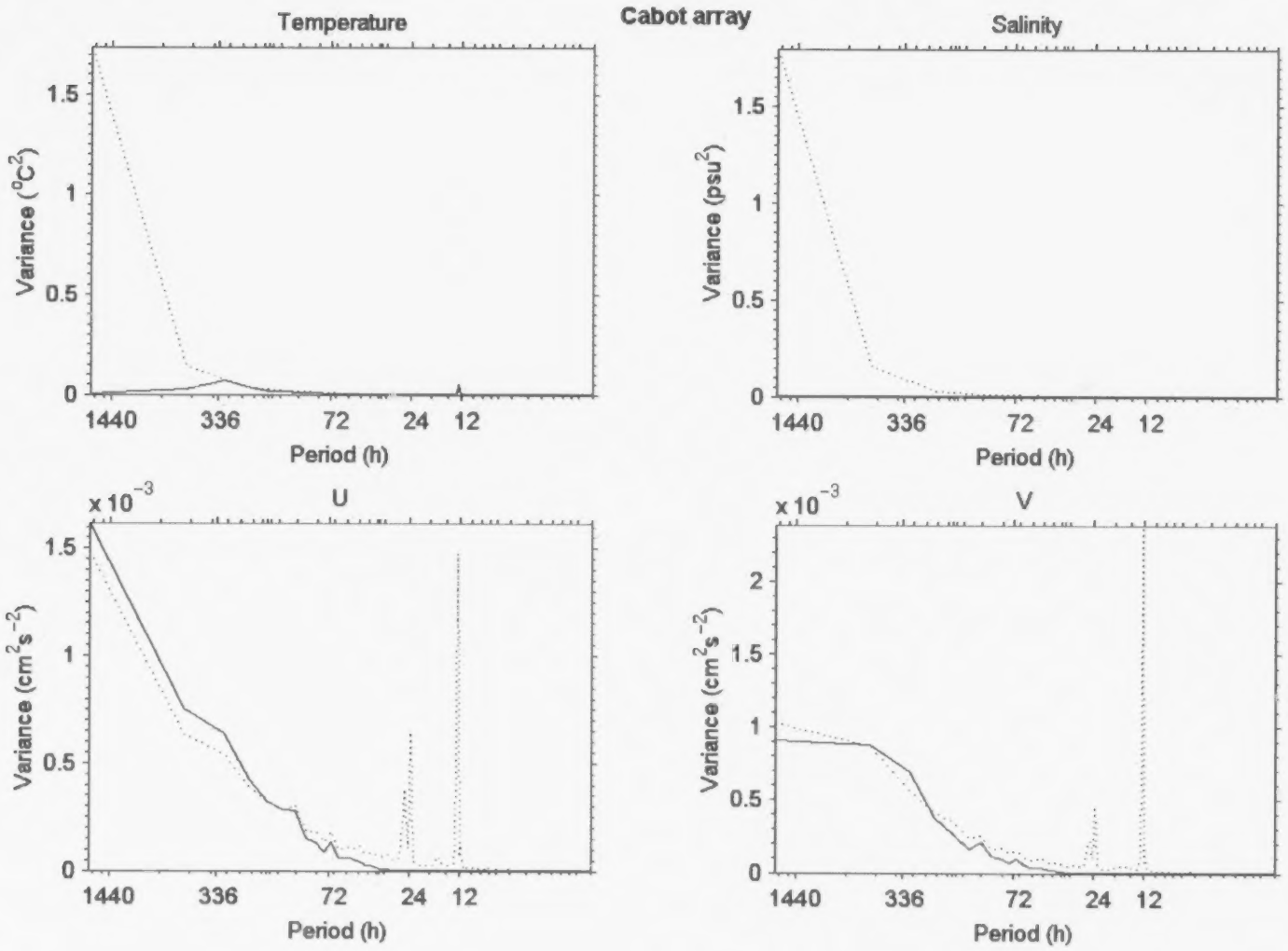
Cabot array
Temperature
Variance (°C²)
1.5
1
0.5
0
1440
336
72
24
12
Period (h)
Salinity
Variance (psu²)
1.5
1
0.5
0
1440
336
72
24
12
Period (h)
x 10⁻³
U
Variance (cm²s⁻²)
1.5
1
0.5
0
1440
336
72
24
12
Period (h)
x 10⁻³
V
Variance (cm²s⁻²)
2
1.5
1
0.5
0
1440
336
72
24
12
Period (h)

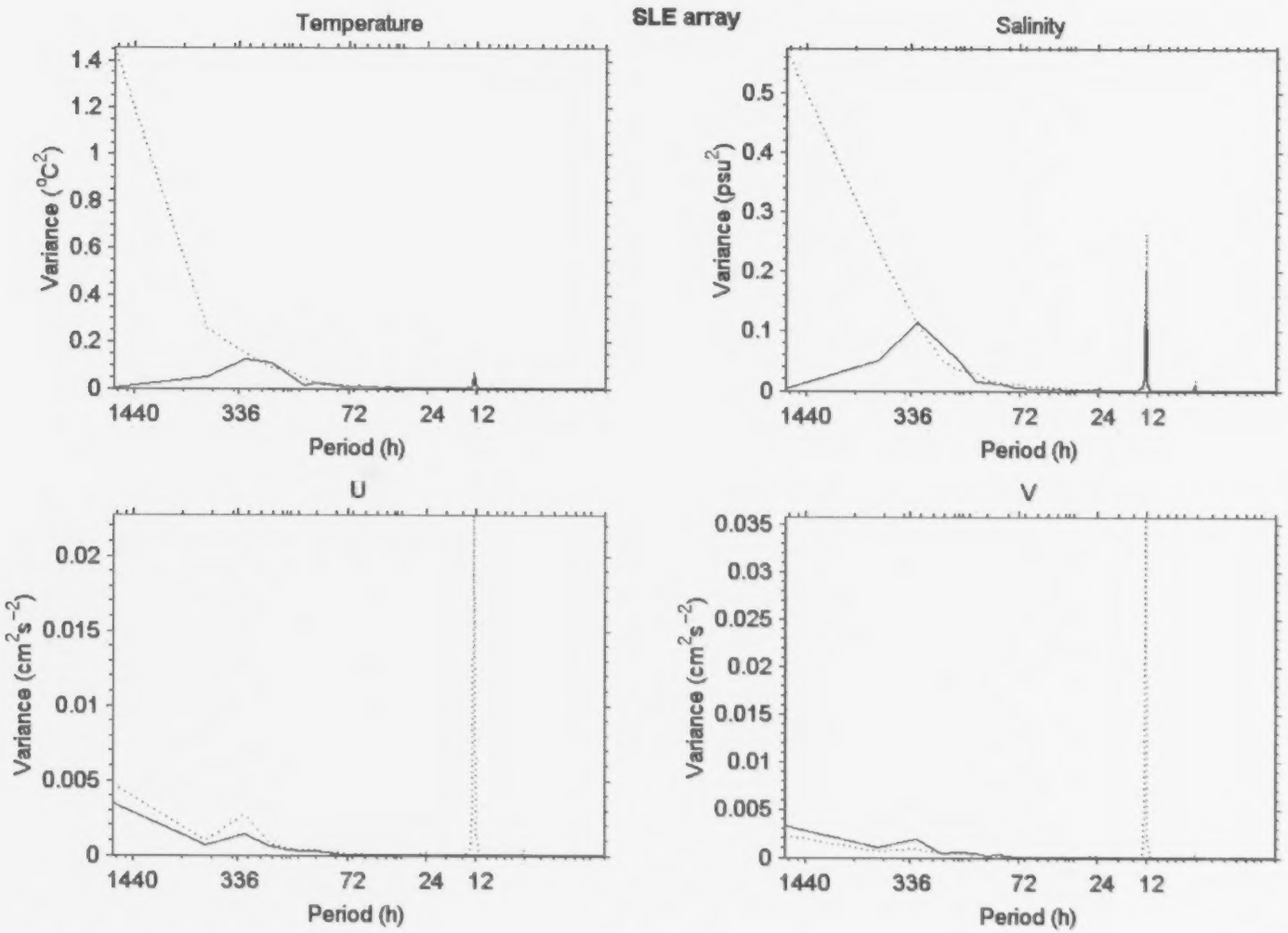
SLE array
Temperature
Variance (°C²)
1.4
1.2
1
0.8
0.6
0.4
0.2
0
1440
336
72
24
12
Period (h)
Salinity
Variance (psu²)
0.5
0.4
0.3
0.2
0.1
0
1440
336
72
24
12
Period (h)
U
Variance (cm²s⁻²)
0.02
0.015
0.01
0.005
0
1440
336
72
24
12
Period (h)
V
Variance (cm²s⁻²)
0.035
0.03
0.025
0.02
0.015
0.01
0.005
0
1440
336
72
24
12
Period (h)

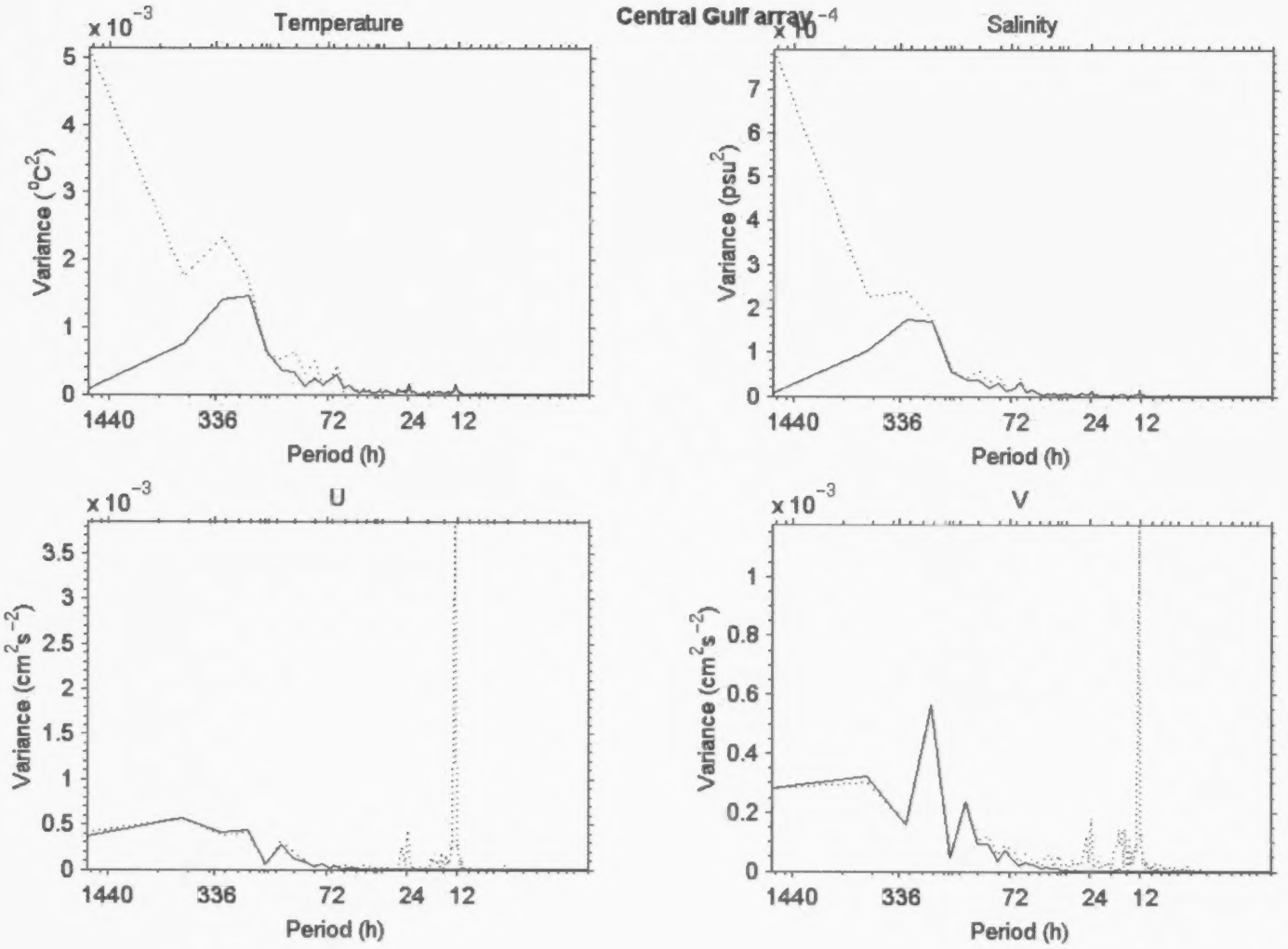
Central Gulf array -4
Temperature
x 10^-3
Variance (°C^2)
Salinity
x 10^-4
Variance (psu^2)
U
x 10^-3
Variance (cm^2 s^-2)
V
x 10^-3
Variance (cm^2 s^-2)
1440
336
72
24
12
Period (h)

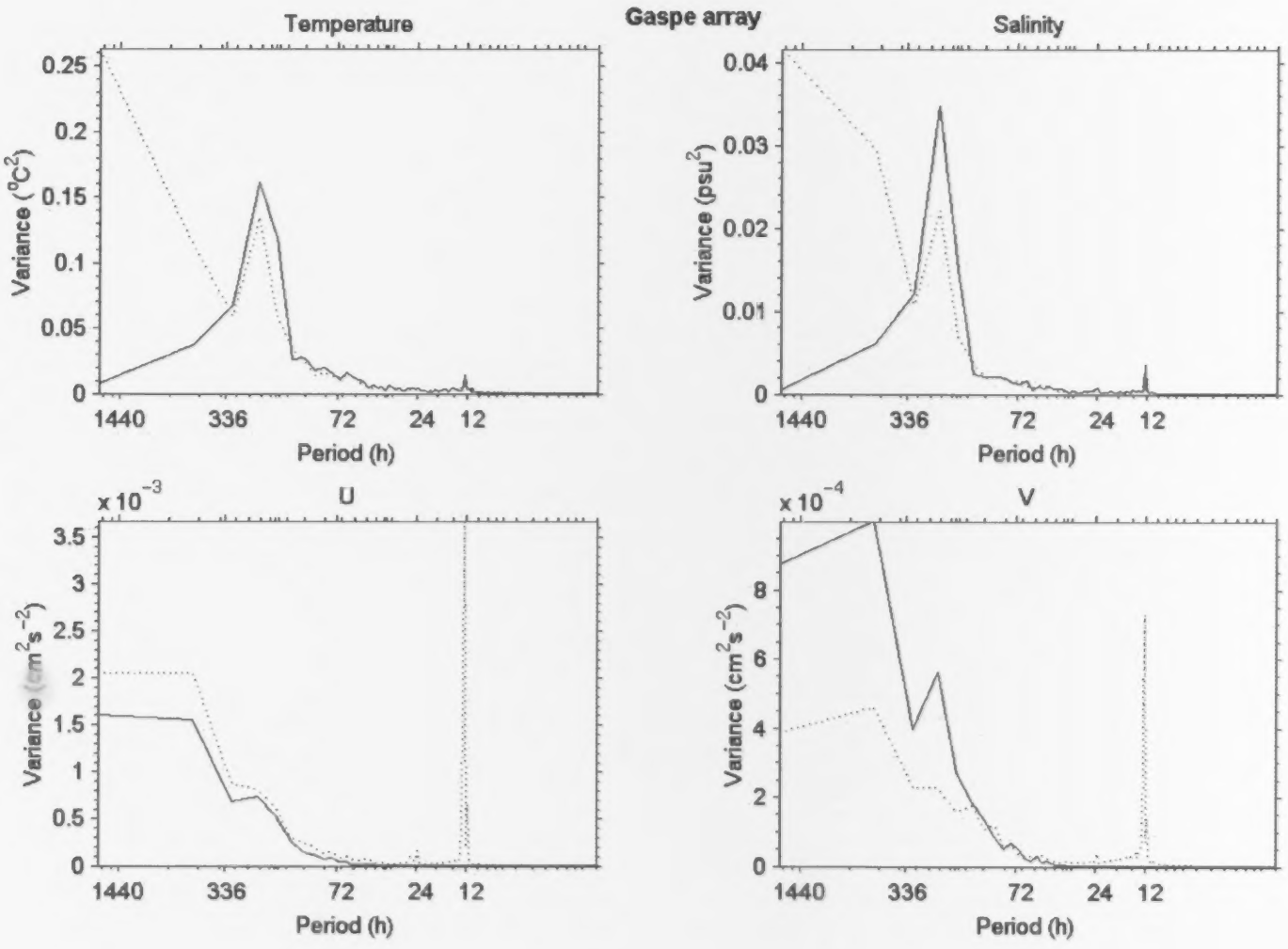
Gaspe array
Temperature
Variance (°C²)
0.25
0.2
0.15
0.1
0.05
0
1440
336
72
24
12
Period (h)
Salinity
Variance (psu²)
0.04
0.03
0.02
0.01
0
1440
336
72
24
12
Period (h)
x 10⁻³
U
Variance (cm²s⁻²)
3.5
3
2.5
2
1.5
1
0.5
0
1440
336
72
24
12
Period (h)
x 10⁻⁴
V
Variance (cm²s⁻²)
8
6
4
2
0
1440
336
72
24
12
Period (h)

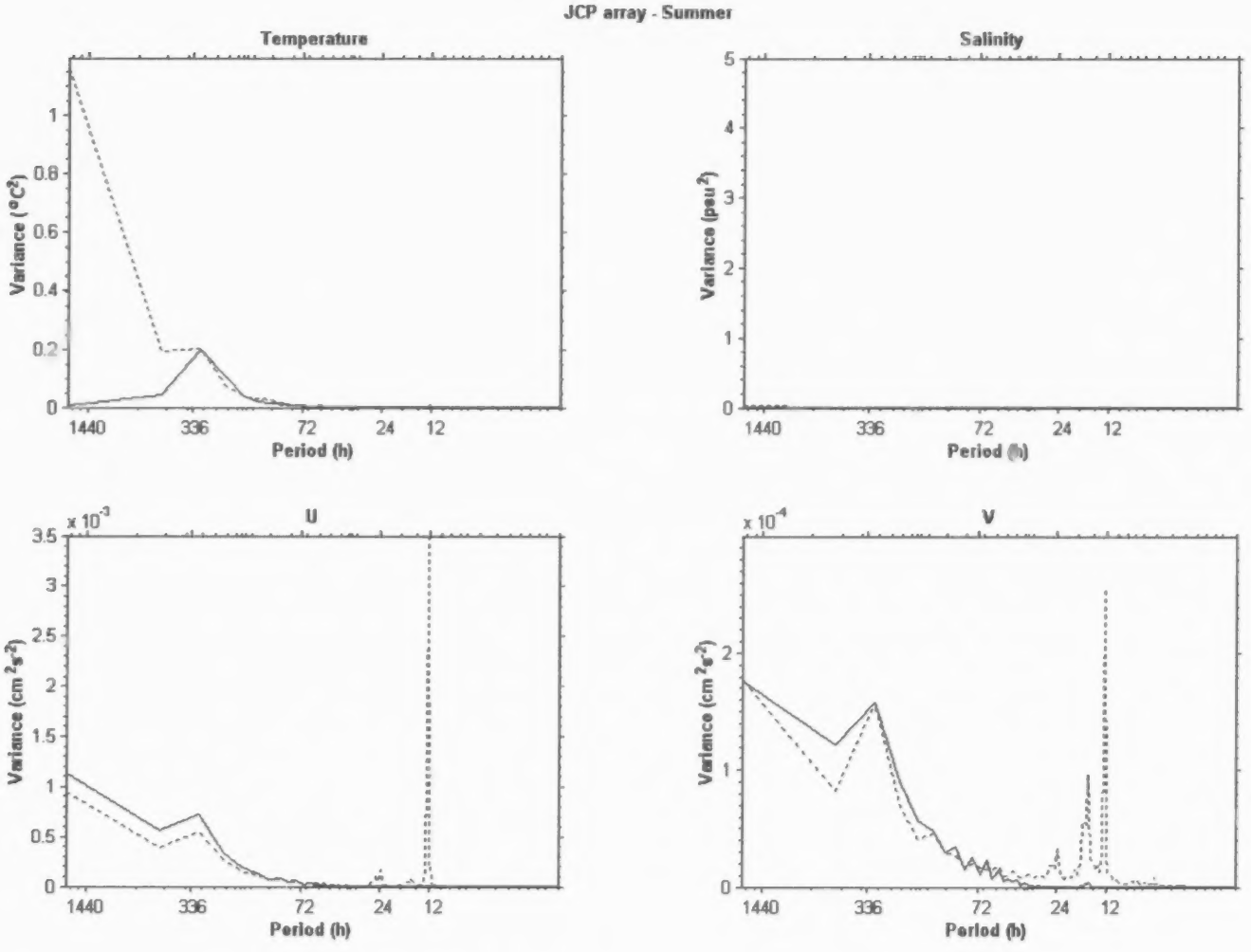
JCP array - Summer
Temperature
Variance (°C²)
Period (h)
Salinity
Variance (psu²)
Period (h)
U
x 10⁻³
Variance (cm²s⁻²)
Period (h)
V
x 10⁻⁴
Variance (cm²s⁻²)
Period (h)
1440
336
72
24
12

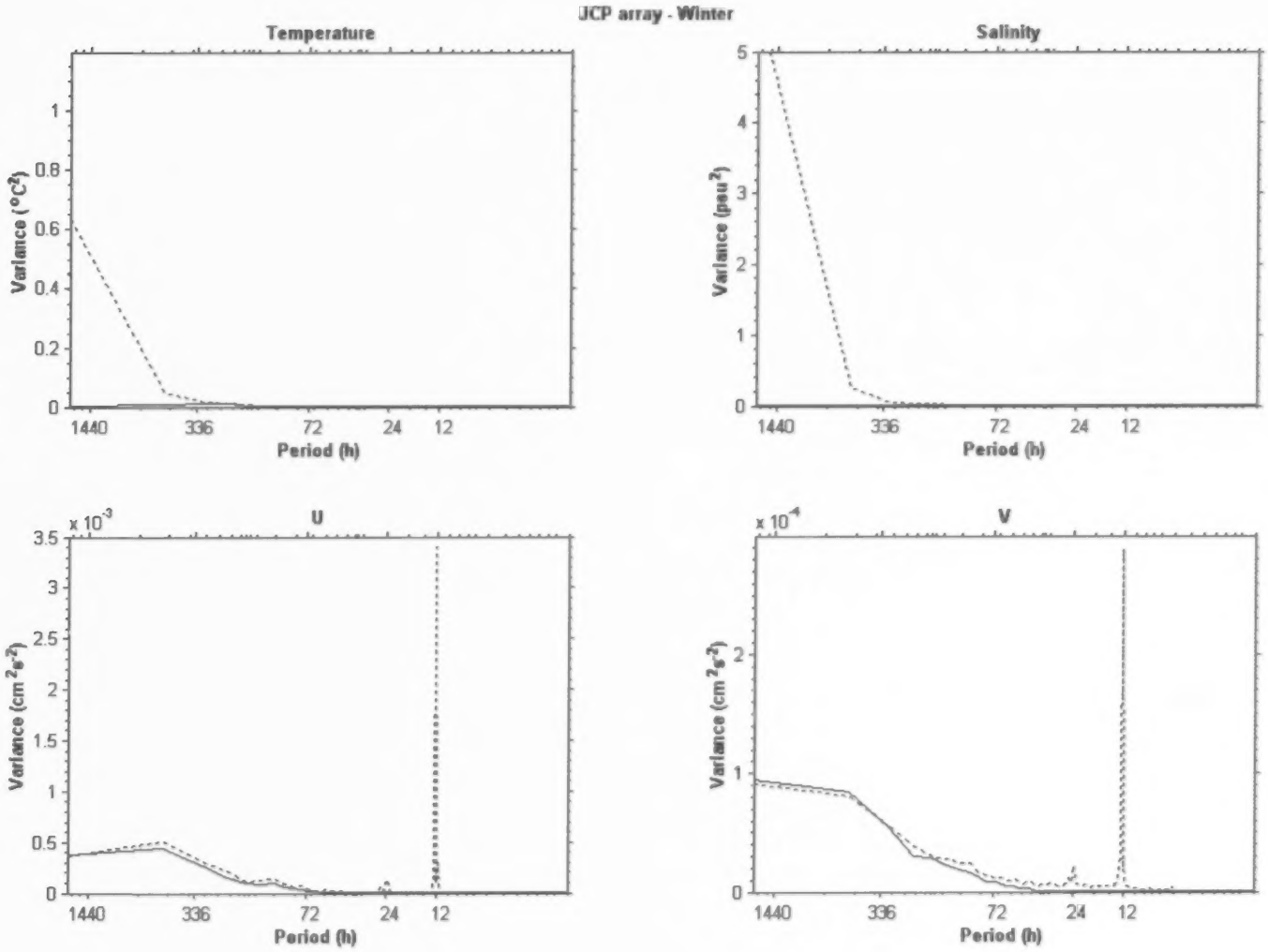
JCP array - Winter
Temperature
Variance (°C²)
Period (h)
1440
336
72
24
12
Salinity
Variance (psu²)
U
x 10⁻³
Variance (cm²s⁻²)
V
x 10⁻⁴

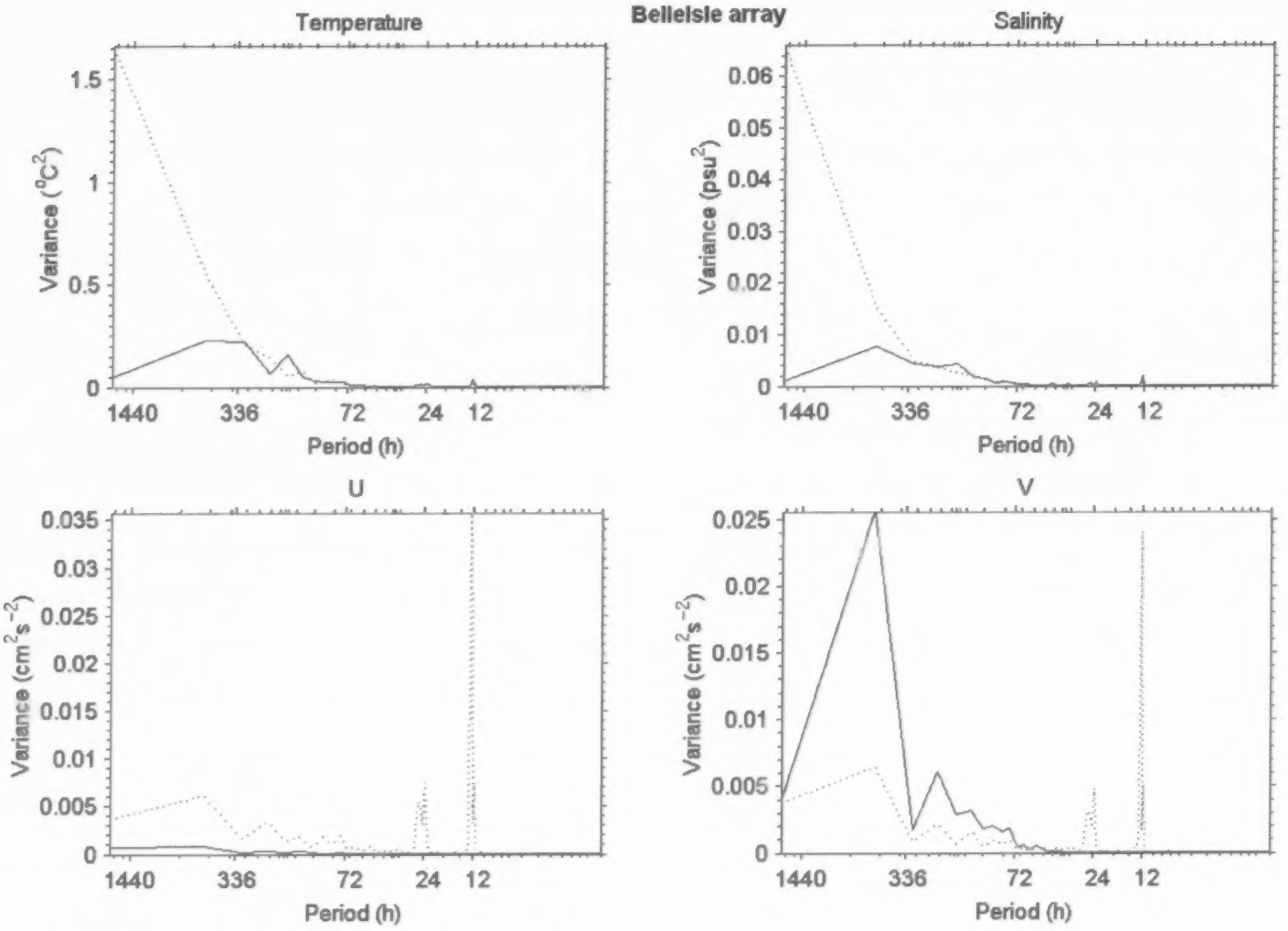
Belleisle array
Temperature
Variance (°C²)
1.5
1
0.5
0
1440
336
72
24
12
Period (h)
Salinity
Variance (psu²)
0.06
0.05
0.04
0.03
0.02
0.01
0
1440
336
72
24
12
Period (h)
U
Variance (cm²s⁻²)
0.035
0.03
0.025
0.02
0.015
0.01
0.005
0
1440
336
72
24
12
Period (h)
V
Variance (cm²s⁻²)
0.025
0.02
0.015
0.01
0.005
0
1440
336
72
24
12
Period (h)